

THE NON-LINEAR BEHAVIOUR OF ELASTIC FRAMES

by

PUI-TAK WONG, M.Sc.(Eng.)

Thesis presented to the Faculty of Engineering of the  
University of London for the degree of Doctor of Philosophy.

Imperial College

January, 1970

ABSTRACT

The non-linear behaviour of elastic plane frames of portal type under static loading is investigated. Both axial loading and non-axial loading problems are discussed.

For axially loaded frames a quick, exact method for evaluating the critical loads is proposed. The possibility of solving buckling problems in approximate, algebraic form is also demonstrated; the new concepts thus developed help to show clearly the effect on the buckling load of the stiffnesses of individual members.

For non-axially loaded frames an iterative method, which is based on small-deflection assumptions, is developed for solving bifurcational problems for which the existing methods are too tedious. The method is also applied to non-bifurcational problems so as to estimate the approximate range of applicability of the small-deflection analysis, by comparing solutions thus found with the experimental results obtained from three model tests.

ACKNOWLEDGMENTS

The author wishes to take this opportunity to express his sincere thanks to the following:

Dr. E.H. Brown, who supervised this work, for his unfailing guidance, inspiration and encouragement.

Professor S.R. Sparkes for permission to pursue the research work at Imperial College.

Surveyer, Nenniger and Chênevert Inc., Montreal, Canada for their granting of an SNC Scholarship.

Messrs. J. Neale and R. Philpott, of the Imperial College structures laboratory, for their assistance in preparing the models for testing.

CONTENTS

	PAGE
<u>ABSTRACT</u>	2
<u>ACKNOWLEDGMENTS</u>	3
<u>CONTENTS</u>	4
<u>CHAPTER I INTRODUCTION</u>	5
<u>CHAPTER II AXIAL LOADING PROBLEMS (I):</u>	15
THE $\gamma$ METHOD AND ITS APPLICATION	
<u>CHAPTER III AXIAL LOADING PROBLEMS (II):</u>	40
THE STABILITY FUNCTION TRANSFORMATION	
AND ITS APPLICATION	
<u>CHAPTER IV NON-AXIAL LOADING PROBLEMS</u>	93
IV.1 GENERAL DESCRIPTION	93
IV.2 EQUILIBRIUM PATHS FOR FRAMES WITHOUT SWAY	98
IV.3 EQUILIBRIUM PATHS FOR FRAMES WITH SWAY	112
IV.4 BIFURCATIONAL BUCKLING	127
<u>CHAPTER V APPLICABILITY OF SMALL-DEFLECTION ANALYSES</u>	132
V.1 EXPERIMENTAL INVESTIGATIONS	132
V.2 DISCUSSION	149
<u>CHAPTER VI CONCLUSIONS</u>	152
<u>NOTATION</u>	157
<u>REFERENCES</u>	161

## CHAPTER I INTRODUCTION

### 1.1 Types of frames and loading

The objective of the thesis is to investigate the non-linear behaviour of elastic plane frames under static loading. Frames are of portal type, i.e., they possess a kinematic degree of freedom when pins are introduced at all joints and supports. If  $M$  denotes the number of members,  $R$  denotes the number of support reactions, and  $J$  denotes the number of joints where members meet, then portal frames are characterized by the inequality

$$F = M + R - 2J < 0, \quad (1.1)$$

in which  $F$  represents the kinematic degree of freedom.

Portal frames are to be distinguished from triangulated frames, which become statically determinate if all rigid joints are replaced by pinned joints; or they satisfy the relation

$$M + R - 2J = 0. \quad (1.2)$$

The common feature of these two types of frames is that they can be treated as being composed of inextensible members: deformation may be attributed solely to the flexural bending of members. This assumption of inextensibility, however, is not applicable to rigidly jointed trusses, which possess the property

$$M + R - 2J > 0. \quad (1.3)$$

Loads considered in this thesis are applied in such a way that their directions and relative magnitudes remain unchanged during deformation of the frame, and their points of application remain fixed in relation to the deformed frame.

Both axial loading and non-axial loading problems are discussed in this thesis. Axial loading of a frame of inextensible members is defined as a system of external loads which satisfy simultaneously the following two requirements:

- (1) that the loads are acting along the centroidal axes of members.
- (2) that they can be expressed as self-equilibrating systems of loads applied to individual members.

Fig.(1.1) shows one such axial loading problem, with the typical possibility of the trivial response of zero deformation.

All other loading systems are classified as non-axial loading systems; some such systems are shown in Fig.(1.2).

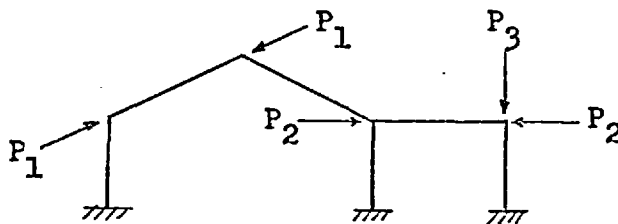


Fig.(1.1)

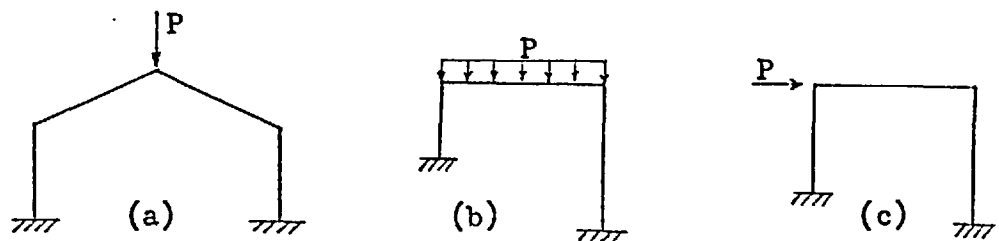


Fig.(1.2)

## 1.2 Frame problems

Both bifurcation and non-bifurcation problems will be discussed in this thesis. A point of bifurcation is a point at which there is branching of the equilibrium path, for example, from a non-sway mode to a sway mode. Thompson (20) remarked that the point of bifurcation is actually the point of intersection of two distinct equilibrium paths. This viewpoint, however, was questioned by Sewell (24) after examining the behaviour of elastic/plastic columns.

Cases in which bifurcational buckling may occur include:

- (1) frames under axial loading.
- (2) symmetrical frames under symmetrical non-axial loading.
- (3) unsymmetrical frames under special distributions of non-axial loading.

Case (3) represents a rare, coincidental or artificial arrangement of the loading system and will not be discussed; case (1) will be discussed in Chapter II and Chapter III, and case (2) will be discussed in Chapter IV.4.

All other frame problems are classified as non-bifurcation problems, to which Chapter IV.2 and Chapter IV.3 will be devoted. For this type of problem, equilibrium paths leading to local maximum load points will be determined.

### 1.3 Axial loading problems, bifurcational buckling

For frames under axial loading (Case 1 of Section (1.2)) several methods of evaluating the bifurcation load have been proposed. For example, Merchant (5) applied disturbing moments to a symmetrical single-bay frame and derived the relation between the critical load factor and other parameters for the sway mode. McMinn (13) applied to both sway and non-sway buckling the criterion that the stiffness matrix corresponding to all possible disturbances is singular. Johnson (10) suggested an energy method, assuming for the displacement function of a multistorey frame a third degree polynomial in a non-dimensional length parameter; he finally used moment distribution to satisfy the equilibrium requirements. Bleich (4) applied four-moment equations to solve the side-sway buckling of two-storey rectangular frames with fixed bases. The same frames were also solved by Livesley and Chandler (8) using a relaxation technique with disturbing forces exciting a side-sway mode, and by Gregory (27) who extracted latent roots from the corresponding stiffness matrix. The cases of single-storey continuous bents were investigated by Timoshenko (1) and Goldberg (12).

New methods of evaluating the bifurcation loads for axially loaded frames will be proposed in Chapter II and Chapter III; frames previously solved by Bleich, McMinn and some other researchers will be solved again as examples of the application of these new ideas.



#### 1.4 Axial loading problems, post-critical behaviour

Non-linear studies concerned with the equilibrium path configurations in the vicinity of a critical equilibrium state were pioneered by Koiter (3) in the structural field. The significance of Koiter's work is in determining the behaviour of an imperfect system which, depending on the type of structure and the degree of imperfection, might differ considerably from that of the perfect or idealized system.

Following Koiter's work, Thompson (23) established in terms of generalized co-ordinates the criteria of elastic stability for both snapping and bifurcation conditions, and rederived in explicit form results similar to those contained in Koiter's work. Results parallel to Thompson's (23) were developed by Sewell (24) using static perturbation techniques in terms of a parameter representing progress along any prospective equilibrium path. Aspects of non-conservative systems were also discussed in Sewell's work.

In the specialized field of frame stability, the post-buckling behaviour of triangulated frames was investigated by Britvec and Chilver (18), and the corresponding behaviour of portal-type frames was investigated by Godley and Chilver (26). These studies lead to the conclusion that the initial elastic buckling of continuous frames is in general unstable. Thus the study of imperfect systems is of practical importance in predicting the behaviour of frames under axial loading.

### 1.5 Non-axial loading problems, bifurcational buckling

For symmetrical frames under symmetrical non-axial loading (Case 2 of Section (1.2)), the possibility of bifurcation was first demonstrated by Chwalla (2) in studying the effects of elastic restraints on the buckling strength of columns in a portal frame. Chwalla derived the governing equations for both symmetrical and antisymmetrical deflected modes by setting up and solving linear differential equations and boundary conditions for each member. The load that satisfied simultaneously these two governing equations represented the critical load at bifurcation. Chilver (7) confirmed Chwalla's finding, by examining a simplified portal frame, that buckling loads corresponding to sway modes are only slightly affected by the presence of primary bending effects, for those types of frames studied. Chilver, however, also showed that for similar frames subjected to symmetrical distortions the maximum loads reduced notably due to primary bending effects.

Horne (15) solved non-axial loading problems by expressing the general deflection  $y$  of an elastic system in terms of generalized co-ordinates  $\zeta$  in the form

$$y = \sum \zeta_i w_i \quad (i = 1, 2, 3, \dots) \quad (1.4)$$

in which  $w_i$  is a normalized eigenfunction deflection and  $\zeta_i$  is a coefficient. Orthogonality relations between slopes and between

curvatures of different critical modes were derived for the eigenfunction system. Differentiated forms of Equ.(1.4) were then substituted into the virtual work equations governing the true loading system.

Horne applied this method to analyse the frame proposed by Chwalla. Solutions were given both for the bifurcation point and the equilibrium path leading to it.

A solution by Horne's approach requires the evaluation of consecutive critical (eigenfunction) load factors and deflection modes for a statically indeterminate frame. An improved approach was proposed by Brown (29,30), who gave rigorous derivations of new non-linear virtual work equations for frames under arbitrary loading. The equations were used to derive the orthogonality relations for axially loaded frames, and to produce results similar to those of Horne for non-axial loading, but with much reduced computational effort.

In their attempt to solve Chwalla's frame, Masur, Chang and Donnell (11) formulated incremental equations from the original unbuckled state of the frame. Basic unknown quantities, which were in incremental form, were selected as independent variables in linear homogeneous equations. The condition that the determinant which was formed by coefficients of such a set of equations should be singular represented a non-trivial, or bifurcational, solution. This method was subsequently applied by Lu (16) in

evaluating buckling loads for portal frames with uniform loads distributed on the cross beam. Experimental and theoretical results were reported to be in fair agreement.

A new approach for solving bifurcational problems of non-axially loaded frames will be proposed in Chapter IV.4 of this thesis; the method can be used with advantage in solving frame problems for which the existing methods are too tedious.

#### 1.6 Non-axial loading problems, large-deflection analysis

Parallel to the small-deflection theory which was employed in the works discussed in Section (1.5) for non-axial loading problem the large-deflection theory presents solutions which can be beyond the range of validity of the former theory. Though there are complete solutions for large-deflections of columns, investigators in the corresponding field for frame structures are few and have directed their analysis to specific structural models.

For example, Williams (21) derived the load-deformation relation for beam-columns, taking into account the effects of finite deflection and flexural shortening. The derivation was fairly general, although certain restrictions were placed on the magnitudes of the shearing forces and the deflected member slopes. The analysis was applied to a symmetrical two-leg frame in a symmetrical mode of buckling. Kerr (22) solved the elastica of a

square frame with loads applied at the mid-points of two opposite sides. For the case of tensile loading numerical values were given and were confirmed by a model test. The symmetrical buckling of a gable frame was solved by Saafan (17), taking into account the effects of finite deflections and flexural shortening of frame members.

Recently Lee, Manuel and Rossow (28) have successfully developed a systematic and general method for analysing large deflections of frames. Frame members, which were assumed to have no initial imperfections, were sub-divided into more members which would end at joints, loading points, or inflection points. Thus recursive equilibrium and compatibility equations could be written for each member and the solution proceeded from the first nodal point, where trial values were initiated, to the last one. Unsatisfied boundary conditions would recommend new trial values and the process went on until it converged.

There are, however, two drawbacks to this approach:

- (1) instability of the systems of equations will occur when a point of inflection of any member falls into the close vicinity of other nodal points.
- (2) it is unsuitable for handling bifurcational problems, since the bifurcation point cannot be directly located by the incremental load method.

Provided that frames are not sensitive to small changes in loads, and that a suitable choice of the initial values could be made, the method described should be able to give a reliable answer, and thus represents a valuable source of reference for other future methods.

Comparisons between solutions based on large-deflection theory and those based on small-deflection theory for non-axial loading problems will be made in Chapter V of this thesis.

### 1.7 General assumptions and limitations

The general assumptions and limitations of the present work are as follows:

- (1) Frames are of portal type. All joints are considered rigid and frame members piecewise prismatic.
- (2) The loading plane and the plane of bending coincide with the plane of the structure.
- (3) The applied loads are static in nature; their relative magnitudes and their positions relative to the frame do not alter during deformation of the frame.
- (4) Deformations are assumed to be within the range of validity of the small-deflection theory. Shear and axial deformations, as well as flexural shortening of members, are neglected.
- (5) Deformations are assumed to occur in the elastic range.

CHAPTER II AXIAL LOADING PROBLEMS (I)THE  $\gamma$  METHOD AND ITS APPLICATIONS2.1 Introduction

The  $\gamma$  method proposed in this chapter is a quick, exact method for evaluating the bifurcation loads of certain types of structures. The common characteristic of these structures is that they should consist of open, but no closed, loops. Two such structures are shown in Fig.(2.1). The method can be extended to be a general one, but its speed, which is its virtue, is only apparent when either there is no joint displacement or, in certain symmetrical cases, the shearing force is zero in the structure; such cases include

- (1) continuous beams (Fig.(2.2a)).
- (2) viaducts or multi-bay bents (Fig.(2.2b)).
- (3) multistorey single-bay frames with equal stanchions under symmetrical loading (Fig.(2.2c)) - since such frames can be divided, across the line of symmetry, into two continuous "open-loop" bents with known support conditions.

One useful feature of the  $\gamma$  method is that it can be readily applied as well to structures with rotational elastic support.

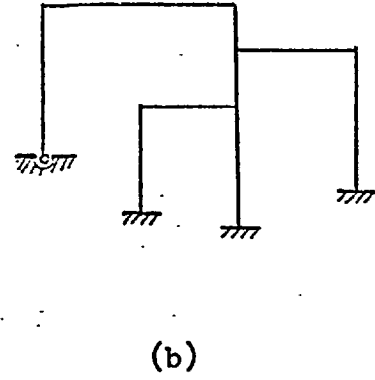
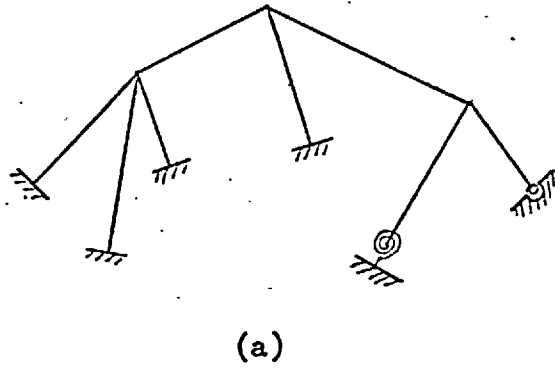


Fig.(2.1)

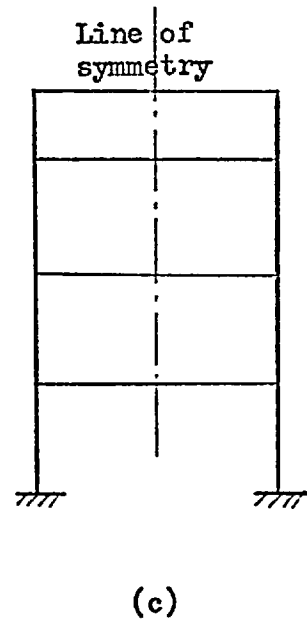
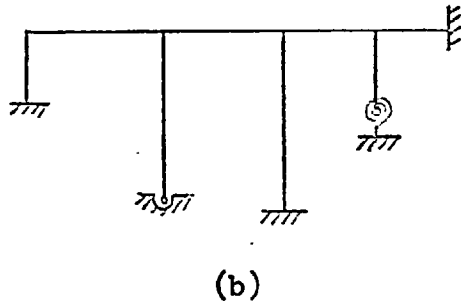
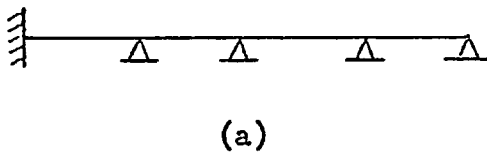


Fig.(2.2)



## 2.2 Theoretical derivation

Consider a typical linear elastic member connecting joints 1 and 2 as shown in Fig.(2.3). All quantities are to be considered positive in the senses shown. Let  $E$  be the modulus of elasticity,  $I$  the second moment of area of the cross section, and  $L$  the length of member; let  $K = EI/L$  and  $\phi = L\sqrt{|P|/EI}$ . Then the "stability functions"  $c$  and  $s$  are given by

$$c = (1 - \phi \cot \phi) / \phi^2 \quad \text{for } P > 0 \quad (2.1)$$

$$= 1/3 \quad \text{for } P = 0$$

$$= (\phi \coth \phi - 1) / \phi^2 \quad \text{for } P < 0$$

$$s = (\phi \csc \phi - 1) / \phi^2 \quad \text{for } P > 0 \quad (2.2)$$

$$= 1/6 \quad \text{for } P = 0$$

$$= (1 - \phi \operatorname{csch} \phi) / \phi^2 \quad \text{for } P < 0.$$

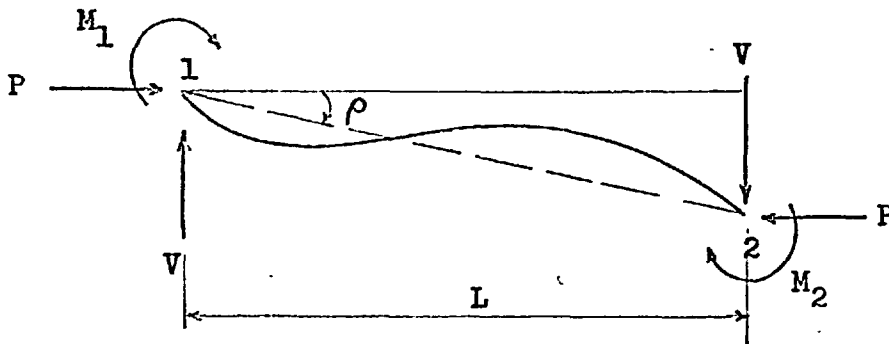


Fig.(2.3)

If the square of the slope is small compared with unity the angular displacements at joints 1 and 2 may be expressed in terms of the bending moments and the angle of rigid body rotation  $\rho$  as follows:

$$\begin{cases} \theta_1 = (c M_1 - s M_2) / K + \rho \\ \theta_2 = (c M_2 - s M_1) / K + \rho \end{cases} \quad (2.3)$$

(see for example Bleich (4), where  $s$  and  $c$  are tabulated for positive  $P$ ).

We will define

$$Y_i = M_i / K \theta_i \quad (i = 1, 2) \quad (2.4)$$

and consider the following two cases:

(1) The case when  $\rho = 0$ .

Equ. (2.3) becomes

$$\begin{cases} K \theta_1 = c K Y_1 \theta_1 - s K Y_2 \theta_2 \\ K \theta_2 = c K Y_2 \theta_2 - s K Y_1 \theta_1 \end{cases}$$

or

$$\begin{cases} (1 - c Y_1) \theta_1 + s Y_2 \theta_2 = 0 \\ s Y_1 \theta_1 + (1 - c Y_2) \theta_2 = 0. \end{cases}$$

Either  $\theta_1 = \theta_2 = 0$ , or

$$(1 - c Y_1) (1 - c Y_2) - s^2 Y_1 Y_2 = 0 \quad (2.5)$$

i.e.,

$$1 - c \gamma_1 = \gamma_2 \left[ c + (s^2 - c^2) \gamma_1 \right].$$

Thus, solving for  $\gamma_2$  :

$$\gamma_2 = \frac{1 - c \gamma_1}{c + d \gamma_1} \quad (2.6)$$

where

$$\begin{aligned} d &= s^2 - c^2 & (2.7) \\ &= \left( 1 - \frac{2}{\phi} \tan \frac{\phi}{2} \right) \frac{1}{\phi^2} & \text{for } P > 0 \\ &= -1/12 & \text{for } P = 0 \\ &= \left( \frac{2}{\phi} \tanh \frac{\phi}{2} - 1 \right) \frac{1}{\phi^2} & \text{for } P < 0. \end{aligned}$$

(2) The case when  $V = 0$ .

Moment equilibrium gives

$$P L \rho + M_1 + M_2 = 0.$$

Equ. (2.3) thus becomes, when  $\rho$  is eliminated,

$$\begin{cases} P L \theta_1 = P L (c M_1 - s M_2) / K - M_1 - M_2 \\ P L \theta_2 = P L (c M_2 - s M_1) / K - M_1 - M_2 \end{cases}$$

or

$$\begin{cases} \left[ \phi^2 + (1 - c \phi^2) \gamma_1 \right] \theta_1 + (1 + s \phi^2) \gamma_2 \theta_2 = 0 \\ (1 - s \phi^2) \gamma_1 \theta_1 + \left[ \phi^2 + (1 - c \phi^2) \gamma_2 \right] \theta_2 = 0. \end{cases}$$

Again, either  $\theta_1 = \theta_2 = 0$ , or

$$\left[ \phi^2 + (1 - c \phi^2) \gamma_1 \right] \left[ \phi^2 + (1 - c \phi^2) \gamma_2 \right] - (1 + s \phi^2)^2 \gamma_1 \gamma_2 = 0. \quad (2.8)$$

Since

$$\phi^2 + (1 - c \phi^2) \gamma_i \equiv \phi^2 + \phi \cot \phi \gamma_i \quad (i = 1, 2)$$

and

$$(1 + s \phi^2)^2 \equiv \phi^2 \csc^2 \phi,$$

Equ. (2.8) becomes

$$\phi^2 \left[ 1 + \frac{1}{\phi \tan \phi} (\gamma_1 + \gamma_2) \right] = \gamma_1 \gamma_2$$

or solving for  $\gamma_2$  :

$$\gamma_2 = \frac{1 - a \gamma_1}{a + b \gamma_1} \quad (2.9)$$

where

$$\begin{aligned} a &= -\frac{1}{\phi \tan \phi} && \text{for } P > 0 \\ &= -\infty && \text{for } P = 0 \\ &= -\frac{1}{\phi \tanh \phi} && \text{for } P < 0 \end{aligned} \quad (2.10)$$

and

$$\begin{aligned} b &= 1/\phi^2 && \text{for } P > 0 \\ &= \infty && \text{for } P = 0 \\ &= -1/\phi^2 && \text{for } P < 0. \end{aligned} \quad (2.11)$$

Values of a, b, c, d, and s for compressive members are listed in Table (2.1) for convenient reference.

Table (2.1)

$\phi$	a	b	c	d	s
0.00	$-\infty$	$\infty$	0.3333	-0.0833	0.1667
0.02	-2499.6667	2500.0001	0.3334	-0.0833	0.1667
0.04	-624.6666	625.0000	0.3334	-0.0833	0.1667
0.06	-277.4444	277.7778	0.3334	-0.0834	0.1667
0.08	-155.9165	156.2500	0.3335	-0.0834	0.1668
0.10	-99.6664	100.0000	0.3336	-0.0834	0.1669
0.12	-69.1108	69.4444	0.3337	-0.0835	0.1669
0.14	-50.6866	51.0204	0.3338	-0.0835	0.1670
0.16	-38.7286	39.0625	0.3339	-0.0835	0.1672
0.18	-30.5301	30.8642	0.3341	-0.0836	0.1673
0.20	-24.6658	25.0000	0.3342	-0.0837	0.1674
0.22	-20.3267	20.6612	0.3344	-0.0837	0.1676
0.24	-17.0265	17.3611	0.3346	-0.0838	0.1678
0.26	-14.4581	14.7929	0.3348	-0.0839	0.1680
0.28	-12.4200	12.7551	0.3351	-0.0840	0.1682
0.30	-10.7758	11.1111	0.3354	-0.0841	0.1684
0.32	-9.4300	9.7656	0.3356	-0.0842	0.1687
0.34	-8.3146	8.6505	0.3359	-0.0843	0.1689
0.36	-7.3798	7.7160	0.3362	-0.0844	0.1692
0.38	-6.5886	6.9252	0.3366	-0.0846	0.1695
0.40	-5.9131	6.2500	0.3369	-0.0847	0.1698
0.42	-5.3316	5.6689	0.3373	-0.0848	0.1702
0.44	-4.8276	5.1653	0.3377	-0.0850	0.1705
0.46	-4.3878	4.7259	0.3381	-0.0851	0.1709
0.48	-4.0017	4.3403	0.3386	-0.0853	0.1713
0.50	-3.6610	4.0000	0.3390	-0.0855	0.1717
0.52	-3.3587	3.6982	0.3395	-0.0856	0.1721
0.54	-3.0894	3.4294	0.3400	-0.0858	0.1725
0.56	-2.8483	3.1888	0.3405	-0.0860	0.1730
0.58	-2.6316	2.9727	0.3411	-0.0862	0.1734
0.60	-2.4362	2.7778	0.3416	-0.0864	0.1739
0.62	-2.2593	2.6015	0.3422	-0.0867	0.1745
0.64	-2.0986	2.4414	0.3428	-0.0869	0.1750
0.66	-1.9523	2.2957	0.3434	-0.0871	0.1755
0.68	-1.8185	2.1626	0.3441	-0.0874	0.1761
0.70	-1.6961	2.0408	0.3448	-0.0876	0.1767
0.72	-1.5836	1.9290	0.3455	-0.0879	0.1773
0.74	-1.4800	1.8262	0.3462	-0.0882	0.1780
0.76	-1.3844	1.7313	0.3469	-0.0884	0.1786
0.78	-1.2960	1.6437	0.3477	-0.0887	0.1793
0.80	-1.2140	1.5625	0.3485	-0.0890	0.1800
0.82	-1.1379	1.4872	0.3493	-0.0893	0.1807
0.84	-1.0671	1.4172	0.3501	-0.0897	0.1815
0.86	-1.0011	1.3521	0.3510	-0.0900	0.1823
0.88	-0.9394	1.2913	0.3519	-0.0903	0.1831
0.90	-0.8817	1.2346	0.3528	-0.0907	0.1839
0.92	-0.8277	1.1815	0.3538	-0.0910	0.1847
0.94	-0.7770	1.1317	0.3548	-0.0914	0.1856
0.96	-0.7293	1.0851	0.3558	-0.0918	0.1865
0.98	-0.6844	1.0412	0.3568	-0.0922	0.1874
1.00	-0.6421	1.0000	0.3579	-0.0926	0.1884

Table (2.1) (continued)

$\phi$	a	b	c	d	s
1.02	-0.6022	0.9612	0.3590	-0.0930	0.1894
1.04	-0.5644	0.9246	0.3601	-0.0935	0.1904
1.06	-0.5287	0.8900	0.3613	-0.0939	0.1914
1.08	-0.4948	0.8573	0.3625	-0.0944	0.1925
1.10	-0.4627	0.8264	0.3637	-0.0948	0.1936
1.12	-0.4322	0.7972	0.3650	-0.0953	0.1948
1.14	-0.4031	0.7695	0.3663	-0.0958	0.1959
1.16	-0.3755	0.7432	0.3677	-0.0963	0.1971
1.18	-0.3491	0.7182	0.3690	-0.0968	0.1984
1.20	-0.3240	0.6944	0.3705	-0.0974	0.1997
1.22	-0.2999	0.6719	0.3719	-0.0979	0.2010
1.24	-0.2769	0.6504	0.3734	-0.0985	0.2023
1.26	-0.2549	0.6299	0.3750	-0.0991	0.2037
1.28	-0.2338	0.6104	0.3765	-0.0997	0.2051
1.30	-0.2136	0.5917	0.3782	-0.1003	0.2066
1.32	-0.1941	0.5739	0.3798	-0.1010	0.2081
1.34	-0.1754	0.5569	0.3816	-0.1016	0.2097
1.36	-0.1573	0.5407	0.3833	-0.1023	0.2113
1.38	-0.1400	0.5251	0.3851	-0.1030	0.2129
1.40	-0.1232	0.5102	0.3870	-0.1037	0.2146
1.42	-0.1070	0.4959	0.3889	-0.1044	0.2164
1.44	-0.0914	0.4823	0.3909	-0.1052	0.2182
1.46	-0.0762	0.4691	0.3929	-0.1060	0.2200
1.48	-0.0615	0.4565	0.3950	-0.1068	0.2219
1.50	-0.0473	0.4444	0.3972	-0.1076	0.2239
1.52	-0.0334	0.4328	0.3994	-0.1085	0.2259
1.54	-0.0200	0.4217	0.4017	-0.1093	0.2280
1.56	-0.0069	0.4109	0.4040	-0.1102	0.2301
1.58	0.0058	0.4006	0.4064	-0.1112	0.2324
1.60	0.0183	0.3906	0.4089	-0.1121	0.2346
1.62	0.0304	0.3810	0.4114	-0.1131	0.2370
1.64	0.0423	0.3718	0.4141	-0.1141	0.2394
1.66	0.0539	0.3629	0.4168	-0.1152	0.2419
1.68	0.0653	0.3543	0.4196	-0.1163	0.2445
1.70	0.0764	0.3460	0.4224	-0.1174	0.2472
1.72	0.0874	0.3380	0.4254	-0.1185	0.2499
1.74	0.0982	0.3303	0.4285	-0.1197	0.2527
1.76	0.1088	0.3228	0.4316	-0.1209	0.2557
1.78	0.1193	0.3156	0.4349	-0.1222	0.2587
1.80	0.1296	0.3086	0.4383	-0.1235	0.2618
1.82	0.1398	0.3019	0.4417	-0.1249	0.2651
1.84	0.1499	0.2954	0.4453	-0.1263	0.2684
1.86	0.1600	0.2891	0.4490	-0.1277	0.2719
1.88	0.1699	0.2829	0.4529	-0.1292	0.2755
1.90	0.1798	0.2770	0.4568	-0.1307	0.2792
1.92	0.1896	0.2713	0.4609	-0.1323	0.2830
1.94	0.1995	0.2657	0.4652	-0.1340	0.2870
1.96	0.2092	0.2603	0.4696	-0.1357	0.2911
1.98	0.2190	0.2551	0.4741	-0.1375	0.2954
2.00	0.2288	0.2500	0.4788	-0.1394	0.2999

Table (2.1) (continued)

$\phi$	a	b	c	d	s
2.02	0.2387	0.2451	0.4837	-0.1413	0.3045
2.04	0.2485	0.2403	0.4888	-0.1433	0.3093
2.06	0.2584	0.2356	0.4941	-0.1453	0.3143
2.08	0.2684	0.2311	0.4996	-0.1475	0.3195
2.10	0.2785	0.2268	0.5053	-0.1497	0.3249
2.12	0.2887	0.2225	0.5112	-0.1521	0.3305
2.14	0.2990	0.2184	0.5174	-0.1545	0.3364
2.16	0.3094	0.2143	0.5238	-0.1570	0.3425
2.18	0.3201	0.2104	0.5305	-0.1597	0.3489
2.20	0.3309	0.2066	0.5375	-0.1624	0.3556
2.22	0.3419	0.2029	0.5448	-0.1653	0.3626
2.24	0.3531	0.1993	0.5524	-0.1683	0.3699
2.26	0.3646	0.1958	0.5604	-0.1715	0.3776
2.28	0.3764	0.1924	0.5687	-0.1748	0.3856
2.30	0.3885	0.1890	0.5775	-0.1783	0.3940
2.32	0.4009	0.1858	0.5867	-0.1819	0.4029
2.34	0.4137	0.1826	0.5964	-0.1857	0.4122
2.36	0.4270	0.1795	0.6065	-0.1898	0.4220
2.38	0.4407	0.1765	0.6172	-0.1940	0.4323
2.40	0.4549	0.1736	0.6285	-0.1985	0.4432
2.42	0.4696	0.1708	0.6404	-0.2033	0.4548
2.44	0.4850	0.1680	0.6530	-0.2083	0.4670
2.46	0.5011	0.1652	0.6663	-0.2136	0.4800
2.48	0.5178	0.1626	0.6804	-0.2192	0.4937
2.50	0.5355	0.1600	0.6955	-0.2252	0.5084
2.52	0.5540	0.1575	0.7115	-0.2316	0.5240
2.54	0.5735	0.1550	0.7285	-0.2384	0.5406
2.56	0.5942	0.1526	0.7467	-0.2457	0.5585
2.58	0.6160	0.1502	0.7663	-0.2536	0.5776
2.60	0.6393	0.1479	0.7873	-0.2620	0.5982
2.62	0.6642	0.1457	0.8098	-0.2710	0.6203
2.64	0.6907	0.1435	0.8342	-0.2808	0.6443
2.66	0.7193	0.1413	0.8606	-0.2914	0.6703
2.68	0.7501	0.1392	0.8893	-0.3029	0.6986
2.70	0.7835	0.1372	0.9206	-0.3155	0.7294
2.72	0.8198	0.1352	0.9549	-0.3293	0.7633
2.74	0.8594	0.1332	0.9926	-0.3445	0.8005
2.76	0.9030	0.1313	1.0342	-0.3612	0.8417
2.78	0.9511	0.1294	1.0805	-0.3799	0.8874
2.80	1.0045	0.1276	1.1321	-0.4007	0.9386
2.82	1.0644	0.1257	1.1901	-0.4241	0.9962
2.84	1.1319	0.1240	1.2559	-0.4506	1.0614
2.86	1.2087	0.1223	1.3309	-0.4809	1.1360
2.88	1.2969	0.1206	1.4175	-0.5159	1.2220
2.90	1.3994	0.1189	1.5183	-0.5567	1.3224
2.92	1.5201	0.1173	1.6374	-0.6048	1.4409
2.94	1.6643	0.1157	1.7800	-0.6625	1.5830
2.96	1.8399	0.1141	1.9541	-0.7329	1.7565
2.98	2.0585	0.1126	2.1711	-0.8207	1.9731
3.00	2.3384	0.1111	2.4495	-0.9334	2.2509

Table (2.1) (continued)

$\phi$	a	b	c	d	s
3.02	2.7098	0.1096	2.8194	-1.0832	2.6203
3.04	3.2268	0.1082	3.3350	-1.2920	3.1353
3.06	3.9963	0.1068	4.1031	-1.6032	3.9029
3.08	5.2647	0.1054	5.3701	-2.1166	5.1693
3.10	7.7512	0.1041	7.8553	-3.1237	7.6539
3.12	14.8413	0.1027	14.9440	-5.9965	14.7420
3.14	199.9607	0.1014	200.0622	-81.0219	199.8598
3.16	-17.1899	0.1001	-17.0897	6.9866	-17.2929
3.18	-8.1836	0.0989	-8.0847	3.3371	-8.2885
3.20	-5.3443	0.0977	-5.2466	2.1870	-5.4511
3.22	-3.9527	0.0964	-3.8563	1.6237	-4.0614
3.24	-3.1262	0.0953	-3.0310	1.2894	-3.2367
3.26	-2.5785	0.0941	-2.4844	1.0680	-2.6908
3.28	-2.1887	0.0930	-2.0957	0.9106	-2.3028
3.30	-1.8970	0.0918	-1.8051	0.7930	-2.0128
3.32	-1.6703	0.0907	-1.5796	0.7018	-1.7880
3.34	-1.4892	0.0896	-1.3995	0.6289	-1.6086
3.36	-1.3409	0.0886	-1.2524	0.5695	-1.4622
3.38	-1.2174	0.0875	-1.1298	0.5200	-1.3403
3.40	-1.1127	0.0865	-1.0262	0.4781	-1.2375
3.42	-1.0230	0.0855	-0.9375	0.4423	-1.1494
3.44	-0.9451	0.0845	-0.8606	0.4113	-1.0733
3.46	-0.8768	0.0835	-0.7933	0.3842	-1.0067
3.48	-0.8165	0.0826	-0.7339	0.3604	-0.9481
3.50	-0.7627	0.0816	-0.6811	0.3391	-0.8961
3.52	-0.7146	0.0807	-0.6339	0.3202	-0.8497
3.54	-0.6711	0.0798	-0.5913	0.3031	-0.8079
3.56	-0.6317	0.0789	-0.5528	0.2877	-0.7703
3.58	-0.5958	0.0780	-0.5178	0.2737	-0.7360
3.60	-0.5629	0.0772	-0.4858	0.2609	-0.7049
3.62	-0.5327	0.0763	-0.4564	0.2492	-0.6764
3.64	-0.5048	0.0755	-0.4293	0.2384	-0.6502
3.66	-0.4790	0.0747	-0.4043	0.2285	-0.6261
3.68	-0.4550	0.0738	-0.3811	0.2193	-0.6038
3.70	-0.4326	0.0730	-0.3596	0.2108	-0.5831
3.72	-0.4117	0.0723	-0.3395	0.2028	-0.5640
3.74	-0.3922	0.0715	-0.3207	0.1954	-0.5461
3.76	-0.3738	0.0707	-0.3031	0.1885	-0.5295
3.78	-0.3565	0.0700	-0.2865	0.1820	-0.5139
3.80	-0.3402	0.0693	-0.2709	0.1759	-0.4993
3.82	-0.3248	0.0685	-0.2562	0.1702	-0.4857
3.84	-0.3102	0.0678	-0.2424	0.1648	-0.4728
3.86	-0.2963	0.0671	-0.2292	0.1597	-0.4607
3.88	-0.2832	0.0664	-0.2167	0.1549	-0.4493
3.90	-0.2706	0.0657	-0.2049	0.1504	-0.4386
3.92	-0.2587	0.0651	-0.1936	0.1460	-0.4284
3.94	-0.2473	0.0644	-0.1829	0.1419	-0.4188
3.96	-0.2364	0.0638	-0.1726	0.1380	-0.4097
3.98	-0.2259	0.0631	-0.1628	0.1343	-0.4010
4.00	-0.2159	0.0625	-0.1534	0.1308	-0.3928



Table (2.1) (continued)

$\phi$	a	b	c	d	s
4.02	-0.2063	0.0619	-0.1444	0.1274	-0.3851
4.04	-0.1971	0.0613	-0.1358	0.1242	-0.3777
4.06	-0.1882	0.0607	-0.1275	0.1211	-0.3706
4.08	-0.1796	0.0601	-0.1195	0.1182	-0.3639
4.10	-0.1713	0.0595	-0.1118	0.1153	-0.3576
4.12	-0.1634	0.0589	-0.1044	0.1126	-0.3515
4.14	-0.1556	0.0583	-0.0973	0.1100	-0.3457
4.16	-0.1482	0.0578	-0.0904	0.1075	-0.3402
4.18	-0.1409	0.0572	-0.0837	0.1051	-0.3349
4.20	-0.1339	0.0567	-0.0772	0.1028	-0.3299
4.22	-0.1271	0.0562	-0.0710	0.1006	-0.3251
4.24	-0.1205	0.0556	-0.0649	0.0985	-0.3205
4.26	-0.1141	0.0551	-0.0590	0.0964	-0.3161
4.28	-0.1078	0.0546	-0.0532	0.0945	-0.3119
4.30	-0.1017	0.0541	-0.0477	0.0925	-0.3079
4.32	-0.0958	0.0536	-0.0422	0.0907	-0.3041
4.34	-0.0900	0.0531	-0.0369	0.0889	-0.3005
4.36	-0.0843	0.0526	-0.0317	0.0872	-0.2970
4.38	-0.0788	0.0521	-0.0267	0.0855	-0.2937
4.40	-0.0734	0.0517	-0.0217	0.0839	-0.2905
4.42	-0.0681	0.0512	-0.0169	0.0823	-0.2875
4.44	-0.0629	0.0507	-0.0122	0.0808	-0.2846
4.46	-0.0578	0.0503	-0.0075	0.0794	-0.2818
4.48	-0.0528	0.0498	-0.0030	0.0779	-0.2792
4.50	-0.0479	0.0494	0.0015	0.0766	-0.2767
4.52	-0.0431	0.0489	0.0058	0.0752	-0.2743
4.54	-0.0384	0.0485	0.0102	0.0739	-0.2721
4.56	-0.0337	0.0481	0.0144	0.0727	-0.2700
4.58	-0.0291	0.0477	0.0186	0.0714	-0.2679
4.60	-0.0245	0.0473	0.0227	0.0703	-0.2660
4.62	-0.0201	0.0469	0.0268	0.0691	-0.2642
4.64	-0.0156	0.0464	0.0308	0.0680	-0.2625
4.66	-0.0113	0.0460	0.0348	0.0669	-0.2609
4.68	-0.0069	0.0457	0.0387	0.0658	-0.2594
4.70	-0.0026	0.0453	0.0426	0.0648	-0.2581
4.72	0.0016	0.0449	0.0465	0.0638	-0.2568
4.74	0.0058	0.0445	0.0503	0.0628	-0.2556
4.76	0.0100	0.0441	0.0541	0.0618	-0.2545
4.78	0.0142	0.0438	0.0579	0.0609	-0.2535
4.80	0.0183	0.0434	0.0617	0.0600	-0.2525
4.82	0.0224	0.0430	0.0655	0.0591	-0.2517
4.84	0.0265	0.0427	0.0692	0.0582	-0.2510
4.86	0.0306	0.0423	0.0729	0.0574	-0.2504
4.88	0.0347	0.0420	0.0767	0.0565	-0.2498
4.90	0.0387	0.0416	0.0804	0.0557	-0.2494
4.92	0.0428	0.0413	0.0841	0.0549	-0.2490
4.94	0.0469	0.0410	0.0879	0.0542	-0.2488
4.96	0.0510	0.0406	0.0916	0.0534	-0.2486
4.98	0.0551	0.0403	0.0954	0.0527	-0.2485
5.00	0.0592	0.0400	0.0992	0.0520	-0.2486

Table (2.1) (continued)

$\phi$	a	b	c	d	s
5.02	0.0633	0.0397	0.1030	0.0512	-0.2487
5.04	0.0674	0.0394	0.1068	0.0506	-0.2489
5.06	0.0716	0.0391	0.1107	0.0499	-0.2493
5.08	0.0758	0.0388	0.1146	0.0492	-0.2497
5.10	0.0801	0.0384	0.1185	0.0486	-0.2502
5.12	0.0843	0.0381	0.1225	0.0479	-0.2509
5.14	0.0887	0.0379	0.1265	0.0473	-0.2517
5.16	0.0930	0.0376	0.1306	0.0467	-0.2525
5.18	0.0975	0.0373	0.1348	0.0461	-0.2535
5.20	0.1020	0.0370	0.1390	0.0455	-0.2547
5.22	0.1066	0.0367	0.1433	0.0450	-0.2559
5.24	0.1112	0.0364	0.1476	0.0444	-0.2573
5.26	0.1159	0.0361	0.1521	0.0439	-0.2588
5.28	0.1208	0.0359	0.1566	0.0433	-0.2605
5.30	0.1257	0.0356	0.1613	0.0428	-0.2623
5.32	0.1307	0.0353	0.1660	0.0423	-0.2643
5.34	0.1359	0.0351	0.1709	0.0418	-0.2664
5.36	0.1411	0.0348	0.1759	0.0413	-0.2687
5.38	0.1465	0.0345	0.1811	0.0408	-0.2712
5.40	0.1521	0.0343	0.1864	0.0403	-0.2739
5.42	0.1578	0.0340	0.1919	0.0398	-0.2768
5.44	0.1637	0.0338	0.1975	0.0394	-0.2800
5.46	0.1698	0.0335	0.2034	0.0389	-0.2833
5.48	0.1761	0.0333	0.2094	0.0385	-0.2869
5.50	0.1826	0.0331	0.2157	0.0380	-0.2908
5.52	0.1894	0.0328	0.2222	0.0376	-0.2949
5.54	0.1964	0.0326	0.2290	0.0372	-0.2994
5.56	0.2038	0.0323	0.2361	0.0367	-0.3041
5.58	0.2114	0.0321	0.2435	0.0363	-0.3093
5.60	0.2194	0.0319	0.2513	0.0359	-0.3148
5.62	0.2278	0.0317	0.2594	0.0355	-0.3207
5.64	0.2366	0.0314	0.2680	0.0352	-0.3271
5.66	0.2458	0.0312	0.2770	0.0348	-0.3339
5.68	0.2556	0.0310	0.2866	0.0344	-0.3414
5.70	0.2659	0.0308	0.2967	0.0340	-0.3494
5.72	0.2769	0.0306	0.3075	0.0337	-0.3580
5.74	0.2885	0.0304	0.3189	0.0333	-0.3674
5.76	0.3010	0.0301	0.3311	0.0329	-0.3776
5.78	0.3143	0.0299	0.3442	0.0326	-0.3887
5.80	0.3286	0.0297	0.3583	0.0323	-0.4008
5.82	0.3440	0.0295	0.3736	0.0319	-0.4141
5.84	0.3607	0.0293	0.3901	0.0316	-0.4286
5.86	0.3789	0.0291	0.4080	0.0313	-0.4447
5.88	0.3987	0.0289	0.4276	0.0309	-0.4624
5.90	0.4205	0.0287	0.4492	0.0306	-0.4821
5.92	0.4445	0.0285	0.4730	0.0303	-0.5040
5.94	0.4711	0.0283	0.4995	0.0300	-0.5287
5.96	0.5010	0.0282	0.5291	0.0297	-0.5565
5.98	0.5346	0.0280	0.5625	0.0294	-0.5881
6.00	0.5727	0.0278	0.6005	0.0291	-0.6243

Table (2.1) (continued)

$\phi$	a	b	c	d	s
6.02	0.6165	0.0276	0.6441	0.0288	-0.6661
6.04	0.6673	0.0274	0.6947	0.0285	-0.7150
6.06	0.7271	0.0272	0.7543	0.0282	-0.7728
6.08	0.7983	0.0271	0.8254	0.0280	-0.8421
6.10	0.8849	0.0269	0.9118	0.0277	-0.9268
6.12	0.9924	0.0267	1.0191	0.0274	-1.0325
6.14	1.1297	0.0265	1.1562	0.0271	-1.1679
6.16	1.3112	0.0264	1.3375	0.0269	-1.3475
6.18	1.5626	0.0262	1.5888	0.0266	-1.5971
6.20	1.9345	0.0260	1.9605	0.0264	-1.9672
6.22	2.5411	0.0258	2.5669	0.0261	-2.5720
6.24	3.7086	0.0257	3.7343	0.0259	-3.7377
6.26	6.8887	0.0255	6.9142	0.0256	-6.9160
6.28	49.9901	0.0254	50.0154	0.0254	-50.0157
6.30	-9.4391	0.0252	-9.4139	0.0251	9.4152
6.32	-4.2960	0.0250	-4.2710	0.0249	4.2739
6.34	-2.7732	0.0249	-2.7483	0.0247	2.7528
6.36	-2.0429	0.0247	-2.0182	0.0244	2.0242
6.38	-1.6139	0.0246	-1.5893	0.0242	1.5969
6.40	-1.3315	0.0244	-1.3071	0.0240	1.3162
6.42	-1.1314	0.0243	-1.1071	0.0237	1.1178
6.44	-0.9821	0.0241	-0.9580	0.0235	0.9702
6.46	-0.8663	0.0240	-0.8424	0.0233	0.8561
6.48	-0.7739	0.0238	-0.7501	0.0231	0.7654
6.50	-0.6984	0.0237	-0.6748	0.0229	0.6915
6.52	-0.6355	0.0235	-0.6120	0.0227	0.6302
6.54	-0.5822	0.0234	-0.5589	0.0225	0.5786
6.56	-0.5366	0.0232	-0.5133	0.0223	0.5345
6.58	-0.4969	0.0231	-0.4738	0.0220	0.4965
6.60	-0.4621	0.0230	-0.4392	0.0218	0.4634
6.62	-0.4314	0.0228	-0.4086	0.0216	0.4343
6.64	-0.4040	0.0227	-0.3813	0.0214	0.4085
6.66	-0.3794	0.0225	-0.3569	0.0213	0.3855
6.68	-0.3572	0.0224	-0.3348	0.0211	0.3649
6.70	-0.3371	0.0223	-0.3148	0.0209	0.3464
6.72	-0.3187	0.0221	-0.2966	0.0207	0.3296
6.74	-0.3019	0.0220	-0.2799	0.0205	0.3144
6.76	-0.2864	0.0219	-0.2645	0.0203	0.3004
6.78	-0.2720	0.0218	-0.2503	0.0201	0.2877
6.80	-0.2588	0.0216	-0.2371	0.0199	0.2760
6.82	-0.2464	0.0215	-0.2249	0.0198	0.2652
6.84	-0.2348	0.0214	-0.2135	0.0196	0.2553
6.86	-0.2241	0.0212	-0.2028	0.0194	0.2460
6.88	-0.2139	0.0211	-0.1928	0.0192	0.2375
6.90	-0.2044	0.0210	-0.1834	0.0191	0.2295
6.92	-0.1954	0.0209	-0.1745	0.0189	0.2221
6.94	-0.1869	0.0208	-0.1661	0.0187	0.2152
6.96	-0.1788	0.0206	-0.1582	0.0186	0.2088
6.98	-0.1712	0.0205	-0.1507	0.0184	0.2027
7.00	-0.1639	0.0204	-0.1435	0.0182	0.1970

### 2.3 Procedure of solution

The process for solving axial loading problems by the  $\gamma$  method is as follows:

- (1) Select the  $\phi$  value of a reference member as  $\phi_R$ . Compute the ratio  $\phi_k/\phi_R$  ( $k = 1, 2, \dots$ ) for all members which sustain loads (this ratio is of course independent of load level for the type of loading specified in Section (1.7)).
- (2) Assume a value of  $\phi_R$ . Compute the  $\phi_k$  and the corresponding stability functions a and b, or c and d of each loaded member, according to whether the member falls in category 1 or 2 of Section (2.2).
- (3) Use Equ.(2.6) or Equ.(2.9) to compute the  $\gamma$  value at the inner end of all loaded "end members" (members having one end connected to the support foundation). For members which are not subjected to load, some  $\gamma$  values which appear frequently can be read off directly from Table (2.2) shown in Section (2.4).
- (4) Start with any joint at which all  $\gamma$  values are known except one. Apply the moment equilibrium condition

$$\theta \sum \gamma_K = 0$$

or, since we assume a priori that  $\theta \neq 0$ ,

$$\sum \gamma_K = 0 \quad (2.12)$$

where summation is extended over all members framing into the joint. Thus the one unknown  $\gamma$  value can be evaluated.

- (5) Apply Equ.(2.6) or Equ.(2.9) to compute the  $\gamma$  at the other end of the member treated in step (4).
- (6) Repeat steps (4) and (5) until the last internal joint is reached.
- (7) At the last joint, all  $\gamma$  values will be known, and if the assumption of  $\Theta \neq 0$  is to be maintained the equilibrium equation (2.12) must in general be modified by the inclusion of an externally applied couple  $M_0$  :

$$\Theta \sum \gamma K = M_0 .$$

If positive  $M_0$  is needed to excite a positive  $\Theta$  the structure is stable. On the other hand if negative  $M_0$  is needed to maintain the deformation, the structure is unstable. Thus we have the stability criterion:

$$\begin{array}{rcl} & > & \text{stable equilibrium} \\ \sum \gamma K & = & 0 \quad \text{neutral equilibrium} \quad (2.13) \\ & < & \text{unstable equilibrium} . \end{array}$$

The condition for locating the critical  $\phi_R$  value,  $\phi_R^c$ , is thus

$$\phi_R^c \begin{array}{c} \geq \\ \leq \end{array} \phi_R \quad (2.14)$$

where the equality/inequality sign corresponds to that found in Equ.(2.13).

- (8) After the value of  $\phi_R$  is thus revised once, the subsequent  $\phi_R$  values can, in principle, be estimated by interpolation or extrapolation, based on two previous  $\phi_R$  values and their

corresponding remainders  $\epsilon$  ( $= \sum Y K$  for the last internal joint). Thus

$$\phi_{(n)} = \phi_{(n-1)} + (\phi_{(n-1)} - \phi_{(n-2)}) \frac{\epsilon_{(n-1)}}{\epsilon_{(n-2)} - \epsilon_{(n-1)}} \dots (2.15)$$

where  $\phi_{(n)}$  denotes the  $n$ th estimate of  $\phi_R$ .

However, it should be noted that there exists a possibility of having a  $\phi$  value extrapolated into the range of convergence of a higher order critical mode; one such case is illustrated by  $\phi_{(3)}$  in Fig.(2.4).

This undesirable situation can be avoided by refraining from the use of Equ.(2.15) for extrapolation. Instead, the value of  $\phi_R$  should be increased until the  $\epsilon$  value changes sign;  $\phi'_{(3)}$  in Fig.(2.4) was located by such a process. Subsequent values of  $\phi_R$  can be interpolated by Equ.(2.15).

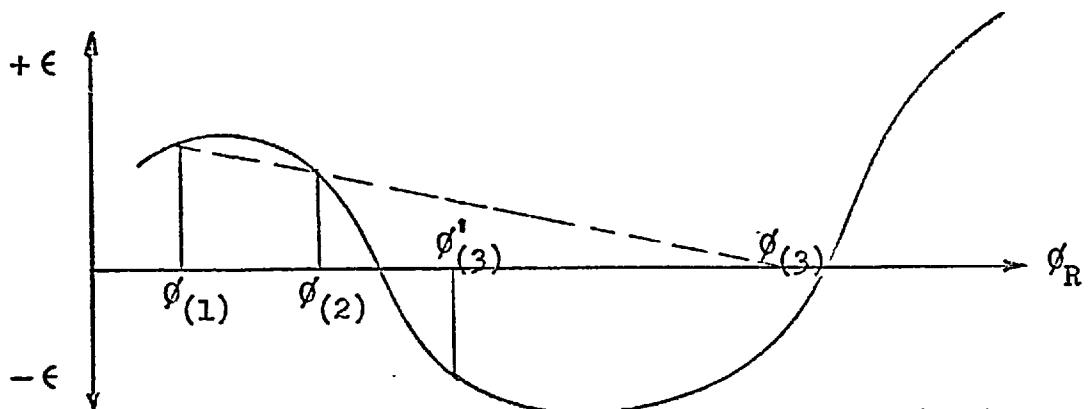


Fig.(2.4)

## 2.4 Illustrative examples

The  $\gamma$  method described in the previous section will be applied to two models. The modulus of elasticity  $E$  in each model is assumed to be the same for all members composing the frame; the quantity  $K (=EI/L)$  shown in the diagrams is a relative value. Computations in the examples are carried out to an accuracy of not more than 3 significant figures.

Some useful  $\gamma$  values which appear frequently are listed in Table (2.2); all these values correspond to zero load and so do not vary in magnitude. In addition, it should be noted that a moment-free end has  $\gamma = 0$  and an encastré end has  $\gamma = -\infty$ .

Table (2.2)

Type	Member	$\theta_1$	$\gamma_1$
1		$M/2K$	2
2		$M/3K$	3
3		$M/4K$	4
4		$M/6K$	6

Example 1 The unsymmetrical continuous bent shown in Fig.(2.5), restrained against side-sway.

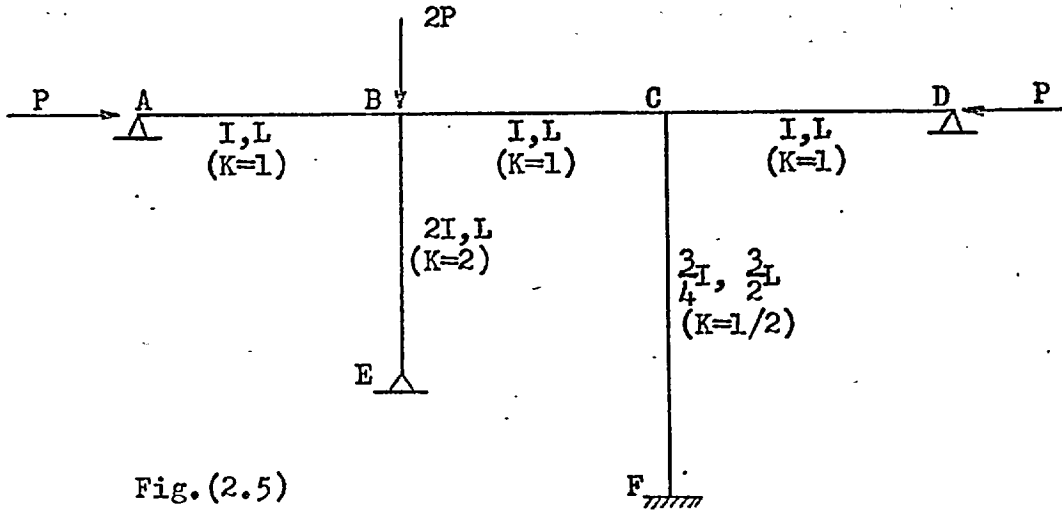


Fig.(2.5)

The process of solution will follow that of Section (2.3) and is shown in the following steps:

- (1) Select  $\phi_R = \phi_{AB}$ , and compute the ratio  $\phi/\phi_R$  for all other members:

$$\phi_{BE}/\phi_R = 1,$$

$$\phi_{BC}/\phi_R = \phi_{CD}/\phi_R = 1, \quad \text{and} \quad \phi_{CF}/\phi_R = 0.$$

- (2) Since  $\phi_{AB} \cong \pi$  (the value corresponding to having both joints A and B pinned), assume  $\phi_R = \pi$  as a convenient start. Thus

$$\phi_{BC} = \phi_{CD} = \phi_{BE} = \phi_R = \pi.$$

Since it is a non-sway problem, stability functions  $c$  and  $d$  will be computed. From Table (2.1) corresponding to  $\phi = \pi$ ,  $c = \pm \infty$  and  $d = \pm \infty$ ; these values of  $c$  and  $d$  are the same for all loaded members since their  $\phi$  values are the same in this example.



(3) The loaded "end members" are AB, BE and CD. Since

$$Y_{AB} = Y_{EB} = Y_{DC} = 0 \quad (\text{hinged end})$$

$$Y_{FC} = -\infty \quad (\text{encastré end}),$$

Equ.(2.6) gives

$$Y_{BA} = (1 - c Y_{AB}) / (c + d Y_{AB}) = 1/c = 0, \quad \text{and}$$

$$Y_{BE} = Y_{CD} = 0.$$

For the unloaded member CF,  $Y_{CF} = 4$ , corresponding to Type 3 of Table (2.2). This value of  $Y_{CF}$  remains unaltered for all computational cycles.

(4) Both joint B and joint C contain only one unknown value of  $Y$  (namely,  $Y_{BC}$  and  $Y_{CB}$  respectively); thus any one of these two joints can be used as the first internal joint. If joint B is selected Equ.(2.12) gives

$$Y_{BA} + 2 Y_{BE} + Y_{BC} = 0$$

which gives  $Y_{BC} = 0$ .

(5)  $Y_{CB}$  in member CB is computed by Equ.(2.6):

$$Y_{CB} = 0.$$

(6) The last internal joint is joint C; therefore we can proceed directly to step (7).

(7) At joint C, Equ.(2.13) gives

$$Y_{CB} + \frac{1}{2} Y_{CF} + Y_{CD} = 0 + \frac{1}{2} (4) + 0 = 2.$$

Thus  $\phi_{(1)} = \eta$  gives  $\epsilon_{(1)} = 2$ , which is  $> 0$ . Therefore  $\phi_R^c > \eta$  according to Equ.(2.14).

The first cycle of computation is thus completed; the computed values of  $\gamma$  and  $\epsilon$  are shown in the first horizontal line of Table (2.3).

The second cycle starts from step (2) as follows:

(2) Assume  $\phi_R = 3.20$ . Thus  $\phi_{BC} = \phi_{CD} = \phi_{BE} = 3.20$  and from Table (2.1)  $c = -5.25$  and  $d = 2.19$ , for all members.

(3) Equ.(2.6) gives  $\gamma_{BA} = \gamma_{BE} = \gamma_{CD} = 1/c = -0.191$ .

(4) At joint B Equ.(2.12) gives  $\gamma_{BC} = 0.573$ .

(5) At member CB Equ.(2.6) gives  $\gamma_{CB} = -1.00$ .

(6) The last joint is joint C.

(7) At joint C, Equ.(2.13) gives

$$\gamma_{CB} + \frac{1}{2} \gamma_{CF} + \gamma_{CD} = +0.809.$$

Thus

$$\phi_{(2)} = 3.20, \quad \epsilon_{(2)} = 0.809 > 0, \quad \text{and} \quad \phi_R^c > 3.20.$$

The second cycle of computation is thus completed; the computed values of  $\gamma$  and  $\epsilon$  are shown in the second horizontal line of Table (2.3). The  $\phi_R$  value for the subsequent cycle may be estimated by Equ.(2.15):

$$\begin{aligned} \phi_{(3)} &= \phi_{(2)} + (\phi_{(2)} - \phi_{(1)}) \epsilon_{(2)} / (\epsilon_{(1)} - \epsilon_{(2)}) \\ &= 3.20 + 0.06 (0.809)/1.19 = 3.24. \end{aligned}$$

A new cycle of computation may thus be started with  $\phi_R = 3.24$ . The  $\phi_R$  value of 3.22 at the 4th cycle is accurate to the second

decimal and is accepted as the final value. The critical value of P is thus computed from member AB:

$$P = ( \phi^2 EI/L^2 )_{AB} = (3.22)^2 EI/L^2 \\ = 1.05 \pi^2 EI/L^2.$$

Table (2.3)

Cycle	$\phi_R$	$\gamma_{BA} =$ $\gamma_{BE} = \gamma_{CD}$	$\gamma_{BC}$	$\gamma_{CB}$	$\epsilon$	Remark
1	$\pi$ (assumed)	0	0	0	+2.00	$\phi_R^c > \phi_R$
2	3.20 (assumed)	-0.191	+0.573	-1.00	+0.81	$\phi_R^c > \phi_R$
3	3.24 (extrapoln.)	-0.330	+0.990	-2.28	-0.61	$\phi_R^c < \phi_R$
4	3.22 (interpoln.)	-0.259	+0.778	-1.54	-0.20	$\phi_R^c \doteq \phi_R$

Example 2 The three-storey symmetrical frame shown in Fig.(2.6a), not prevented from side-sway. The effects of primary bending are to be neglected. Thus loads are assumed to be carried equally by the two columns and axial forces in the beams are ignored; the equivalent loading system is shown in Fig.(2.6b). The Euler load ( $P_E$ ) for column CD is given as 59.2 tons. Reference : McMinn (14), pp.193-196.

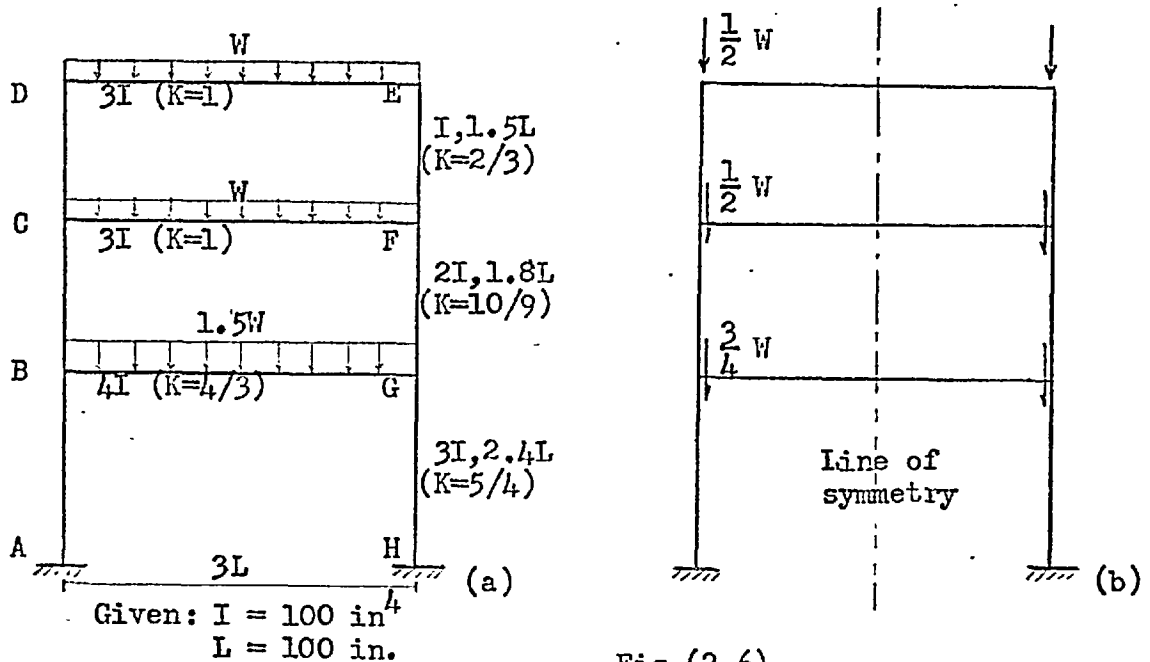


Fig.(2.6)

Sway is possible in this frame, so in the columns  $\rho \neq 0$ . However, symmetry suggests that the two columns will deform similarly and horizontal equilibrium then requires zero horizontal shears, so that Equ.(2.9) is applicable. Only columns at one side of the frame need be analysed; computational steps corresponding to those outlined in Section (2.3) are as follows:

(1) Select  $\phi_R = \phi_{CD}$ . The ratio of  $\phi$  for other members are

$$\frac{\phi_{BC}}{\phi_R} = \sqrt{\frac{W/2EI \cdot 1.8L}{W/2EI \cdot 1.5L}} = 1.20$$

$$\frac{\phi_{AB}}{\phi_R} = \sqrt{\frac{7W/12EI \cdot 2.4L}{W/2EI \cdot 1.5L}} = 1.73$$

and  $\frac{\phi_{DE}}{\phi_R} = \frac{\phi_{CF}}{\phi_R} = \frac{\phi_{BG}}{\phi_R} = 0.$

(2) Since member CD is elastically supported at C and D,  $0 < \phi_R < \pi$  (corresponding to the case of  $V = 0$ , for the first critical mode).

Try  $\phi = \pi/2 = 1.57$  as a start. Thus

$$\phi_{CD} = 1.57, \quad a_{CD} = 0, \quad b_{CD} = 0.406,$$

$$\phi_{BC} = 1.88, \quad a_{BC} = 0.172, \quad b_{BC} = 0.282,$$

and

$$\phi_{AB} = 2.71, \quad a_{AB} = 0.808, \quad b_{AB} = 0.136.$$

(3) The loaded "end member" is AB. Since

$$Y_{AB} = -\infty \quad (\text{encastré end}),$$

Equ.(2.9) gives

$$Y_{BA} = - (a/b)_{AB} = -5.94.$$

For the unloaded members DE, CF, and BG Table (2.2) gives

$$Y_{DE} = Y_{CF} = Y_{BG} = 6. \quad \text{These values of } Y \text{ remain}$$

unaltered for all computational cycles.

(4) Joint D contains one unknown  $Y$  value (namely  $Y_{DC}$ ) while joint C contains two unknowns (namely  $Y_{CD}$  and  $Y_{CB}$ ) and joint B contains

one unknown (namely  $Y_{BC}$ ); thus either joint D or joint B can be assigned as the first internal joint. If joint D is selected Equ.(2.12) gives

$$\frac{2}{3} Y_{DC} + Y_{DE} = 0, \quad \text{or} \quad Y_{DC} = -9.$$

This value of  $Y_{DC}$  is constant for all computational cycles, since it relates only to  $Y_{DE}$  which itself is a constant.

(5) Equ.(2.9) gives  $Y_{CD} = -0.272$ .

(6)  $Y_{CB}$  is evaluated by applying Equ.(2.12) at joint C:

$$\frac{10}{9} Y_{CB} + Y_{CF} + \frac{2}{3} Y_{CD} = 0, \quad \text{or} \quad Y_{CB} = -5.24$$

and  $Y_{BC}$  is equal to  $-1.46$  by Equ.(2.9).

(7) The remaining internal joint is joint B, at which Equ.(2.13) gives

$$\frac{5}{4} Y_{BA} + \frac{4}{3} Y_{BG} + \frac{10}{9} Y_{BC} = -1.05.$$

The first cycle of computation is thus completed with  $\phi_{(1)} = 1.57$  and  $\epsilon_{(1)} = -1.05 < 0$  which indicates, according to Equ.(2.14), that  $\phi_R^C < 1.57$ . The computed values of  $Y$  (except  $Y_{DC}$  which is of constant value of  $-9$ ) and  $\epsilon$  are shown in the first line of Table (2.4). The  $\phi_R$  value of  $1.54$  at the 3rd cycle is accurate to the second decimal and is accepted as the final value.

The critical value of  $W$  is thus computed from member CD:

$$\begin{aligned} W &= 2 (\phi^2 EI/L^2)_{CD} = 2 (\phi^2 P_E/\pi^2)_{CD} \\ &= 2 (1.54/\pi)^2 (59.2) \text{ tons} \\ &= 28.5 \text{ tons.} \end{aligned}$$

The same answer is given by McMinn.

Table (2.4)

Cycle	$\phi_R (= \phi_{CD})$	$\gamma_{CD}$	$\gamma_{CB}$	$\gamma_{BC}$	$\gamma_{BA}$	$\epsilon$	Remark
1	1.57 (assumed)	-0.272	-5.24	-1.46	-5.94	-1.05	$\phi_R^c < \phi_R$
2	1.50 (assumed)	-0.142	-5.31	-1.12	-4.24	+1.46	$\phi_R^c > \phi_R$
3	1.54 (interpoln.)	-0.215	-5.27	-1.30	-5.11	+0.17	$\phi_R^c \doteq \phi_R$

CHAPTER III AXIAL LOADING PROBLEMS (II)

THE STABILITY FUNCTION TRANSFORMATION AND ITS APPLICATION

3.1 The  $\tan \phi$  transformation

For the types of structure discussed in Chapter II it is possible to transform the exact transcendental equations into approximate algebraic equations. The critical load can then be expressed in explicit terms of the properties of members composing the frame. Consequently the relative influence of each member on the critical load can be examined, and this will be of use during the process of design.

The basic idea arises from the observation that if  $P$  is positive the only non-algebraic function in both Equ.(2.5) and Equ.(2.8) is  $\tan \phi$ ; i.e., terms involving  $\sin \phi$  or  $\cos \phi$  in their separate form will not be present. For example, if  $\rho = 0$  the governing equation for a typical member is Equ.(2.5):

$$s^2 \gamma_1 \gamma_2 - (1 - c \gamma_1) (1 - c \gamma_2) = 0$$

or, for  $P > 0$ ,

$$\frac{1}{\phi^4} \left( \frac{\phi}{\sin \phi} - 1 \right)^2 \gamma_1 \gamma_2 - \left[ 1 - \frac{1}{\phi^2} (1 - \phi \cot \phi) \gamma_1 \right] \left[ 1 - \frac{1}{\phi^2} (1 - \phi \cot \phi) \gamma_2 \right] = 0$$

which may be written as



$$1 - \frac{1}{\phi^2} (1 - \phi \cot\phi) Y_1 - Y_2 \left[ \frac{1}{\phi^2} (1 - \phi \cot\phi) + \frac{1}{\phi^2} \left(1 - \frac{2}{\phi} \tan\frac{\phi}{2}\right) Y_1 \right] = 0. \quad (3.1)$$

Similarly if  $V = 0$  the governing equation for a typical member is Equ.(2.8):

$$(1 + s \phi^2)^2 Y_1 Y_2 - \left[ \phi^2 + (1 - c \phi^2) Y_1 \right] \left[ \phi^2 + (1 - c \phi^2) Y_2 \right] = 0$$

or, for  $P > 0$ ,

$$\csc^2\phi Y_1 Y_2 - (\phi + Y_1 \cot\phi) (\phi + Y_2 \cot\phi) = 0.$$

After rearranging this becomes

$$\phi^2 + \phi \cot\phi (Y_1 + Y_2) = Y_1 Y_2. \quad (3.2)$$

The problem of transforming the transcendental equations into algebraic equations is thus reduced to the problem of finding a suitable expansion for  $\tan \phi$ .

The well-known  $\tan \phi$  expression, namely,

$$\tan\phi = \phi + \frac{1}{3} \phi^3 + \frac{2}{15} \phi^5 + \frac{17}{315} \phi^7 + \dots$$

is prohibitive for such a purpose, since a satisfactory algebraic expression thus derived would involve many high order terms of  $\phi$ , and the purpose of pursuing a simple yet accurate approximation would be defeated.

However, it is observed that the function  $\tan \phi$  has the following properties:

$$\begin{aligned} \tan \phi &= 0 && \text{at } \phi = 0, \pm\pi, \pm 2\pi, \pm 3\pi \dots \\ &= \pm\infty && \text{at } \phi = \pm\frac{\pi}{2}, \pm\frac{3}{2}\pi, \pm\frac{5}{2}\pi, \pm\frac{7}{2}\pi \dots \end{aligned}$$

A possible transformation of  $\tan \phi$ , after grouping together proper quadratic terms, would then be

$$\tan \phi = \frac{\phi \left[ 1 - \left(\frac{\phi}{\pi}\right)^2 \right] \left[ 1 - \left(\frac{1}{2\pi} \phi\right)^2 \right] \dots \left[ 1 - \left(\frac{1}{n\pi} \phi\right)^2 \right]}{\left[ 1 - \left(\frac{2}{\pi} \phi\right)^2 \right] \left[ 1 - \left(\frac{2}{3\pi} \phi\right)^2 \right] \dots \left[ 1 - \left(\frac{2}{(2n-1)\pi} \phi\right)^2 \right]} \quad (3.3)$$

This intuitively derived form has all the correct zeros and singularities, and its general validity will be established in the following section.

### 3.2 Proof of the tan $\phi$ transformation

The tan  $\phi$  transformation given by Equ.(3.3) will be exact if

$$\sin \phi = \phi \left[ 1 - \left( \frac{\phi}{\pi} \right)^2 \right] \left[ 1 - \left( \frac{1}{2\pi} \phi \right)^2 \right] \dots \left[ 1 - \left( \frac{1}{n\pi} \phi \right)^2 \right]$$

and

$$\cos \phi = \left[ 1 - \left( \frac{2}{\pi} \phi \right)^2 \right] \left[ 1 - \left( \frac{2}{3\pi} \phi \right)^2 \right] \dots \left[ 1 - \left( \frac{2}{(2n-1)\pi} \phi \right)^2 \right].$$

#### Proof

##### (1) $\sin \phi$

The theorem of infinite products (see for example, Morse and Feshbach, "Methods of Theoretical Physics", Part I, pp.382-385) is

$$f(\phi) = f(0) e^{\frac{f'(0)}{f(0)} \phi} \prod_{n=1}^{\infty} \left[ \left( 1 - \frac{\phi}{a_n} \right) e^{\frac{\phi}{a_n}} \right] \quad (3.4)$$

in which  $f(\phi)$  is a differentiable function of  $\phi$ ,  $f' = df/d\phi$ , and  $a_n$  is a value of  $\phi$  where the function  $f$  has a zero.

We shall consider, instead of  $\sin \phi$ , which gives  $f(0) = 0$ , the function

$$f(\phi) = \frac{\sin \phi}{\phi} .$$

Thus,

$$f(0) = \left( \frac{\sin \phi}{\phi} \right)_{\phi=0} = \left( 1 - \frac{\phi^2}{3!} + \frac{\phi^4}{5!} \right)_{\phi=0} = 1,$$

$$\begin{aligned}\frac{f'(0)}{f(0)} &= (\cot \phi - \frac{1}{\phi})_{\phi=0} \\ &= \left[ \left( \frac{1}{\phi} - \frac{\phi}{3} - \frac{\phi^3}{45} \right) - \frac{1}{\phi} \right]_{\phi=0} = 0\end{aligned}$$

and

$$a_n = \pm n\pi, \quad n = 1, 2, 3, \dots$$

Equ.(3.4) gives

$$\frac{\sin \phi}{\phi} = \prod_{n=1}^{\infty} \left[ \left( 1 - \frac{\phi}{n\pi} \right) e^{\frac{\phi}{n\pi}} \right] \left[ \left( 1 + \frac{\phi}{n\pi} \right) e^{-\frac{\phi}{n\pi}} \right]$$

Hence,

$$\sin \phi = \phi \prod_{n=1}^{\infty} \left[ 1 - \left( \frac{\phi}{n\pi} \right)^2 \right] \quad \text{Q.E.D.}$$

(2)  $\cos \phi$

The function  $f(\phi) = \cos \phi$  has the following properties:

$$f(0) = 1,$$

$$f'(0) = 0$$

and

$$a_n = \pm (2n - 1)\pi/2, \quad n = 1, 2, 3, \dots$$

Equ.(3.4) gives directly

$$\cos \phi = \prod_{n=1}^{\infty} \left\{ \left[ 1 - \frac{2\phi}{(2n-1)\pi} \right] e^{\frac{2\phi}{(2n-1)\pi}} \right\} \left\{ \left[ 1 + \frac{2\phi}{(2n-1)\pi} \right] e^{-\frac{2\phi}{(2n-1)\pi}} \right\}$$

or,

$$\cos \phi = \prod_{n=1}^{\infty} \left\{ 1 - \left[ \frac{2\phi}{(2n-1)\pi} \right]^2 \right\}$$

Q.E.D.

Thus,

$$\tan \phi = \frac{\sin \phi}{\cos \phi} = \frac{\phi \prod_{n=1}^{\infty} \left[ 1 - \left( \frac{\phi}{n\pi} \right)^2 \right]}{\prod_{n=1}^{\infty} \left[ 1 - \left( \frac{2\phi}{(2n-1)\pi} \right)^2 \right]}$$

with an expanded form as in Equ.(3.3).

### 3.3 A simple non-sway case

As an illustration of the transformation process, we shall calculate the critical load of the strut shown in Fig.(3.1). End 2 is attached to a spring with rotational stiffness  $S_2$  but allowing no translation; the end 1 is pinned. For such a strut, Equ.(2.6) or Equ.(3.1) gives

$$\gamma_2 = \frac{1}{c} = \frac{\phi^2}{1 - \phi \cot \phi}. \quad (3.5)$$

As an approximation we shall take

$$\tan \phi = \frac{\phi \left[ 1 - \left( \frac{1}{\eta} \phi \right)^2 \right]}{\left[ 1 - \left( \frac{2}{\eta} \phi \right)^2 \right] \left[ 1 - \left( \frac{2}{3\eta} \phi \right)^2 \right]} \quad (3.6)$$

and denote

$$\alpha = \left( \phi / \eta \right)^2.$$

Equ.(3.5) is thus reduced to

$$\gamma_2 = \frac{\eta^2 (1 - \alpha)}{\frac{31}{9} - \frac{16}{9} \alpha} \doteq \frac{9\eta^2 (1 - \alpha)}{16 (2 - \alpha)}. \quad (3.7)$$

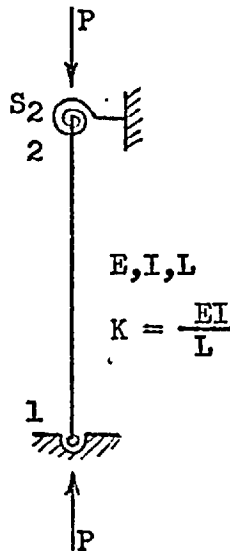
Solving for  $\alpha$  :

$$\alpha = \frac{1 - 2\gamma_2}{1 - \gamma_2} \quad (3.8)$$

in which

$$\gamma_2 = \frac{16}{9\eta^2} \gamma_2$$

Fig.(3.1)



To show the order of error involved in such a transformation, it will be assumed that the spring has a rotational stiffness  $S_2$  of  $2K$ . Then  $\gamma_2 = -S_2/K = -2$ ,  $\nu_2 = -0.36$ , and  $\phi = \pi \sqrt{\alpha} = 3.53$  which compares to the exact critical  $\phi$  value of 3.59. For the limiting case of  $S_2$  being infinite,  $\alpha = 2$ ; then  $\phi = 4.44$  which compares to the exact value of 4.49.

The practical range of  $\phi$  in compression members with one end pinned (Fig.(3.1)) is  $\pi \leq \phi \leq 1.43$ , if only the first critical load is to be considered. In the lower part of this range the approximation given by Equ.(3.6) is good, but for the higher part of the range it is not. Nevertheless the expression for  $\alpha$  thus derived (Equ.(3.8)) is acceptable, as previously demonstrated. The underlying reason for this is best illustrated by plotting the value of  $\gamma_2$  against  $\phi$ , as shown in Fig.(3.2). Curve A, which

represents the exact solution given by Equ.(3.5) for the strut of Fig.(3.1), is plotted alongside curve B which represents the approximate solution given by Equ.(3.7). It is seen that at  $\phi = 4.2$ , for instance, the error in  $\gamma_2$  given by curve B may be more than 50%; but the error in  $\phi$  for a given value of  $\gamma_2$  in this vicinity is less than 3%.

It is also of interest to point out that the rounding off made in deriving Equ.(3.7), namely the simplifying of  $(1.94 - \alpha)$  to  $(2 - \alpha)$ , is actually improving the limiting ( $S_2 = \infty$ )  $\phi$  value from  $\phi = 4.37$  (corresponding to  $\alpha = 1.94$ ) to  $\phi = 4.44$  (corresponding to  $\alpha = 2.00$ ), while the exact value is  $\phi = 4.49$ .

After examining Fig.(3.2), it is obvious that the exact curve can be better fitted. Rewrite Equ.(3.7) in the form

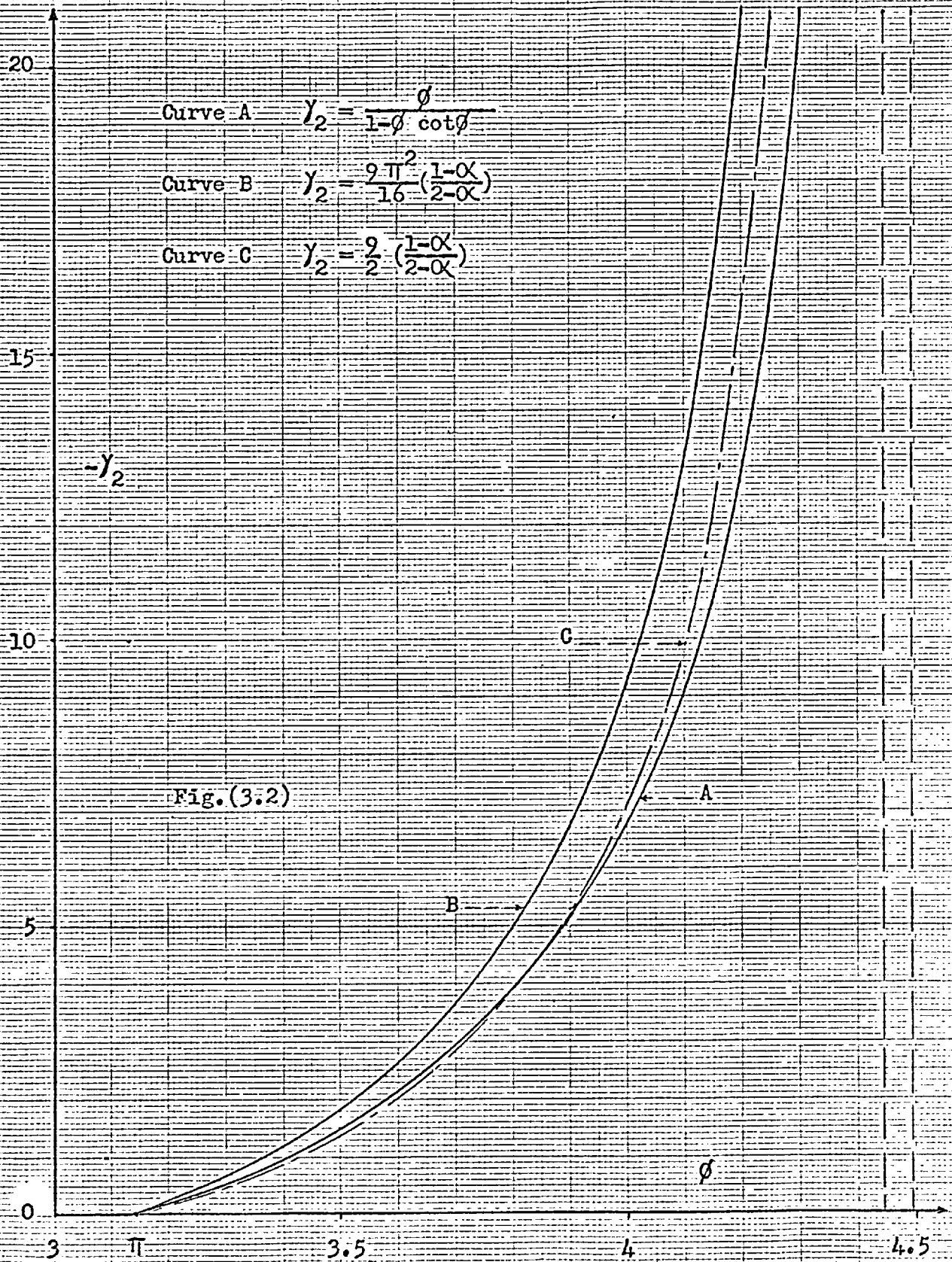
$$\gamma_2 = C_f \frac{(1 - \alpha)}{(2 - \alpha)}$$

and the maximum error can be minimized by a proper choice of the coefficient  $C_f$ . Curve C in Fig.(3.2) represents one such possibility, with

$$C_f = \frac{9}{2}.$$

This particular value of  $C_f$  will be chosen for non-sway problems, since it will be shown to be suitable for the general non-sway case to be discussed in the following section.





### 3.4 The general non-sway case

For the general non-sway case, consider the strut shown in Fig.(3.3). End 1 and end 2 are attached to springs of rotational stiffness  $S_1$  and  $S_2$ , respectively. Both springs allow restrained rotation but no translation. For such a strut the governing equation is given by Equ.(3.1), namely,

$$1 - \frac{1}{\phi^2} (1 - \phi \cot \phi) Y_1 - Y_2 \left[ \frac{1}{\phi^2} (1 - \phi \cot \phi) + \frac{1}{\phi^2} (1 - \frac{2}{\phi} \tan \frac{\phi}{2}) Y_1 \right] = 0 \quad (3.9)$$

in which  $Y_i = -S_i / K$  ( $i = 1, 2$ ).

The practical range of  $\phi$  now extends to  $\phi = 2\pi$  (corresponding to  $S_1 = S_2 = \infty$ ), and a reasonable  $\tan \phi$  approximation for this range requires an additional numerator factor:

$$\tan \phi = \frac{\phi \left[ 1 - \left( \frac{1}{\pi} \phi \right)^2 \right] \left[ 1 - \left( \frac{1}{2\pi} \phi \right)^2 \right]}{\left[ 1 - \left( \frac{2}{\pi} \phi \right)^2 \right] \left[ 1 - \left( \frac{2}{3\pi} \phi \right)^2 \right]} \quad (3.10)$$

It is obvious that substitution of Equ.(3.10) into Equ.(3.9) would lead to a high order polynomial expression for  $\phi$ . Thus the approach of direct substitution is undesirable for the general non-sway case.

A new approach is possible. It has been shown in Section (3.1) how the exact  $\tan \phi$  transformation was formed by merely collecting

terms satisfying the limiting conditions, namely, the zeros and singularities. Possibly therefore, a technique parallel to this might be employed to form an expression for  $\alpha$  in the form

$$\alpha = \alpha_1 \alpha_2 \quad (3.11)$$

in which  $\alpha = (\phi/\pi)^2$  as previously defined, and  $\alpha_1$  and  $\alpha_2$  are functions only of  $Y_1$  and  $Y_2$ , respectively. It is required that the product of  $\alpha_1$  and  $\alpha_2$  should be correct, or nearly so, for all the limiting conditions of the strut; these conditions are listed in Table (3.1).

A possible approximate expression for  $\alpha$ , guided by Equ.(3.8), is thus

$$\alpha = \left( \frac{1 - 2V_1}{1 - V_1} \right) \left( \frac{1 - 2V_2}{1 - V_2} \right) \quad (3.12)$$

in which

$$V_i = \frac{Y_i}{c_f} = \frac{1 - \alpha_i}{2 - \alpha_i} \quad (i = 1,2). \quad (3.13)$$

Table (3.1) shows that Equ.(3.12) satisfies closely all the limiting values of  $\alpha$ . In order to verify that Equ.(3.12) also gives satisfactory approximate solutions under various combinations of the values of  $S_1$  and  $S_2$ , Table (3.2) has been prepared. For comparison the exact solutions are given in Table (3.3). Since

subscripts 1 and 2 are interchangeable, only halves of the tables divided by the diagonal need to be filled in.

It is observed that the approximate solution shown in Table (3.2) involves an error of not more than  $-2\%$  and  $+2\%$  for underestimate and overestimate, respectively, of  $\alpha$ . These errors are deemed acceptable since they are probably less than that of estimating the actual loading in a structure.

Table (3.1)

Limiting Boundary Conditions	Exact $\alpha$	$\alpha$ by Equ.(3.12)
$\gamma_1 = 0$ and $\gamma_2 = 0$	1.00	1.00
$\gamma_1 = 0$ and $\gamma_2 = -\infty$	2.04	2.00
$\gamma_1 = -\infty$ and $\gamma_2 = 0$	2.04	2.00
$\gamma_1 = -\infty$ and $\gamma_2 = -\infty$	4.00	4.00

Fig.(3.3)



The expression of  $\alpha$  given in the form of Equ.(3.12) is particularly useful in visualizing the various effects of  $S_1$  and  $S_2$  on the load carrying capacity of the structure. For example, if the  $\alpha$  value for the frame shown in Fig.(3.4a) is  $\alpha_a$ , then the fixing of the bases of the columns in a similar frame (Fig.(3.4b)) would increase the load factor to  $2\alpha_a$ , as Equ.(3.12) clearly shows. In fact, Table (3.2) has been prepared according to this principle: only the  $\alpha$  values in the first column of the table (corresponding

to  $S_1 = 0$ ) had to be computed; the rest of the table could be formed immediately by taking the products of these values. Thus  $\alpha$  for the case of  $S_1/K = 0.5$  and  $S_2/K = 1.0$  is formed by  $(1.18)(1.10) = 1.30$ ;  $\alpha$  for the case of  $S_1/K = 5.0$  and  $S_2/K = 5.0$  is formed by  $(1.53)^2 = 2.33$ , and so on.

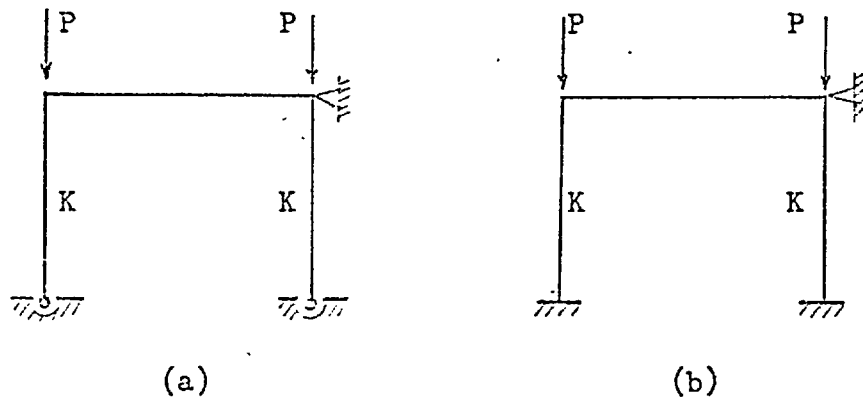


Fig.(3.4)

Table (3.2)

The approximate values of  $\alpha$  given by Equ.(3.12)

$s_2/k$	$s_1/k$					
	0	0.5	1.0	5.0	10.0	$\infty$
0	1.00					
0.5	1.10	1.21				
1.0	1.18	1.30	1.40			
5.0	1.53	1.68	1.80	2.33		
10.0	1.69	1.86	2.00	2.58	2.86	
$\infty$	2.00	2.20	2.36	3.05	3.38	4.00

Table (3.3)

The exact values of  $\alpha$  given by Equ.(3.9)

$s_2/k$	$s_1/k$					
	0	0.5	1.0	5.0	10.0	$\infty$
0	1.00					
0.5	1.10	1.21				
1.0	1.18	1.30	1.38			
5.0	1.54	1.68	1.77	2.31		
10.0	1.73	1.87	1.99	2.55	2.88	
$\infty$	2.04	2.21	2.33	3.00	3.38	4.00

Example The two-storey symmetrical frame shown in Fig.(3.5), prevented from side-sway. Reference: Bleich (4), pp.255-259.

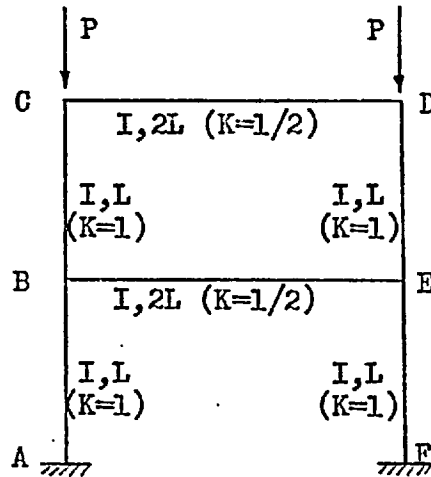


Fig.(3.5)

Since sway is to be prevented the columns will deform symmetrically about the centre line of the frame and consequently only columns at one side of the frame need be analysed. For reference we have  $Y_{CD} = Y_{BE} = 2$  (type 1 of Table (2.2)),  $Y_{AB} = -\infty$ , and  $C_f = 9/2$ .

First we shall consider the ratio of  $\phi$  between columns AB and BC:

$$\frac{\phi_{AB}}{\phi_{BC}} = 1, \quad \text{so that} \quad \frac{\pi \sqrt{\alpha_{AB} \alpha_{BA}}}{\pi \sqrt{\alpha_{BC} \alpha_{CB}}} = 1$$

or,

$$\alpha_{AB} \alpha_{BA} = \alpha_{BC} \alpha_{CB}. \quad (a)$$

Equ.(a) involves four unknowns and thus three auxiliary equations are needed for a solution. These three equations will be obtained at the three joints A, B and C.

At joint A,  $\alpha_{AB}$  is given directly by Equ.(3.12) with  $Y_{AB} = Y_{AB}/C_f = -\infty$ :  $\alpha_{AB} = (1 - 2Y_{AB})/(1 - Y_{AB}) = 2$ . (b)

At joint C Equ.(2.12) gives  $Y_{CB} = -1$ , thus  $V_{CB} = Y_{CB}/C_f = -2/9$   
and Equ.(3.12) gives

$$\alpha_{CB} = (1 - 2V_{CB})/(1 - V_{CB}) = 1.18. \quad (c)$$

Substituting (b) and (c) into (a), we have

$$\alpha_{BC} = 1.69 \alpha_{BA}. \quad (d)$$

The last auxiliary equation will be obtained by applying  
Equ.(2.12) at joint B:

$$Y_{BC} + Y_{BA} + \frac{1}{2} Y_{BE} = 0$$

or, in view of Equ.(3.13),

$$C_f \frac{1 - \alpha_{BC}}{2 - \alpha_{BC}} + C_f \frac{1 - \alpha_{BA}}{2 - \alpha_{BA}} + \frac{1}{2} (2) = 0. \quad (e)$$

Solving (d) and (e) simultaneously we have, after rearranging,

$$\alpha_{BA}^2 - 2.47 \alpha_{BA} + 1.30 = 0$$

which gives

$$\alpha_{BA} = \begin{cases} 0.76 & \text{(first mode)} \\ 1.70. \end{cases}$$

Thus

$$\begin{aligned} P &= (\phi^2 EI/L^2)_{AB} = \pi^2 \alpha_{AB} \alpha_{BA} EI/L^2 \\ &= 1.53 \pi^2 EI/L^2. \end{aligned}$$

The exact value of P given by Bleich is  $1.55 \pi^2 EI/L^2$ .



### 3.5 A simple no shear case

The stability function transforming process for the no shear cases is parallel to that for the non-sway cases discussed in the previous two sections. As an introduction, let us consider the strut shown in Fig.(3.6). End 2 of the strut is attached to a spring of rotational stiffness  $S_2$ ; the spring allows both restrained rotation and free lateral translation; the end 1 is encastré. For such a strut, Equ.(2.9) or Equ.(3.2) gives

$$\gamma_2 = -\frac{a}{b} = \frac{\phi}{\tan\phi}. \quad (3.14)$$

The range of  $\phi$  in compression members is now  $\pi/2 \leq \phi \leq \pi$  if only the lowest critical load is sought. A possible approximation for  $\tan \phi$  is thus

$$\tan \phi = \frac{\phi \left[ 1 - \left( \frac{1}{\pi} \phi \right)^2 \right]}{\left[ 1 - \left( \frac{2}{\pi} \phi \right)^2 \right]}.$$

Denote, as in non-sway cases,

$$\alpha = \left( \phi/\pi \right)^2$$

Equ.(3.14) is thus reduced to

$$\gamma_2 = \frac{(1 - 4\alpha)}{(1 - \alpha)}. \quad (3.15)$$

Solving for  $\alpha$  :

$$\alpha = \frac{1 - \sqrt{2}}{4 - \sqrt{2}} \quad (3.16)$$

in which

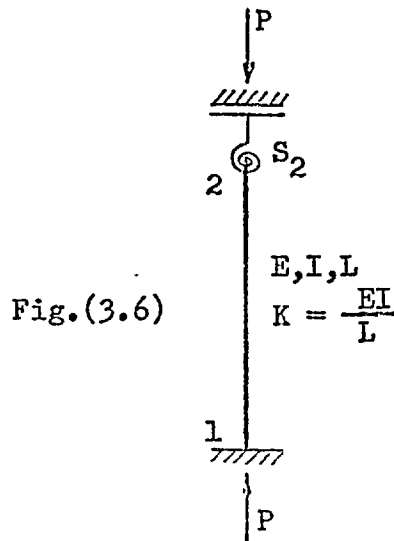
$$\sqrt{2} = \gamma_2$$

To show the order of error involved in such a transformation, it will again be assumed that the spring has a rotational stiffness  $S_2$  of  $2K$ . Then  $\nu_2 = \gamma_2 = -S_2/K = -2$ ,  $\alpha = 0.50$ , and  $\phi = \pi \sqrt{\alpha} = 2.22$  which compares to the exact  $\phi$  value of 2.29. For the limiting case of  $S_2$  being infinite,  $\alpha = 1$  from Equ.(3.16). Then  $\phi = \pi$ , which is the exact value. Curve A in Fig.(3.7) represents the exact solution given by Equ.(3.14), while curve B represents the approximate solution given by Equ.(3.15). Again it is seen that the exact curve can be better approximated. Put Equ.(3.15) in the form

$$\gamma_2 = C_s \frac{(1 - 4\alpha)}{(1 - \alpha)}$$

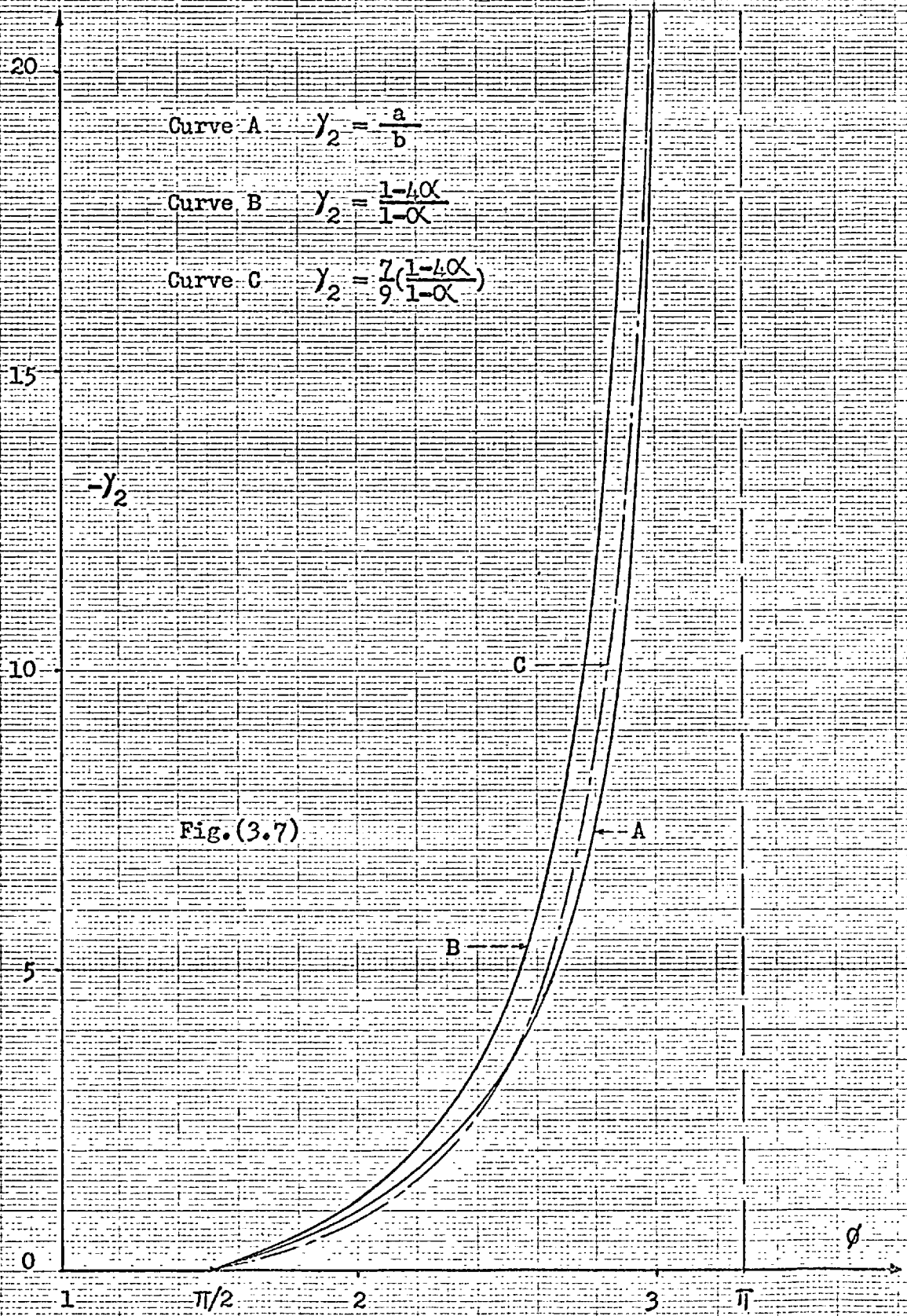
and the maximum error can be minimized by a proper choice of the coefficient  $C_s$ ; curve C in Fig.(3.7) represents one such possibility, with

$$C_s = \frac{7}{9}.$$



This particular value of  $C_s$  will be chosen for sway problems, since it will be shown to be suitable for the general sway cases to be discussed in the following section.

On the other hand curve C, though reducing the absolute value of the maximum error in  $\phi$ , may slightly overestimate  $\phi$  at some values of  $\gamma_2$ , in contrast to curve B which always gives a lower-bound solution. However, since the error involved is so small the overestimate is deemed acceptable.



### 3.6 The general no shear case

For the general no shear case we shall consider the strut shown in Fig.(3.8). End 1 and end 2 are attached to springs with rotational stiffness  $S_1$  and  $S_2$ , respectively. Both springs allow restrained rotation, and one of them allows free lateral translation compelling zero shear. For such a strut the governing equation is given by Equ.(3.2), namely,

$$\phi^2 + \phi \cot\phi (Y_1 + Y_2) = Y_1 Y_2 \quad (3.17)$$

in which  $Y_i = -S_i/K$  ( $i = 1,2$ ).

The  $\tan \phi$  approximation, which will be required from  $\phi = 0$  (corresponding to  $S_1 = S_2 = 0$ ) up to the limiting case of  $\phi = \pi$  (corresponding to  $S_1 = S_2 = \infty$ ), is given by

$$\tan \phi = \frac{\phi \left[ 1 - \left( \frac{1}{\pi} \phi \right)^2 \right]}{\left[ 1 - \left( \frac{2}{\pi} \phi \right)^2 \right]} \quad (3.18)$$

The substitution of Equ.(3.18) into Equ.(3.17) leads to

$$Y_2 = - \frac{\alpha \pi^2 (1 - \alpha) + (1 - 4\alpha) Y_1}{(1 - 4\alpha) - (1 - \alpha) Y_1} \quad (3.19)$$

which is the transformed Equ.(2.9). Thus  $\alpha$  can be solved in a quadratic form by Equ.(3.19), or the  $Y$  method described in Chapter II may be employed, with Equ.(3.19) replacing Equ.(2.9).

Following closely the argument of Section (3.4), it is possible to approximate the solution of  $\alpha$  in the form

$$\alpha = \alpha_1 \alpha_2 \quad (3.20)$$

in which  $\alpha = (\phi/\pi)^2$  and  $\alpha_1$  and  $\alpha_2$  are functions only of  $\gamma_1$  and  $\gamma_2$  respectively. It is required, as before, that the product  $\alpha_1 \alpha_2$  should be satisfactory for all the limiting condition of the strut; these conditions are listed in Table (3.4).

A possible approximate expression for  $\alpha$ , guided by Equ.(3.16), is thus

$$\alpha = \left( \frac{1 - \nu_1}{4 - \nu_1} \right) \left( \frac{1 - \nu_2}{4 - \nu_2} \right) \quad (3.21)$$

in which

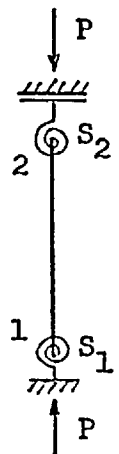
$$\nu_i = \frac{\gamma_i}{C_s} = \frac{1 - 4\alpha_i}{1 - \alpha_i} \quad (i = 1, 2). \quad (3.22)$$

Table (3.4) shows that Equ.(3.21) satisfies all the limiting conditions except the case of  $\gamma_1 = \gamma_2 = 0$ .

Table (3.4)

Limiting Boundary Conditions	Exact $\alpha$	$\alpha$ by Equ.(3.21)
$\gamma_1 = 0$ and $\gamma_2 = 0$	0	1/16
$\gamma_1 = 0$ and $\gamma_2 = -\infty$	1/4	1/4
$\gamma_1 = -\infty$ and $\gamma_2 = 0$	1/4	1/4
$\gamma_1 = -\infty$ and $\gamma_2 = -\infty$	1	1

Fig.(3.8)



In order to verify that Equ.(3.21) also gives satisfactory approximate solutions at most combined values of  $S_1$  and  $S_2$ , Table (3.5) has been prepared. For comparison the exact solutions are given in Table (3.6). Since subscripts 1 and 2 are interchangeable only halves of the tables divided by the diagonal need to be filled in.

It is to be noted that due to the violation of the limiting condition at  $\gamma_1 = \gamma_2 = 0$  Equ.(3.21) should not be applied to structures in which columns are connected to very flexible members. For most well-proportioned structures, however, the possibility of encountering this situation is remote. Whenever in doubt, Equ. (3.19) instead of Equ.(3.21) should be used to evaluate  $\alpha$ .

It is observed in Table (3.5) that the approximate solutions, except those values shown in brackets which are outside the applicability of Equ.(3.21), involve an error of not more than -4% and +5% for underestimate and overestimate of  $\alpha$ , respectively.

Table (3.5) was prepared in this manner: first the values in the last row of the table (corresponding to  $S_2 = \infty$ ) were computed; then the rest of the table could be formed immediately by taking the products of these values. Thus  $\alpha$  for the case of  $S_1/K = 1.0$  and  $S_2/K = 5.0$  was formed by  $(0.43)(0.71) = 0.31$ ;  $\alpha$  for the case of  $S_1/K = 5.0$  and  $S_2/K = 5.0$  was formed by  $(0.71)^2 = 0.51$  and so on.

Table (3.5)

The approximate values of  $\alpha$  given by Equ.(3.21)

$s_2/k$	$s_1/k$				
	0	1.0	5.0	10.0	$\infty$
0	(0.06)				
1.0	(0.11)	(0.19)			
5.0	0.18	0.31	0.51		
10.0	0.21	0.36	0.59	0.68	
$\infty$	0.25	0.43	0.71	0.82	1.00

Table (3.6)

The exact values of  $\alpha$  given by Equ.(3.17)

$s_2/k$	$s_1/k$				
	0	1.0	5.0	10.0	$\infty$
0	0				
1.0	0.08	0.17			
5.0	0.17	0.31	0.53		
10.0	0.21	0.36	0.61	0.70	
$\infty$	0.25	0.42	0.72	0.83	1.00



Example

The two-storey symmetrical frame shown in Fig.(3.9), not prevented from side-sway. Reference: Livesley and Chandler (8), pp.10-12, or Gregory (27), pp.340-342.

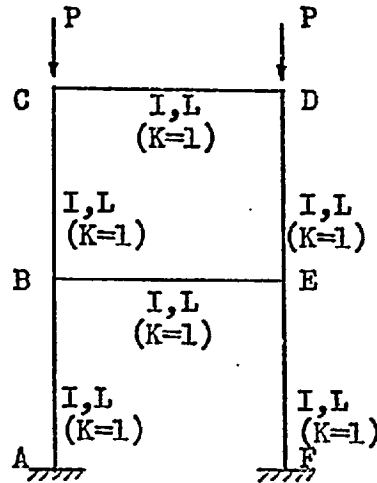


Fig.(3.9)

This is a no shear problem since symmetry suggests that the two columns will deform similarly and horizontal equilibrium then requires zero horizontal shear. Again, only columns at one side of the frame need be analysed. For reference we have  $\gamma_{CD} = \gamma_{BE} = 6$  (type 4 of Table (2.2)),  $\gamma_{AB} = -\infty$  and  $C_s = 7/9$ .

First we shall take the ratio of  $\phi$  between columns AB and BC:

$$\frac{\phi_{AB}}{\phi_{BC}} = 1, \quad \text{so that} \quad \frac{\pi \sqrt{\alpha_{AB} \alpha_{BA}}}{\pi \sqrt{\alpha_{BC} \alpha_{CB}}} = 1$$

or,

$$\alpha_{AB} \alpha_{BA} = \alpha_{BC} \alpha_{CB}. \quad (a)$$

Equ.(a) involves four unknowns and thus three auxiliary equations are needed for a solution. These three equations will be obtained at the three joints A, B and C.

At joint A,  $\alpha_{AB}$  is given directly by Equ.(3.21) with  $\gamma_{AB} = \gamma_{AB}/C_s = -\infty$ :

$$\alpha_{AB} = (1 - \nu_{AB}) / (4 - \nu_{AB}) = 1. \quad (b)$$

At joint C Equ.(2.12) gives  $\gamma_{CB} = -6$ , thus  $\nu_{CB} = \gamma_{CB}/C_s = -54/7$  and Equ.(3.21) gives

$$\alpha_{CB} = (1 - \nu_{CB}) / (4 - \nu_{CB}) = 0.74. \quad (c)$$

Substituting (b) and (c) into (a), we have

$$\alpha_{BC} = 1.34 \alpha_{BA}. \quad (d)$$

The last auxiliary equation is given by applying Equ.(2.12) at joint B:

$$\gamma_{BC} + \gamma_{BA} + \gamma_{BE} = 0$$

or, in view of Equ.(3.22),

$$C_s \frac{1 - 4 \alpha_{BC}}{1 - \alpha_{BC}} + C_s \frac{1 - 4 \alpha_{BA}}{1 - \alpha_{BA}} + 6 = 0. \quad (e)$$

Solving (d) and (e) simultaneously we have, after rearranging,

$$\alpha_{BA}^2 - 1.41 \alpha_{BA} + 0.46 = 0$$

which gives

$$\alpha_{BA} = \begin{cases} 0.51 & \text{(first mode)} \\ 0.90. \end{cases}$$

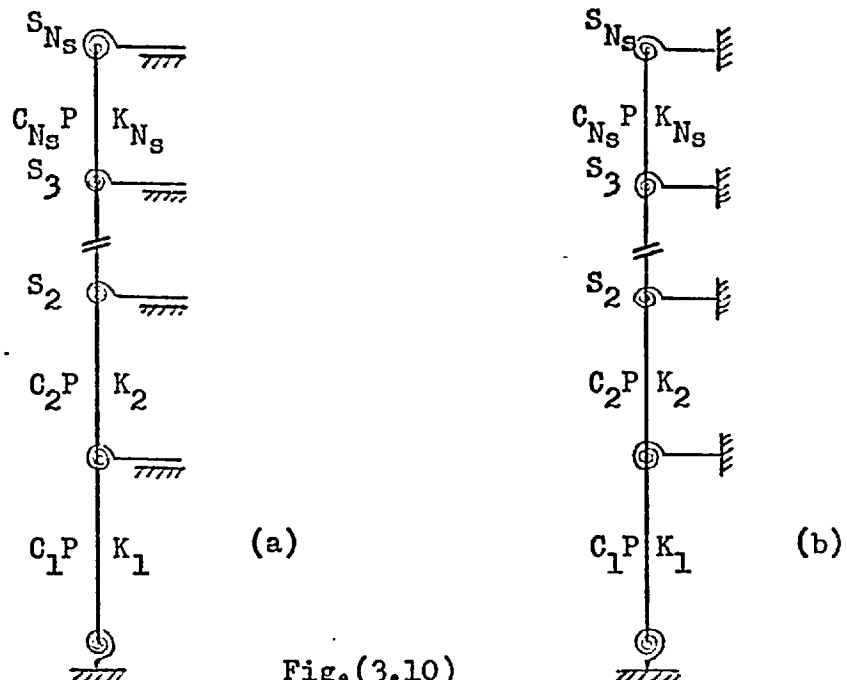
Thus

$$\begin{aligned} P &= (\sigma^2 EI/L^2)_{AB} = \pi^2 \alpha_{AB} \alpha_{BA} EI/L^2 \\ &= 0.51 \pi^2 EI/L^2. \end{aligned}$$

The exact value of P given by Livesley and Chandler, or by Gregory, is  $0.52 \pi^2 EI/L^2$ .

3.7 Multistorey single-bay frames under either no shear or non-sway condition

It was mentioned in Section (3.4) and Section (3.6) that for a multistorey single-bay frame under symmetrical loading condition the rotational stiffnesses of the beams are known, and thus only one stanchion at either side of the frame need be analysed. Fig.(3.10a) and Fig.(3.10b) illustrate stanchions with  $N_s$  storeys in no-shear and non-sway conditions, respectively, with  $S_k$  ( $k = 1 \dots N_s$ ) representing the rotational stiffness of beam at the  $k$ th floor. As in the previous sections external loads acting on the stanchion are proportional and are given in terms of a common load multiplier  $P$ , the critical value of which is to be determined. The corresponding axial force in the  $k$ th column can thus be expressed as  $C_k P$ , with  $C_k$  representing the numerical part of the axial force (Fig.(3.10)).



The critical value of P is given by

$$P = \left( \alpha \frac{\pi^2 EI}{C L^2} \right)_1 = \left( \alpha \frac{\pi^2 EI}{C L^2} \right)_2 = \dots = \left( \alpha \frac{\pi^2 EI}{C L^2} \right)_{N_s}$$

and the problem is solved if any of the  $\alpha$  values is evaluated.

It can be readily shown that the direct evaluation of  $\alpha_k$  for the kth column in a frame of  $N_s$  storeys requires the solution of a polynomial in  $\alpha_k$  of degree  $N_s$ . For the particular case of

$$S_0 = \infty,$$

$$S_1 = S_2 = S_3 = \dots = S_{N_s}$$

and 
$$C_1 = C_2 = C_3 = \dots = C_{N_s},$$

the resulting polynomial for  $\alpha_k$  will be similar to that derived by Merchant (5).

However, this direct approach of solving for  $\alpha_k$  is not advisable when  $N_s$  is large and when the axial forces and/or beam stiffness vary from storey to storey. A modified approach will now be proposed.

We have noted in the previous sections that the value of  $\alpha$  at an end of a column is in general insensitive to the variation of  $\gamma$  at the corresponding end. Consequently one value of  $\gamma$  at each internal joint may be assumed; the  $\gamma$  value at the other side of the joint may be found from Equ.(2.12), namely,

$$\left( \sum \gamma \right)_k = 0 \quad k = 1 \dots N_s. \quad (3.23)$$

After all  $\gamma$  values are thus obtained the corresponding  $\alpha$  value at top and bottom of each column can be computed by Equ.(3.13) or Equ.(3.22), or can be read off directly from Table (3.7) which has been prepared for this purpose.

If we write  $\alpha_t$  and  $\alpha_b$  as the  $\alpha$  values at top and bottom of each column and denote

$$P_k^B = \pi^2 \left( \frac{EI}{CL^2} \right)_k \quad k = 1 \dots N_s \quad (3.24)$$

the corresponding value of P estimated from the kth column is given by

$$P_k = (\alpha_t \alpha_b P_k^B)_k \quad (3.25)$$

and the critical value of P may be conveniently approximated by the arithmetic mean:

$$P = \frac{1}{N_s} \sum_{k=1}^{N_s} P_k \quad (3.26)$$

A satisfactory approximate value of P is reached when the condition

$$P_1 = P_2 = P_3 = \dots = P_{N_s} \quad (3.27)$$

is satisfied (or nearly so); any subsequent cycle of trial-and-error may be guided by the value of P computed by Equ.(3.26) in a previous cycle.

Table (3.7) Value of  $\alpha$  (Equ.(3.13) and Equ.(3.22))

$y$	$\alpha_{(\rho=0)}$	$\alpha_{(v=0)}$	$y$	$\alpha_{(\rho=0)}$	$\alpha_{(v=0)}$
2.0	0.200		-3.0	1.400	0.618
1.9	0.269		-3.1	1.403	0.624
1.8	0.333		-3.2	1.416	0.630
1.7	0.393		-3.3	1.423	0.636
1.6	0.448		-3.4	1.430	0.642
1.5	0.500		-3.5	1.437	0.647
1.4	0.548		-3.6	1.444	0.652
1.3	0.594		-3.7	1.451	0.657
1.2	0.636		-3.8	1.458	0.662
1.1	0.676		-3.9	1.464	0.667
1.0	0.714		-4.0	1.471	0.672
0.9	0.750		-4.1	1.477	0.676
0.8	0.784		-4.2	1.483	0.681
0.7	0.816	0.032	-4.3	1.489	0.685
0.6	0.846	0.071	-4.4	1.494	0.689
0.5	0.875	0.106	-4.5	1.500	0.693
0.4	0.902	0.139	-4.6	1.505	0.697
0.3	0.929	0.170	-4.7	1.511	0.701
0.2	0.953	0.198	-4.8	1.516	0.705
0.1	0.977	0.225	-4.9	1.521	0.709
0.	1.000	0.250	-5.0	1.526	0.712
-0.1	1.022	0.273	-5.1	1.531	0.716
-0.2	1.043	0.295	-5.2	1.536	0.719
-0.3	1.062	0.316	-5.3	1.541	0.723
-0.4	1.082	0.335	-5.4	1.545	0.726
-0.5	1.100	0.354	-5.5	1.550	0.729
-0.6	1.118	0.371	-5.6	1.554	0.732
-0.7	1.135	0.388	-5.7	1.559	0.735
-0.8	1.151	0.403	-5.8	1.563	0.738
-0.9	1.167	0.418	-5.9	1.567	0.741
-1.0	1.182	0.432	-6.0	1.571	0.744
-1.1	1.196	0.446	-7.0	1.609	0.769
-1.2	1.211	0.459	-8.0	1.640	0.790
-1.3	1.224	0.471	-9.0	1.667	0.807
-1.4	1.237	0.483	-10.0	1.690	0.822
-1.5	1.250	0.494	-11.0	1.710	0.835
-1.6	1.262	0.505	-12.0	1.727	0.846
-1.7	1.274	0.515	-13.0	1.743	0.855
-1.8	1.286	0.525	-14.0	1.757	0.864
-1.9	1.297	0.534	-15.0	1.769	0.871
-2.0	1.308	0.543	-16.0	1.780	0.878
-2.1	1.318	0.552	-17.0	1.791	0.884
-2.2	1.328	0.561	-18.0	1.800	0.889
-2.3	1.338	0.569	-19.0	1.809	0.894
-2.4	1.348	0.577	-20.0	1.816	0.899
-2.5	1.357	0.584	-30.0	1.870	0.930
-2.6	1.366	0.591	-40.0	1.899	0.946
-2.7	1.375	0.598	-50.0	1.917	0.956
-2.8	1.384	0.605	-60.0	1.930	0.963
-2.9	1.392	0.612	-70.0	1.940	0.968
			$-\infty$	2.000	1.000

The method described is essentially a trial-and-error one, so a quick solution depends on a reasonable estimate of the  $\gamma$  values. The following procedure may be helpful in initiating the  $\gamma$  values.

We notice that the column having the minimum value of  $P^B$  (given by Equ.(3.24)) is probably the controlling, or critical, column. If we can roughly estimate the  $\alpha$  values at the ends of this critical column the critical load thus computed will not be far from the correct value and thus will give a valuable guide in estimating the  $\gamma$  values for other members.

If column  $c$  is the assigned critical column with columns  $u$  and  $v$  connecting to its top and bottom respectively, a good approximation of  $\alpha_{tc}$ , or  $\alpha_{bc}$ , will be obtained by establishing the relationship between columns  $c$  and  $u$ , or between columns  $c$  and  $v$ , respectively. Thus for estimating  $\alpha_{tc}$  we relate

$$(\alpha_t \alpha_b P^B)_c = (\alpha_t \alpha_b P^B)_u$$

which gives

$$\alpha_{bu} = \alpha_{tc} \frac{\alpha_{bc} P_c^B}{\alpha_{tu} P_u^B} \quad (3.28)$$

and denote

$$A_t = \alpha_{tc} + \alpha_{bu}. \quad (3.29)$$

Substituting Equ.(3.28) into Equ.(3.29) we have

$$\alpha_{tc} = \frac{A_t}{1 + \frac{\alpha_{bc} P_c^B}{\alpha_{tu} P_u^B}}. \quad (3.30)$$

A good approximate value of  $\alpha_{tc}$  will be obtained if we make rough assumptions on the values of  $\gamma$  at the ends of both columns c and u (a convenient way is to assume equal distribution of S values between consecutive columns at every joint) and evaluate the corresponding  $\alpha$  values, then the revised value of  $\alpha_{tc}$  is given by Equ.(3.30).

For estimating  $\alpha_{bc}$  similar derivation between column c and v gives

$$\alpha_{bc} = \frac{A_b}{1 + \frac{\alpha_{tc} P_c^B}{\alpha_{bv} P_v^B}} \quad (3.31)$$

in which

$$A_b = \alpha_{bc} + \alpha_{tv}. \quad (3.32)$$

The process for evaluating  $\alpha_{bc}$  by Equ.(3.31) is parallel to that for evaluating  $\alpha_{tc}$  (by Equ.(3.30)) described above.

After the values of  $\alpha_{tc}$  and  $\alpha_{bc}$  are thus estimated the first approximation of P is given by

$$P = (\alpha_t \alpha_b P^B)_c. \quad (3.33)$$

This critical value of P is to be maintained throughout all other columns and their  $\gamma$  values will be evaluated accordingly. This evaluation of  $\gamma$  will be starting from the highest and lowest columns (since the  $\gamma$  values at one end of these columns are known constants) and proceed thus towards the critical column. A



satisfactory answer is reached when Equ.(3.27) is satisfied approximately. For subsequent computational cycles Equ.(3.26) will be applied to replace Equ.(3.33) and the computation repeated until it converges.

The computational procedure will be summarized as follows:

(1) Compute  $P^B$  according to Equ.(3.24) and denote the column having the minimum  $P^B$  value as the critical column.

(2) Estimate the  $\alpha$  values at top and bottom of the critical column by assuming equal distributions of S values between the critical column and its adjacent columns and determining the corresponding  $\alpha$  values from Table (3.7). The values of  $\alpha_{tc}$  and  $\alpha_{bc}$  are then given by Equ.(3.30) and Equ.(3.31), respectively, and the initial P value is given by Equ.(3.33).

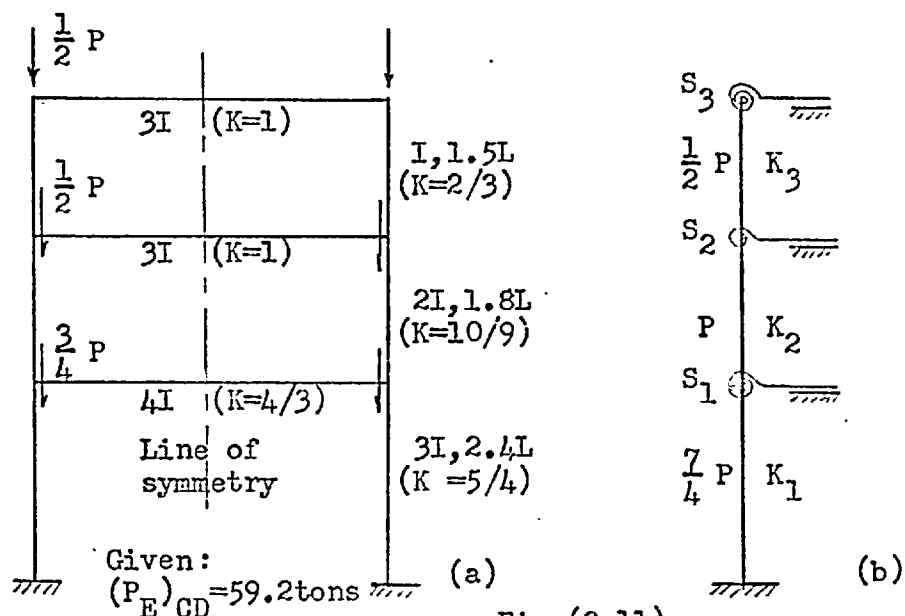
(3) Evaluate the  $\gamma$  values of all other columns in such a way that the P value can be maintained. The process will start systematically from the highest and lowest columns and work towards the critical column. This will result in the revision of the  $\alpha$  values (and, consequently, the P value) of the critical column.

(4) The final solution is reached when Equ.(3.27) is closely satisfied. Until then the value of P for the subsequent computational cycles will be given by Equ.(3.26) and step (3) will be repeated until the convergence is satisfactory.

The process will be illustrated by the following example.

Example

We shall determine the critical load of the symmetrical two-storey frame previously investigated in Section (2.4). The frame, which is permitted to sway, is shown again in Fig.(3.11a) below. Since for this type of side-sway problem  $\gamma = 6$  for all beams (Table (2.2), type 4),  $S_1 = 8.0$  and  $S_2 = S_3 = 6.0$ ; the equivalent column is shown in Fig.(3.11b). The following computational steps correspond to those listed above.



(1) Equ.(3.24) gives

$$P_1^B = (4/7) \pi^2 E (3I) / (2.4L)^2 = 0.30 \pi^2 EI / L^2.$$

Similarly,  $P_2^B = 0.62 \pi^2 EI / L^2$  and  $P_3^B = 0.89 \pi^2 EI / L^2$ ; column 1 is therefore the critical column.

(2) Since  $\gamma_{b1} = -\infty$  Table (3.7) gives  $\alpha_{b1} = 1.0$  and we need only to evaluate  $\alpha_{t1}$ . Assuming

$$S_{t1} = S_{b2} = S_1/2 = 4 \quad \text{and} \quad S_{t2} = S_2/2 = 3,$$

we have

$$Y_{t1} = -4/1.25 = -3.2, \quad Y_{b2} = -3.6, \quad \text{and} \quad Y_{t2} = -2.7.$$

Consequently

$$\alpha_{t1} = 0.63, \quad \alpha_{b2} = 0.65, \quad \text{and} \quad \alpha_{t2} = 0.62$$

and Equ.(3.30) gives

$$\alpha_{t1} = \frac{0.63 + 0.65}{1 + \frac{0.3}{(0.62)(0.62)}} = 0.71.$$

According to Equ.(3.33)

$$P = P_1 = (0.71)(0.30) \pi^2 EI/L^2 = 0.21 \pi^2 EI/L^2.$$

- (3) The evaluation of  $Y$  values will proceed from column 3 to column 1 which is the critical column. Thus we start the first cycle of trial-and-error (Table (3.8)) by letting

$$P_3 = P = 0.21 \pi^2 EI/L^2.$$

Since  $\alpha_{t3} = 0.81$  corresponding to  $Y_{t3} = -9.0$ , we have

$$\alpha_{b3} = P_3 / \alpha_{t3} P_3^B = 0.29$$

and, from Table (3.7)  $Y_{b3} \doteq -0.2$ . Equ.(3.23) gives  $Y_{t2} = -5.3$ , thus  $\alpha_{t2} = 0.72$  from Table (3.7). Similarly we shall let

$$P_2 = P = 0.21 \pi^2 EI/L^2$$

so that  $\alpha_{b2} = P_2 / \alpha_{t2} P_2^B = 0.47$

and, from Table (3.7)  $Y_{b2} \doteq -1.3$ . Equ.(3.23) gives  $Y_{t1} = -5.3$ ;

then  $\alpha_{t1} = 0.72$  from Table (3.7) and  $P_1 = 0.22 \pi^2 EI/L^2$  by Equ.(3.25).

(4) The critical value of P is thus given by Equ.(3.26):

$$P = (1/3) (0.21 + 0.21 + 0.22) \pi^2 EI/L^2 = 0.213 \pi^2 EI/L^2.$$

The solution obtained is deemed accurate enough since Equ.(3.27) is closely satisfied; if another computation cycle is required step (3) will be repeated with  $P = 0.213 \pi^2 EI/L^2$ .

The solution is thus

$$P = 0.213 \pi^2 EI/L^2 = 0.48(P_E)_{CD} = 28.4 \text{ tons,}$$

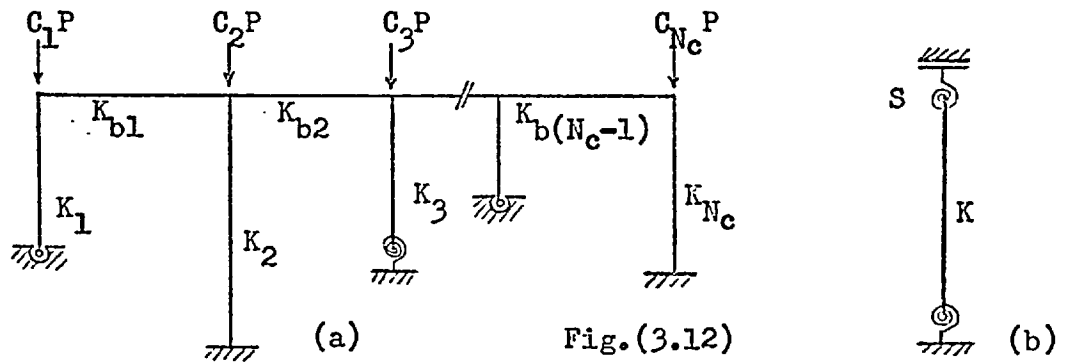
while the exact solution is 28.5 tons.

Table (3.8)

k	Cycle			1		
	S	K	$P_k^B/(\pi^2 EI/L^2)$	$\gamma$	$\alpha$	$P_k/(\pi^2 EI/L^2)$
3	6.0	0.67	0.89	(-9.0)	(0.81)	0.21
				-0.2	0.29	
2	8.0	1.11	0.62	-5.3	0.72	0.21
				-1.3	0.47	
1	8.0	1.25	0.30	-5.3	0.72	0.22
				( $-\infty$ )	(1.00)	

### 3.8 Single-storey multi-bay frames with $V \neq 0$ and $\rho \neq 0$ .

Let us consider the frame consisting of  $N_c$  columns shown in Fig.(3.12a), in which  $C_1, C_2, C_3 \dots$  are numerical constants.



In general any column  $j$  ( $j = 1, 2, \dots, N_c$ ) of the frame has  $V_j \neq 0$  and  $\rho_j \neq 0$ ; thus neither Equ.(3.12) nor Equ.(3.21) is applicable in evaluating the load-carrying capacity of each column. An exact solution would have to equate to zero the sum of the end moments at each joint and apply the condition of shearing force equilibrium at the cross beam:

$$V = \sum_{j=1}^{N_c} V_j = 0. \quad (3.34)$$

This formal approach has been detailed by many previous investigators (for example, Goldberg (12)).

We notice, however, that Equ.(3.34) can be satisfied in the mean if the whole frame is replaced by an equivalent column, as shown in Fig.(3.12b). By doing so individual joints of the frame will not necessarily be accurately in equilibrium but the bending moments

as a whole will satisfy Equ.(3.34). Consequently Equ.(3.21), which was derived under the condition of  $V = 0$ , will be applicable in estimating the average load-carrying capacity of the frame as a whole.

If we denote, as in Section (3.7),  $\alpha_t$  and  $\alpha_b$  as the values of  $\alpha$  at the top and bottom, respectively, of a column subjected to the condition of  $V = 0$  and  $\rho \neq 0$ , then at the  $j$ th column we have

$$C_j P = (\alpha_t \alpha_b \pi^2 EI / L^2)_j \quad j = 1 \dots N_c. \quad (3.35)$$

Since the support condition of every column is specified we shall first determine  $(\alpha_b)_j$  ( $j=1 \dots N_c$ ) by Equ.(3.22), which was derived under the assumption that  $V_j = 0$ , or from Table (3.7). However, the values of  $(\alpha_t)_j$  remain unknown. In order to estimate the average load-carrying capacity of the columns we shall assume that every unknown  $(\alpha_t)_j$  can be approximated by one value  $\alpha_t$ , i.e.,

$$\alpha_t \doteq \alpha_{t1} \doteq \alpha_{t2} \dots \doteq \alpha_{tN_c}. \quad (3.36)$$

Then by summing Equ.(3.35) for all  $j$  the value of  $P$  may be approximated by

$$P = \frac{\alpha_t \sum_{j=1}^{N_c} (\alpha_b \frac{\pi^2 EI}{L^2})_j}{\sum_{j=1}^{N_c} C_j}. \quad (3.37)$$

It should be pointed out that an alternative approximation to  $P$  may be given by

$$P = \frac{\alpha_t \alpha_b \sum_{j=1}^{N_c} \left( \frac{\pi^2 EI}{L^2} \right)_j}{\sum_{j=1}^{N_c} c_j} \quad (3.38)$$

in which

$$\alpha_b = \frac{1}{N_c} \sum_{j=1}^{N_c} \alpha_{bj} \quad (3.39)$$

However, the value of  $P$  thus evaluated would in general be less accurate than that given by Equ.(3.37). The reason is that Equ.(3.37) retains as much of the characteristics of the individual columns as the process permits; this is an advantage for a frame of the type shown in Fig.(3.12a) where the values of  $\alpha_{bj}$  may range from  $1/4$  to  $1$  (corresponding to pinned and encastré ends, respectively), a variation of 400%.

In order to evaluate  $\alpha_t$  we shall form an equivalent column (Fig.(3.12b)) having the property

$$K = \frac{1}{N_c} \sum_{j=1}^{N_c} K_j \quad (3.40)$$

The value of  $S$  at the top of the equivalent column may be estimated as follows: the points of contraflexure of all beams are assumed

to be at their mid-spans; thus if  $(YK)_{b1}$ ,  $(YK)_{b2}$ ,  $(YK)_{b3}$  ..... denote the rotational stiffness of beams to the right of columns 1,2,3....., then

$$\begin{aligned}
 S &\doteq \frac{1}{N_c} \left[ Y_{b1} K_{b1} + (Y_{b1} K_{b1} + Y_{b2} K_{b2}) + \dots \right. \\
 &\quad \left. + Y_{b(N_c-1)} K_{b(N_c-1)} \right] \\
 &= \frac{2}{N_c} \sum_{i=1}^{N_c-1} Y_{bi} K_{bi} . \qquad (3.41)
 \end{aligned}$$

If the beams composing the frame are free from axial forces then

$$Y_{bi} = 6 \qquad i = 1 \dots (N_c - 1), \qquad (3.42)$$

$$S = \frac{12}{N_c} \sum_{i=1}^{N_c-1} K_{bi} \qquad (3.43)$$

and the  $Y$  value at the top of the equivalent column is given by

$$Y_t = -S/K . \qquad (3.44)$$

Thus  $\alpha_t$  can be determined by Equ.(3.22) or from Table (3.7).

It should be noted that the proposed approach is different from the approach of evaluating the critical load directly based on an equivalent column. The reasons are:

- (1) In the proposed method the only purpose of forming an



equivalent column with stiffness  $K$  is for estimating  $\gamma_t$  and, therefore,  $\alpha_t$ . As  $\alpha$  is generally insensitive to the variation of  $\gamma$  it follows that a rather poor approximation of  $K$  will not significantly influence the value of  $\alpha_t$ .

(2) For a general frame (such as that shown in Fig.(3.12a)) in which support conditions of columns may be different (ranging from  $\gamma = 0$  to  $\gamma = -\infty$ ), a direct equivalent column approach is inapplicable since the equivalent support condition for such a column cannot be properly determined. On the other hand the proposed method can handle this type of problem with considerable accuracy since the approach is founded on the principle represented by Equ.(3.21), so that a value of  $\alpha$  can be evaluated by separate consideration of the end conditions of any column; consequently the foundation condition of an equivalent column need not be specified since the determination of  $\alpha_t$  is independent of the foundation conditions.

It is thus seen that the proposed method is more versatile than the equivalent portal method (9), which is mainly applicable to frames composed of columns with equal lengths and uniform support conditions.

In the general case when axial forces at the beams are also present, i.e., if beam  $i$  ( $i = 1, 2, \dots, N_c - 1$ ) is subjected to axial force  $C_{bi}P$  ( $C_{bi}$  being a numerical constant) the corresponding value of  $\gamma_{bi}$  in Equ.(3.41) will have to be modified from the basic

value of 6. The modifying factor is a function of  $\phi_{bi}$ , where

$$\phi_{bi} = \left( \sqrt{\frac{|CP|}{EI}} L \right)_{bi} \quad (3.45)$$

and the modified  $\gamma_{bi}$  is given by

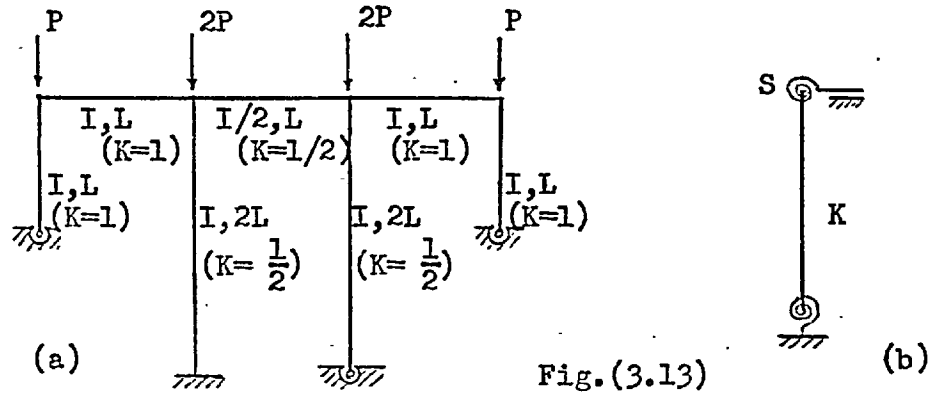
$$\gamma_{bi} = \frac{6}{(3 c_{bi})} \quad (3.46)$$

(see for example Gere (19), p.182) in which  $c_{bi}$  is the stability function, given by Equ.(2.1), of the  $i$ th beam.

In general  $\phi_{bi} \leq 1$ ; then  $0.333 \leq c_{bi} \leq 0.358$  and consequently  $\gamma_{bi}$  seldom differs much from the basic value of 6. A possible approach for solving this type of frame problem would be first to evaluate  $P$  in the frame with the effects of axial forces at the beams neglected (i.e., with all  $\gamma_{bi} = 6$ ); this value of  $P$  would then be used to compute all  $\phi_{bi}$  values given by Equ.(3.45) and the modification to  $\gamma_{bi}$  would be made according to Equ.(3.46). The analysis of the frame would then be repeated, with all previous values of  $\gamma$  at the columns properly modified. In most cases the value of  $P$  thus evaluated would give a good approximate answer.

Example

We shall determine the critical load of the three-bay bent shown in Fig.(3.13a), not prevented from side-sway.



For the equivalent column (Fig.(3.13b)) Equ.(3.40) gives

$$K = \frac{1}{4} \left( 1 + \frac{1}{2} + \frac{1}{2} + 1 \right) = 0.75$$

and Equ.(3.43) gives  $S = (12/4)(2.5) = 7.5$ .

Thus  $\gamma_t = -10.0$  by Equ.(3.44), and  $\alpha_t = 0.822$  from Table (3.7).

The critical load evaluated from the equivalent column is, from Equ.(3.37) with  $\alpha_{b1} = \alpha_{b3} = \alpha_{b4} = 1/4$  and  $\alpha_{b2} = 1$ ,

$$\begin{aligned} P &= \frac{1}{6} \alpha_t \frac{\pi^2 EI}{L^2} \left( \frac{1}{4} + \frac{1}{4} + \frac{1}{16} + \frac{1}{4} \right) = 0.137 \alpha_t \frac{\pi^2 EI}{L^2} \\ &= 0.112 \frac{\pi^2 EI}{L^2}. \end{aligned}$$

The exact solution is  $P = 0.113 \pi^2 EI/L^2$ .

### 3.9 General multistorey multi-bay frames

The method described in Section (3.7) for evaluating the critical load of a multistorey frame and the method described in Section (3.8) for evaluating a multi-bay frame can be combined to estimate the critical load of a multistorey multi-bay frame having  $N_s$  storeys and  $N_c$  columns (Fig.(3.14a)). Columns in each storey are first transformed into an equivalent column (Fig.(3.14b)) according to the procedure described in Section (3.8), and then the vertical distribution of  $\gamma$  can be estimated according to the procedure described in Section (3.7).

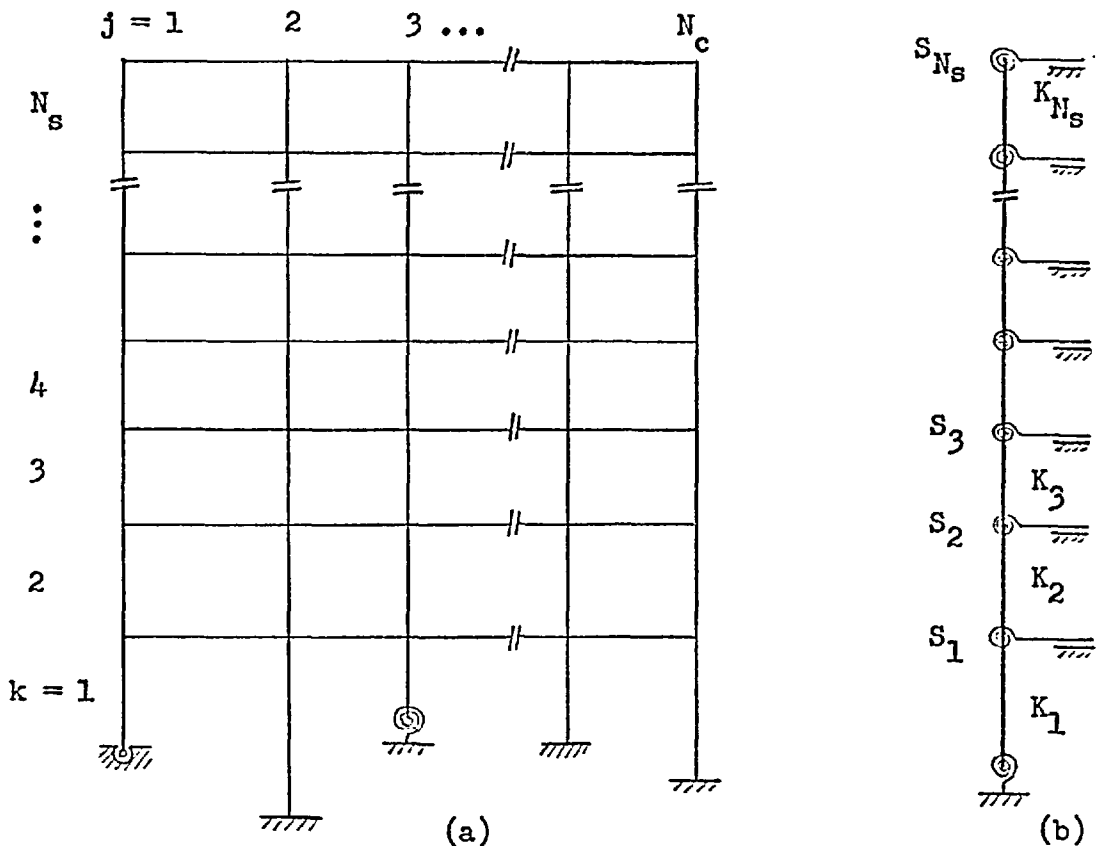


Fig.(3.14)

Thus if we denote (as in Equ.(3.25))  $P_k$  as the value of  $P$  estimated from the equivalent column at storey  $k$  ( $k = 1 \dots N_s$ ) then at the  $k$ th storey Equ.(3.35) reads

$$C_{jk} P_k = (\alpha_t \alpha_b \frac{\pi^2 EI}{L^2})_{jk} \quad j = 1 \dots N_c \quad (3.47)$$

Observing that for any column connecting to the foundation  $\alpha_b$  is known while for any other column neither  $\alpha_t$  nor  $\alpha_b$  is known, we shall assume that at any storey  $k$  every unknown  $(\alpha_t)_{jk}$  and  $(\alpha_b)_{jk}$  can be approximated by constant values  $(\alpha_t)_k$  and  $(\alpha_b)_k$ , respectively. Then by summing Equ.(3.47) for all  $j$  the value of  $P_k$  is given by

$$\left\{ \begin{array}{l} P_1 = \left[ \alpha_t \sum_{j=1}^{N_c} (\alpha_b \frac{\pi^2 EI}{L^2})_j / \sum_{j=1}^{N_c} C_j \right]_1 \\ P_m = \left[ \alpha_t \alpha_b \sum_{j=1}^{N_c} (\frac{\pi^2 EI}{L^2})_j / \sum_{j=1}^{N_c} C_j \right]_m \end{array} \right. \quad (3.48)$$

( $m = 2, 3, \dots, N_s$ ).

In order to evaluate the values of  $(\alpha_t)_k$  and  $(\alpha_b)_k$  we shall form an equivalent column (Fig.(3.14b)) having the property

$$K_k = \frac{1}{N_c} \left( \sum_{j=1}^{N_c} K_j \right)_k \quad k = 1 \dots N_s \quad (3.49)$$

If we denote  $S_k$  as the value of rotational stiffness of an equivalent spring attached to the upper joint of the  $k$ th column then Equ.(3.41) becomes

$$S_k = \frac{2}{N_c} \left( \sum_{i=1}^{N_c-1} \gamma_{bi} K_{bi} \right)_k \quad k = 1 \dots N_s \quad (3.50)$$

The vertical distribution of  $\gamma$  may thus proceed as in Section (3.7).

However, in order to conform with the computational pattern established in Section (3.7) in initiating the value of  $P$ , we shall denote

$$\left\{ \begin{array}{l} P_1^B = \left[ \sum_{j=1}^{N_c} \left( \alpha_b \frac{\pi^2 EI}{L^2} \right)_j / \sum_{j=1}^{N_c} C_j \right]_1 \left( \frac{1}{\alpha_{b1}} \right) \\ P_m^B = \left[ \sum_{j=1}^{N_c} \left( \frac{\pi^2 EI}{L^2} \right)_j / \sum_{j=1}^{N_c} C_j \right]_m \quad (m = 2, 3, \dots, N_s) \end{array} \right. \quad (3.51)$$

so that Equ.(3.48) may be rewritten in a single form, similar to Equ.(3.25), as

$$P_k = \left( \alpha_t \alpha_b P^B \right)_k \quad k = 1 \dots N_s \quad (3.52)$$

It is observed that the actual value of  $\alpha_{b1}$  is immaterial since  $\alpha_{b1}$  will be cancelled out in computing  $P_1$  by Equ.(3.52); we may

thus employ Equ.(3.39), namely,

$$\alpha_{b1} = \frac{1}{N_c} \left( \sum_{j=1}^{N_c} \alpha_{bj} \right)_1 \quad (3.53)$$

for the purpose of estimating  $P_1^B$ .

The process of transforming a multi-bay frame into an equivalent column is thus as follows:

(1) Compute the K value of the equivalent column at each storey by Equ.(3.49) and the equivalent spring stiffness at each floor level by Equ.(3.50).

(2) Compute  $P^B$  values according to Equ.(3.51) and denote the column having the minimum  $P^B$  value as the critical column.

After that the computational procedure follows exactly steps (2) to (4) listed in Section (3.7).

The complete process will be best illustrated by the following example.

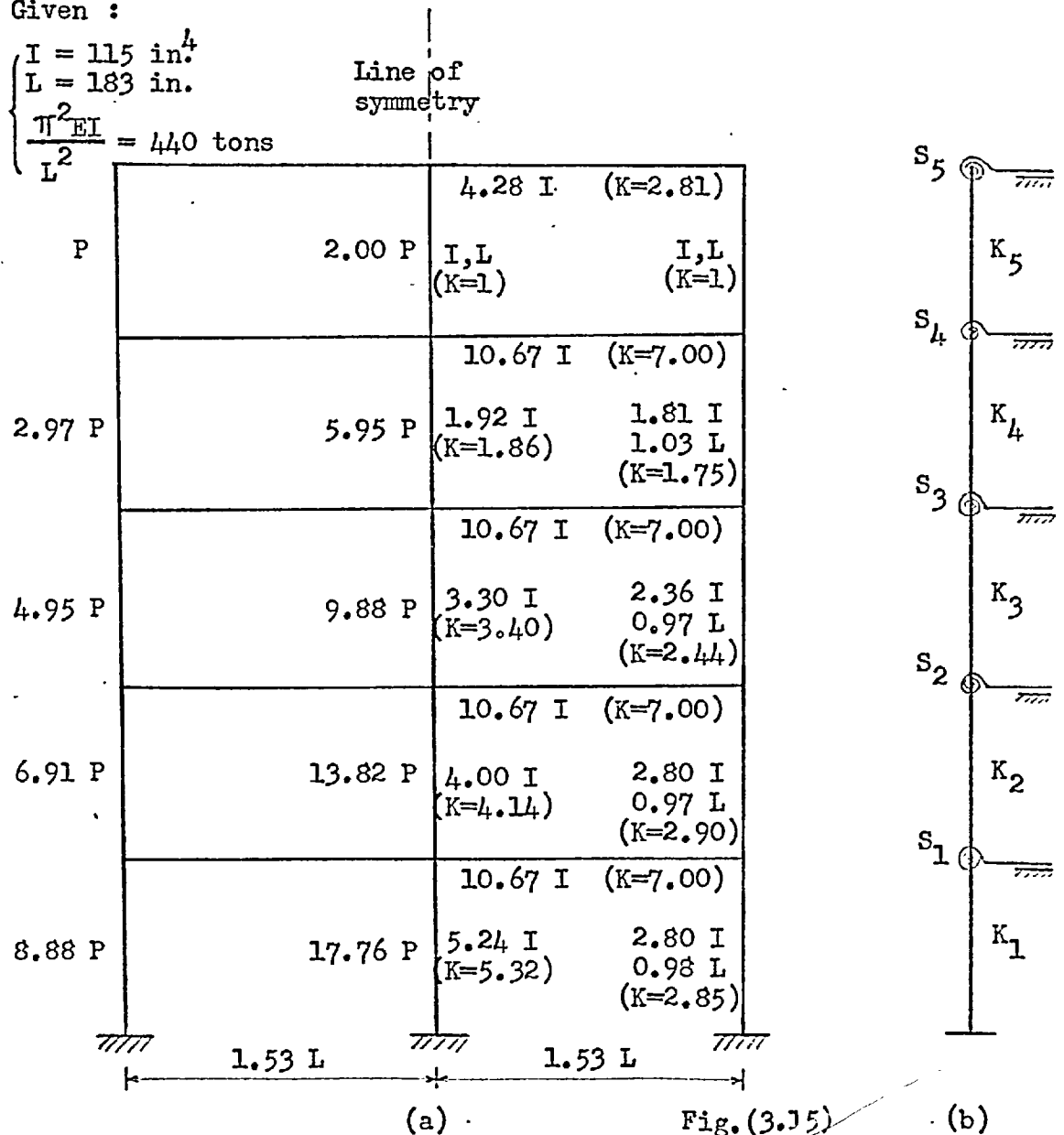
Example

We shall evaluate the critical value of  $P$  for the frame shown in Fig.(3.15a); the frame is allowed to sway. The axial forces of the columns are as shown and those for the beams are zero.

Reference: Bowles and Merchant (6), and McMinn (14).

Given :

$$\begin{cases} I = 115 \text{ in}^4 \\ L = 183 \text{ in.} \\ \frac{\pi^2 EI}{L^2} = 440 \text{ tons} \end{cases}$$





Computational steps:

(1) Transform the frame into an equivalent column (Fig.(3.15b)):

(a) Equ.(3.49) gives

$$K_1 = (1/3) (2.85 + 5.32 + 2.85) = 3.7 ;$$

similar computation gives

$$K_2 = 3.3, \quad K_3 = 2.8, \quad K_4 = 1.8, \quad \text{and} \quad K_5 = 1.0 .$$

(b) Equ.(3.50) gives

$$S_1 = S_2 = S_3 = S_4 = (12/3)(7 + 7) = 56.0$$

$$\text{while } S_5 = (12/3)(2.81 + 2.81) = 22.5 .$$

(c) Equ.(3.51) gives, with  $(\alpha_{bj})_1 = 1,$

$$P_1^B = \frac{(2)(\frac{2.85}{0.98}) + \frac{5.32}{0.98}}{(2)(8.88) + 17.76} \left( \frac{\pi^2 EI}{L^2} \right) = 0.317 \frac{\pi^2 EI}{L^2} ;$$

$$\text{similarly } P_2^B = 0.370 \pi^2 EI/L^2, \quad P_3^B = 0.432 \pi^2 EI/L^2,$$

$$P_4^B = 0.438 \pi^2 EI/L^2, \quad \text{and} \quad P_5^B = 0.750 \pi^2 EI/L^2.$$

Thus column 1 will be regarded as the critical column; these values of  $P^B$ , as well as those of  $S$  and  $K$ , are recorded in Table (3.9). The process of determining the vertical distribution of  $\gamma$  for the equivalent column then follows steps (2) to (4) listed in Section (3.7).

(2) Estimate the  $\alpha$  values at the ends of the critical column.

In this case, since column 1 is connected to known support

condition, we need only to estimate the value of  $\alpha_{t1}$ . If we assume equal distribution of  $S_1$  between column 1 and column 2, then Equ.(3.30) gives

$$\alpha_{t1} = 1.58/(1 + 1.08) = 0.76$$

and, according to Equ.(3.33),

$$P = P_1 = (0.76)(0.317) \pi^2 EI/L^2 = 0.241 \pi^2 EI/L^2.$$

(3) The evaluation of  $\gamma$  values will thus proceed from column 5, which is connecting to the roof, to the critical column. Thus we start the first cycle of computation by letting

$$P_5 = P = 0.241 \pi^2 EI/L^2.$$

Since  $\alpha_{t5} = 0.906$  corresponding to  $\gamma_{t5} = -S_5 = -22.5$ , we have

$$\alpha_{b5} = P_5/(\alpha_{t5} P_5^B) = 0.355$$

and, from Table (3.7)  $\gamma_{b5} \doteq -0.5$ . Equ.(3.23) then gives

$$\gamma_{t4} = -31.0, \text{ thus } \alpha_{t4} = 0.932 \text{ from Table (3.7).}$$

Similarly we shall let

$$P_4 = P = 0.241 \pi^2 EI/L^2,$$

$$\text{thus } \alpha_{b4} = P_4/(\alpha_{t4} P_4^B) = 0.590$$

and, from Table (3.7)  $\gamma_{b4} \doteq -2.6$ . Equ.(3.23) gives  $\gamma_{t3} = -18.6$ , thus  $\alpha_{t3} = 0.892$  from Table (3.7).

Subsequent computation for the remaining floors will be similar to that described and the result is clearly shown in Table (3.9). After  $\alpha_{t1}$  is thus revised we have, by Equ.(3.25),

$$P_1 = 0.260 \pi^2 EI/L^2.$$

(4) The critical value of P is thus given by Equ.(3.26):

$$P = (1/5) [(4)(0.241) + 0.260] \pi^2 EI/L^2 = 0.245 \pi^2 EI/L^2.$$

The second cycle of computation starts from step (3) with  $P = 0.245 \pi^2 EI/L^2$ . The subsequent solution of  $P = 0.247 \pi^2 EI/L^2$  is considered accurate enough since Equ.(3.27) is approximately satisfied. If another computation cycle is required step (3) will be repeated with  $P = 0.247 \pi^2 EI/L^2$ .

The critical value of P is thus given by

$$\begin{aligned} P &= 0.247 \pi^2 EI/L^2 = (0.247)(440) \text{ tons} \\ &= 109 \text{ tons} . \end{aligned}$$

For comparison, Bowles and Merchant employed a relaxation method and obtained  $P = 107$  tons while McMinn applied the equivalent portal method with a matrix approach and gave  $P = 112$  tons.

Table (3.9)

Cycle				1			2		
k	s	K	$\frac{P_k^B L^2}{\pi^2 EI}$	$\gamma$	$\alpha$	$\frac{P_k L^2}{\pi^2 EI}$	$\gamma$	$\alpha$	$\frac{P_k L^2}{\pi^2 EI}$
5	56.	1.0	0.750	(-22.5)	(0.906)	0.241		(0.906)	0.245
				-0.5	0.355		-0.5	0.361	
4	56.	1.8	0.438	-31.0	0.932	0.241	-31.0	0.932	0.245
				-2.6	0.590		-2.7	0.600	
3	56.	2.8	0.432	-18.6	0.892	0.241	-18.6	0.892	0.245
				-3.1	0.625		-3.3	0.638	
2	56.	3.3	0.370	-14.3	0.866	0.241	-14.1	0.865	0.245
				-6.2	0.750		-6.8	0.765	
1	56.	3.7	0.317	-9.6	0.816	0.260	-9.1	0.808	0.256
				(-∞)	(1.000)			(1.000)	

## CHAPTER IV NON-AXIAL LOADING PROBLEMS

### IV.1 GENERAL DESCRIPTIONS

#### 4.1.1 The method

An iterative method is developed to determine the equilibrium paths of rigidly jointed frames under non-axial loading, according to small displacement theory. The characteristic of this approach is that a reference deformation parameter, rather than the load factor, is treated as the independent variable. The usual approach of incrementing the load factor has to limit its increments to small steps, or there is a danger that the assumed load factor might be greater than its maximum equilibrium value. The present method is aimed to avoid such a difficulty: by incrementing from zero the value of a reference deformation parameter  $\rho_R$ , as shown in Fig.(4.1.1), a continuous equilibrium path will be determined.

The main advantage of this approach is that bifurcation buckling can be solved directly, without resorting to laborious formulations based on the existing bifurcation criteria such as that proposed by Masur et al (11). In this thesis the proposed method will be applied to rectangular frames which suffer no side-sway deflection prior to bifurcation (Fig.(4.1.2a)). For such a frame the bifurcation load may be found directly by assigning an infinitesimal value to the reference side-sway parameter  $\rho_R$ , as illustrated in Fig.(4.1.2b).

This approach of evaluating the bifurcation load for rectangular frames may be extended to include other type of frames, such as gable frames, in which  $\rho_R$  is non-zero prior to bifurcation. For example, Fig.(4.1.3a) shows a symmetrical gable frame under symmetrical loading; if the sum of the side-sway rotations of the two stations is plotted against the load factor  $\lambda$  (Fig.(4.1.3b)), the bifurcation load may be found under the condition  $(\rho_1 + \rho_2) \doteq 0$ .

In general, if the deflection mode of a symmetrical frame under symmetrical loading is expressible in terms of a symmetrical mode function  $f_s$  and an antisymmetrical mode function  $f_a$ , so that

$$w = f_s + f_a,$$

then the critical load factor can be evaluated by assigning an infinitesimal value to  $f_a$  in the  $f_a - \lambda$  plot, provided that after bifurcation the frame deforms in an antisymmetrical mode (Fig.(4.1.4)).

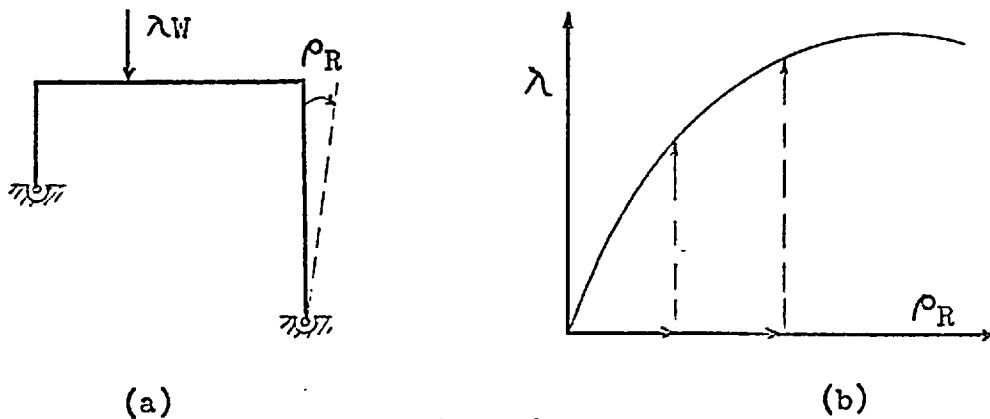
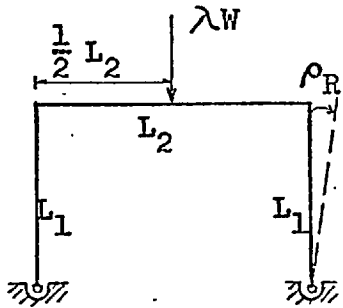
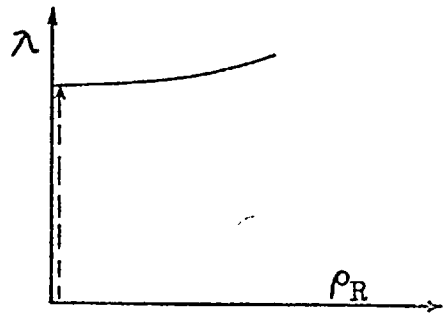


Fig.(4.1.1)

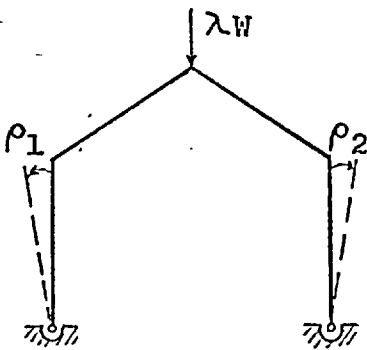


(a)

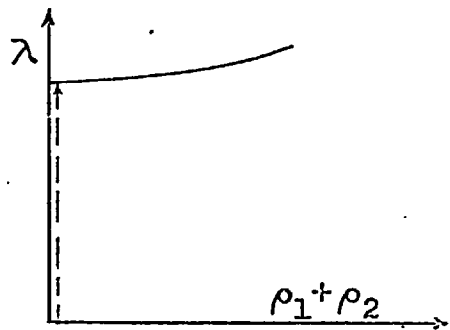


(b)

Fig. (4.1.2)

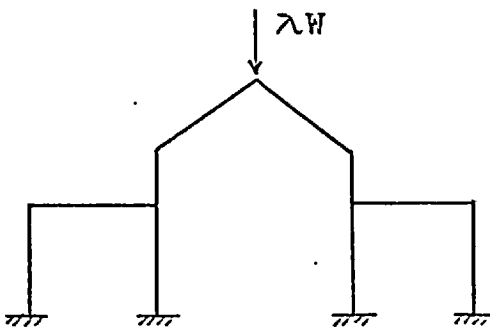


(a)

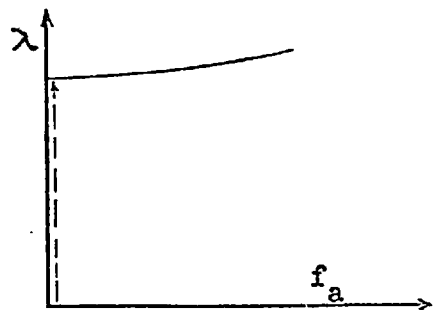


(b)

Fig. (4.1.3)



(a)



(b)

Fig. (4.1.4)

#### 4.1.2 The frame and the loading

Theoretical derivations are based on a "viaduct" (i.e., a single-storey continuous rectangular frame) with non-sinking supports; the general assumptions and limitations of the analysis were listed in Section (1.7).

The following facilities are provided in the derivation:

- (1) The number of spans is unlimited.
- (2) The columns may be of unequal lengths, different materials and different sectional properties; the same applies to the beams.
- (3) Bases of columns may be hinged or fixed.
- (4) Members may have initial (imperfect) slopes.

For the sake of clarity in derivation, the structural members and joints of a viaduct will be designated by numbers as shown in Fig.(4.1.5).

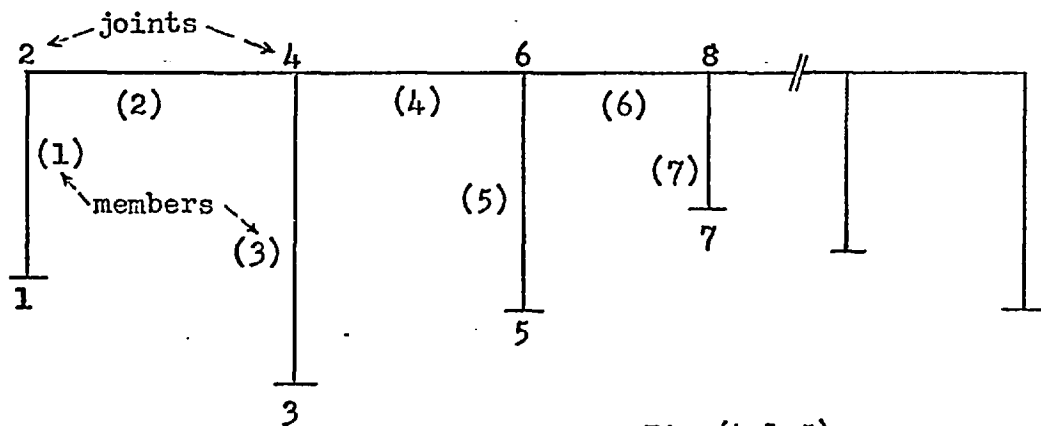


Fig.(4.1.5)



Loads are proportional and are given in terms of a common load factor  $\lambda$  and a common constant multiplier  $P_{ER}$  which is chosen in this thesis as the Euler load of a reference column. If  $N_{wm}$  denotes the number of vertical loads acting on beam  $m$  then vertical loads are given in the form:

$$\lambda W_{mk} P_{ER} \quad \left\{ \begin{array}{l} k = 1, 2, \dots, N_{wm} \\ m = 2, 4, \dots \end{array} \right.$$

Distributed loads are to be simulated by a series of point loads.

Horizontal loads are assumed to be applied only at the beam level; the sum of these horizontal loads is given in the form:

$$\lambda W_h P_{ER}$$

in which  $W_h$  is positive when acting from left to right.

The proposed method, though derived on single-storey frames, can be readily extended to multistorey frames which may be treated as being compounded of single-storey frames. For example, if  $N_s$  denotes the number of storeys in a rectangular frame which is composed of inextensible members and allowed to sway, it then has  $N_s$  degrees of freedom of joint translation at floor levels. One of the joint translations may be assigned as the reference deflection parameter  $\rho_R$ ; the remaining  $N_s - 1$  joint translations and the common load factor  $\lambda$  may be found from conditions of shear equilibrium at floor levels ( $N_s$  of them) and the  $\lambda - \rho_R$  curve may be plotted.

## IV.2 EQUILIBRIUM PATHS FOR FRAMES WITHOUT SWAY

### 4.2.1 The procedure of solution

The procedure of determining the equilibrium paths for frames without side-sway is as follows:

- (1) If the frame has a degree of indeterminacy  $N$  choose  $N$  statically independent bending moments  $Q_n$  ( $n = 1, 2, \dots, N$ ) as the "indeterminacies". For uniformity of analysis these bending moments are to be chosen at the ends of members (the numbering system for members and end moments is as shown in Fig. (4.1.5)).
- (2) Select a reference joint  $J_R$ , and assign its rotation as the reference rotation parameter  $\Theta_R$ . (In general, any internal joint may be selected as the reference joint; the selection is subject only to one condition, that there is at least one non-zero vertical load acting on a beam framing into that joint. The reason for this requirement will become clear in the next section when  $\lambda$  is being evaluated.)
- (3) Choose a small but non-zero value of  $\Theta_R$ .
- (4) Initiate the values of the load factor  $\lambda$  and the indeterminate end-moments.
- (5) Evaluate the axial force in each member in the form

$$P = \lambda P^0 + \sum_{n=1}^N r_n Q_n$$

where  $r_n$  is an influence coefficient. This formula for  $P$  is

- only valid for non-sway cases.
- (6) Evaluate the stability functions of all members, and the primary bending terms for all loaded beams.
  - (7) Evaluate end-moments and joint rotations. Conventional end moment expressions are used (See, for example, Bleich (4)) with terms for initial imperfections and for primary transverse loading. These expressions are derived based on small-deflection assumptions. If the condition of moment equilibrium is applied at all joints ( $J$  of them) except the reference joint,  $J-1$  joint rotations can be evaluated. These joint rotations, incorporating the chosen value of  $\theta_R$ , are then used to evaluate the end moments (including indeterminate end-moments).
  - (8) To facilitate convergence of iteration, the indeterminate end moments may be substituted back to step (5) to modify the axial forces. If this is to be adopted, step (5) to step (7) will be repeated until the values of all indeterminate moments have converged satisfactorily.
  - (9) Apply the condition of moment equilibrium at the reference joint  $J_R$ , then the only remaining unknown - the load factor  $\lambda$  - may be evaluated.
  - (10) Since this iterated value of  $\lambda$  is in general not the correct one, it is to be substituted back in step (5) to re-compute the axial forces. Thus step (5) to step (9) are to be repeated until the value of  $\lambda$  converges. Then a point on the  $\lambda - \theta_R$

curve is located.

(11) The subsequent points on the  $\lambda - \theta_R$  curve can be similarly found, by incrementing the reference rotation parameter  $\theta_R$  in step (3). It is to be noted that step (4) can be henceforth omitted since the initial values of the load factor and the indeterminate moments are conveniently furnished by the corresponding values computed for a previous point.

#### 4.2.2 Formulation

Theoretical derivations will be given in this section for non-axially loaded frames prevented from sway. Computational steps following each subtitle of this section are corresponding to those listed in Section (4.2.1).

##### Evaluating the degree of indeterminacy (step (1))

Let  $M$  denote the number of members in a frame,  $J$  the number of joints where members meet (i.e., internal joints), and  $H$  the number of hinges. Then the number of indeterminate end-moments  $N$  is given by:

$$N = 3(M - J) - H. \quad (4.2.1)$$

##### Evaluation of axial forces (step (5))

The axial force in the  $i$ th member ( $i = 1, 2, \dots, M$ ) of the frame (Fig.(4.1.5)) under a specified loading proportional to a load factor  $\lambda$  may be expressed (exactly) by equilibrium considerations as

$$P_i = \lambda P_i^0 + \sum_{n=1}^N r_{in} Q_n \quad (i = 1 \dots M) \quad (4.2.2)$$

in which

$P_i^0$  = force at member  $i$  when the specified loading acts on the frame, with  $Q_n = 0$  ( $n = 1 \dots N$ ).

$Q_n$  = the  $n$ th indeterminate end-moment.

$r_{in}$  = influence coefficient of the axial force in member  $i$  due to  $Q_n$ .

The influence coefficients  $r$  can be evaluated by statics.

Let  $P_{ER}$  denote the Euler load of a reference column having a length  $L_R$ , modulus of elasticity  $E_R$  and second moment of area  $I_R$  (The external loads have already been referred to this same value  $P_{ER}$  in Section (4.1.2) above). Let

$$\bar{P}_i = P_i / P_{ER},$$

$$\bar{P}_i^0 = P_i^0 / P_{ER},$$

$$\bar{r}_{in} = r_{in} L_R,$$

and

$$\bar{Q}_n = Q_n / (P_{ER} L_R),$$

then Equ.(4.2.2) in non-dimensional form is

$$\bar{P}_i = \lambda \bar{P}_i^0 + \sum_{n=1}^N \bar{r}_{in} \bar{Q}_n \quad (i = 1 \dots M). \quad (4.2.3)$$

Evaluation of stability functions (step (6))

The  $\phi$  value of the  $i$ th member is

$$\begin{aligned}\phi_i &= \sqrt{\left(\frac{|P|}{EI}\right)_i} L_i = \sqrt{P_{ER} \left(\frac{|\bar{P}|}{EI}\right)_i} L_i \\ &= \pi \sqrt{\left(\frac{|\bar{P}|}{\bar{EI}}\right)_i} \bar{L}_i \quad (i = 1 \dots M) \quad (4.2.4)\end{aligned}$$

in which  $\bar{E}_i = E_i/E_R$ ,  $\bar{I}_i = I_i/I_R$ , and  $\bar{L}_i = L_i/L_R$ . The value of  $\phi_i$  may be substituted in Equ.(2.1) and Equ.(2.2) of Chapter II to compute stability functions  $c$  and  $s$ , respectively.

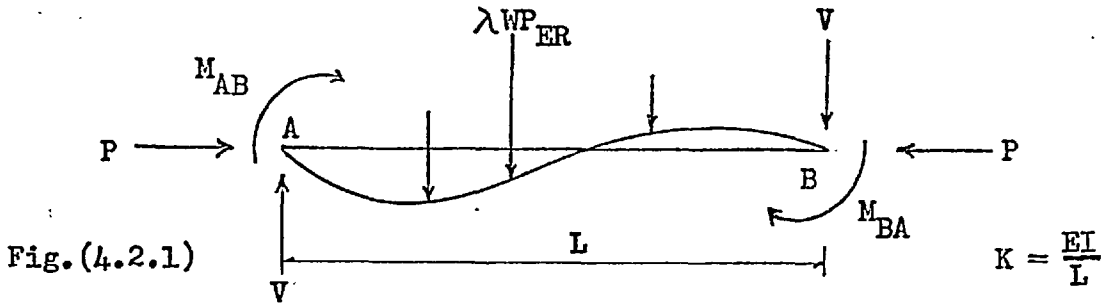
Evaluation of primary bending terms, end-moments and joint rotations

(steps (6) and (7))

Consider a typical linear elastic member connecting joints A and B as shown in Fig.(4.2.1). All quantities are to be considered positive in the senses shown. Provided that the square of the slope is small in comparison with unity the angular displacement at joints A and B are (by modifying Equ.(2.3) of Chapter II):

$$\begin{cases} \theta_A = \frac{1}{K} (c M_{AB} - s M_{BA}) + \theta_{AB}^0 \\ \theta_B = \frac{1}{K} (c M_{BA} - s M_{AB}) + \theta_{BA}^0 \end{cases} \quad (4.2.5)$$

in which  $\theta_{AB}^0$  and  $\theta_{BA}^0$  are primary angles at ends A and B, respectively, due to lateral load and member imperfections, with joints A and B pinned; stability functions  $c$  and  $s$  are as defined in Section (2.2).



Equ. (4.2.5) may be transformed to give

$$\begin{cases} M_{AB} = K [C \theta_A + S \theta_B - (C \theta_{AB}^{\circ} + S \theta_{BA}^{\circ})] \\ M_{BA} = K [C \theta_B + S \theta_A - (C \theta_{BA}^{\circ} + S \theta_{AB}^{\circ})] \end{cases} \quad (4.2.6)$$

in which  $C = c/(c^2 - s^2)$  and  $S = s/(c^2 - s^2)$ . We will denote

$$\bar{M} = M/(P_{ER} L_R),$$

$$\bar{K} = K/(P_{ER} L_R),$$

and

$$\begin{cases} T_{AB} = (C \theta_{AB}^{\circ} + S \theta_{BA}^{\circ}) \\ T_{BA} = (C \theta_{BA}^{\circ} + S \theta_{AB}^{\circ}), \end{cases} \quad (4.2.7)$$

then Equ. (4.2.6) becomes

$$\begin{cases} \bar{M}_{AB} = \bar{K} (C \theta_A + S \theta_B - T_{AB}) \\ \bar{M}_{BA} = \bar{K} (C \theta_B + S \theta_A - T_{BA}) \end{cases} \quad (4.2.8)$$

To evaluate  $\theta_{AB}^{\circ}$  and  $\theta_{BA}^{\circ}$  we shall denote by  $u_k$  and  $v_k$  the location factors of the lateral load  $W_k$  ( $k = 1, 2, \dots$ ) acting on the member, as

shown in Fig.(4.2.2), and by  $\tilde{\theta}_{AB}^{\circ}$  and  $\tilde{\theta}_{BA}^{\circ}$  the initial imperfection angles of the member at joints A and B, respectively, prior to the application of loads. Then for the case of  $P > 0$  the values of  $\theta_{AB}^{\circ}$  and  $\theta_{BA}^{\circ}$  are given (see, for example, Timoshenko (1)) by

$$\begin{cases} \theta_{AB}^{\circ} = \frac{\lambda}{P} \sum_k \left[ W_k \left( \frac{\sin(v_k \theta)}{\sin \theta} - v_k \right) \right] + \tilde{\theta}_{AB}^{\circ} \\ \theta_{BA}^{\circ} = \frac{\lambda}{P} \sum_k \left[ W_k \left( \frac{\sin(u_k \theta)}{\sin \theta} - u_k \right) \right] + \tilde{\theta}_{BA}^{\circ} \end{cases} \quad (4.2.9)$$

in which summations are extended over all lateral loads acting on the member. In the case of  $P < 0$ , hyperbolic functions should replace all the circular functions in Equ.(4.2.9).

For a member with an encastré end B the expression of moments are given by Equ.(4.2.8) with  $\theta_B = 0$ . For a member pinned at end B,  $\bar{M}_{BA} = 0$  and the expression for  $\bar{M}_{AB}$  may be found by substituting  $\theta_B$  from the second of Equ.(4.2.8) into the first:

$$\bar{M}_{AB} = \bar{K} \left( \frac{1}{c} \theta_A + T_{BA} \frac{S}{C} - T_{AB} \right)$$

which may be simplified, in view of Equ.(4.2.7), to

$$\bar{M}_{AB} = \bar{K} \frac{1}{c} (\theta_A - \theta_{AB}^{\circ}). \quad (4.2.10)$$

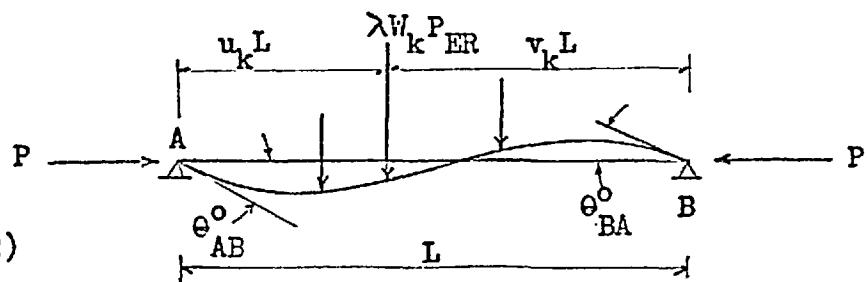


Fig.(4.2.2)



It was mentioned in Section (4.1.2) that horizontal loads of the frame are to be applied only at the beam level. Thus at each end of every column we have

$$\theta^o = \tilde{\theta}^o.$$

When end-moments are expressed in terms of joint rotations by Equ.(4.2.6) the condition of moment equilibrium at every internal joint except the reference joint will give J-1 equations for the J-1 unknown joint rotations. After that the end-moments, including the indeterminate end-moments Q, may be evaluated.

#### Evaluation of $\lambda$ (step (9))

For the purpose of illustration we shall assume that member 2 of the frame shown in Fig.(4.1.5) is subjected to non-zero vertical loads. Then joint 2 may be selected as the reference joint, at which the condition of moment equilibrium reads

$$M_{21} + M_{24} = 0$$

or

$$\bar{M}_{21} + \bar{K}_2 (C_2 \theta_2 + S_2 \theta_4 - T_{24}) = 0, \quad (4.2.11)$$

in which

$$T_{24} = C_2 \theta_{24}^o + S_2 \theta_{42}^o$$

or, in view of Equ.(4.2.9),

$$T_{24} = \frac{\lambda}{\bar{P}_2} \left\{ C_2 \left[ \sum_{k=1}^{N_{w2}} W_{2k} \left( \frac{\sin(v_k \phi_2)}{\sin \phi_2} - v_k \right) + \tilde{\theta}_{24}^o \frac{\bar{P}}{\lambda} \right] + S_2 \left[ \sum_{k=1}^{N_{w2}} W_{2k} \left( \frac{\sin(u_k \phi_2)}{\sin \phi_2} - u_k \right) + \tilde{\theta}_{42}^o \frac{\bar{P}}{\lambda} \right] \right\}.$$

If we denote

$$D_{24} = T_{24}/\lambda \quad (4.2.12)$$

then the load factor may be found by Equ.(4.2.11), in view of Equ.(4.2.12):

$$\lambda = \frac{1}{\bar{K}_2 D_{24}} \left[ \bar{M}_{24} + \bar{K}_2 (C_2 \theta_2 + S_2 \theta_4) \right]. \quad (4.2.13)$$

#### The iterative process

The process of locating a point on the  $\lambda - \theta_R$  curve by iteration is summarized in the simplified flow-chart shown in Fig.(4.2.3).

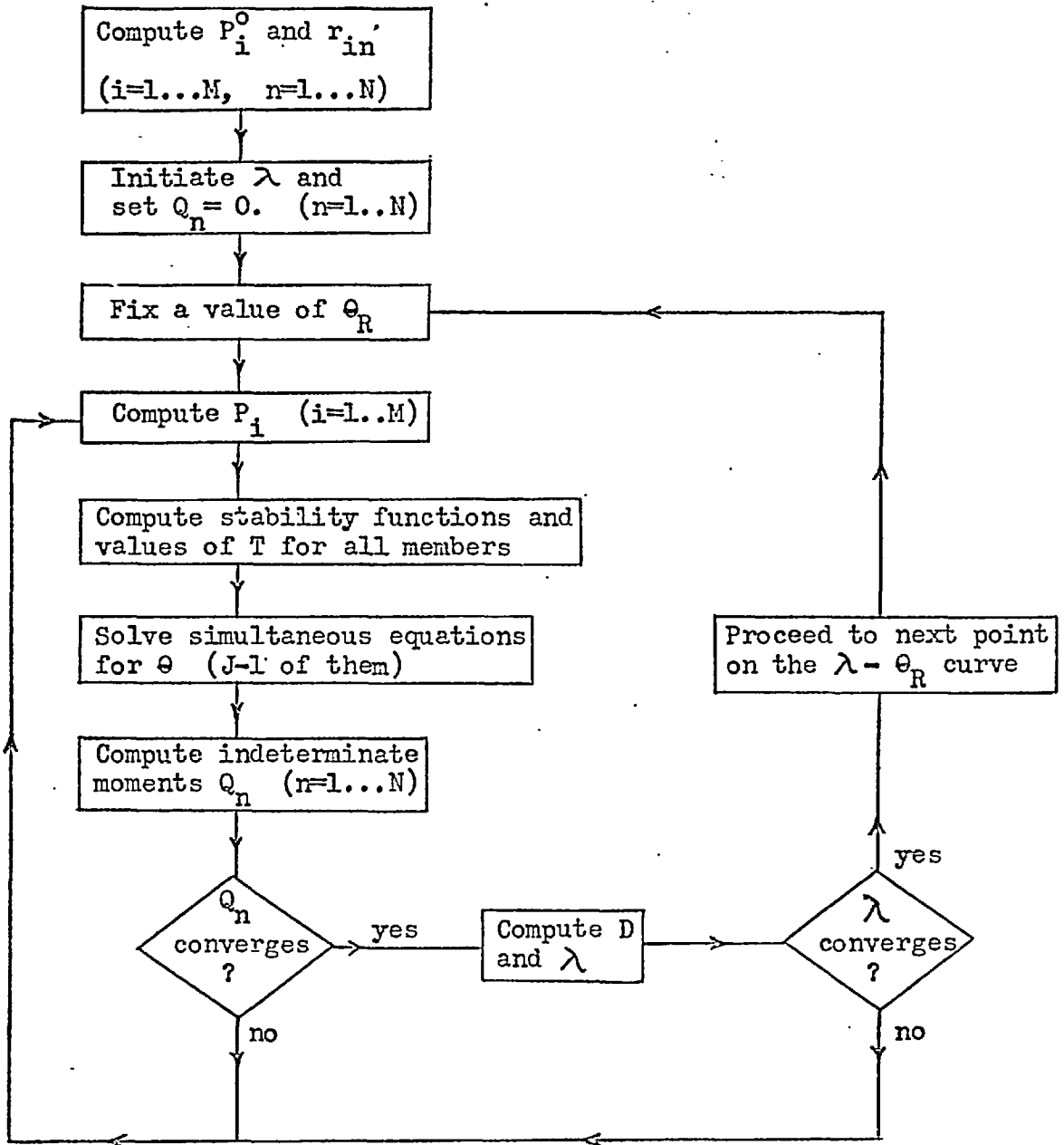


Fig.(4.2.3) Iteration flow-chart for non-sway problems

Example

The frame shown in Fig.(4.2.4) is prevented from sway. The  $E, I, L$  values are as shown; there is no initial imperfection of members.

The degree of indeterminacy for such a frame is obviously one. If the indeterminacy  $Q$  is selected as shown in Fig.(4.2.5), then

$$\bar{Q}_1 = \bar{M}_{24} \text{ and } \bar{P}_1^0 = W(1-u).$$

Since the load is given in terms of  $P_{E1}$ , column 1 is thus the reference column. If we denote  $\bar{L}_i = L_i/L_1$  ( $i=1,2$ ), then the values of  $r_{in}$  are as shown in Table (4.2.1), which was prepared according to Fig.(4.2.6).

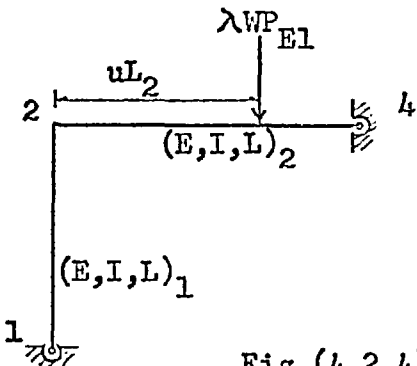


Fig.(4.2.4)

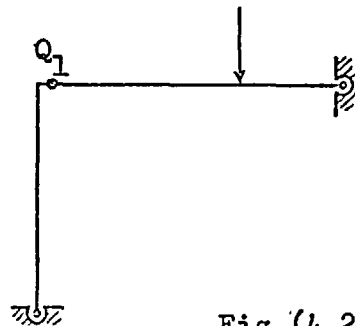
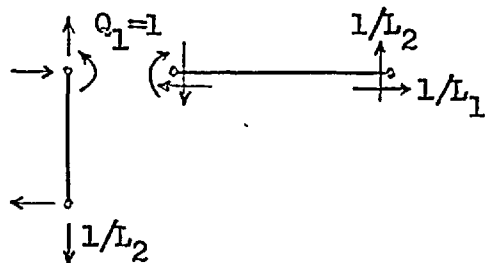


Fig.(4.2.5)

Table (4.2.1)  
The value of  $\bar{r}_{in}$

$n \backslash i$	1	2
1	$-1/\bar{L}_2$	-1

Fig.(4.2.6)  
The value of  $r_{in}$



The axial force is thus, from Equ.(4.2.3),

$$\bar{P}_i = \lambda \bar{P}_i^0 + \bar{r}_{i1} \bar{Q}_1 \quad (i=1,2).$$

These forces are used to generate stability functions  $c_i$  and  $s_i$  ( $i = 1,2$ ), with  $\phi_i$  given by Equ.(4.2.4).

Since joint 2 is the only internal joint in the structure the value of  $\lambda$  can be found directly by applying the condition of equilibrium of moments at that joint:

$$\bar{M}_{21} + \bar{M}_{24} = \bar{K}_1 \frac{1}{c_1} \theta_2 + \bar{K}_2 \frac{1}{c_2} (\theta_2 - \theta_{24}^0) = 0 \quad (4.2.14)$$

in which  $\theta_{24}^0$  is given by Equ.(4.2.9):

$$\theta_{24}^0 = \frac{\lambda}{\bar{P}_2} \left[ W \frac{\sin(1-u)\phi_2}{\sin\phi_2} - (1-u) \right].$$

If we denote  $d = \theta_{24}^0/\lambda$ , then Equ.(4.2.14) may be solved for  $\lambda$  as

$$\lambda = \left( 1 + \frac{\bar{K}_1 c_2}{\bar{K}_2 c_1} \right) \frac{\theta_2}{d}.$$

For the case when the  $E$ ,  $I$ , and  $L$  values are equal for the two members and with  $W = 1$  and  $u = 0.2$ , the numerical solutions are given in Fig.(4.2.7), where  $\lambda$  is plotted against  $\theta_2$ ,  $\bar{Q}_1$ ,  $\bar{P}_1$  and  $\bar{P}_2$ ; the accuracy of the solutions will be revealed by a model test to be shown in Chapter V.

The number of iterative cycles required for a satisfactory convergence increases as  $\lambda$  approaches its maximum equilibrium value. As  $\lambda$  increases, and convergence becomes more difficult, increments

of the reference deflection parameter may be reduced to smaller values to facilitate the convergence; the computation finally ceases when further reduction would be impracticable. In this example the computation stops at  $\theta_2 = 0.96$ ; the corresponding value of  $\lambda$  is 1.56 which is about 84% of the maximum value obtained by Lee et al (28).

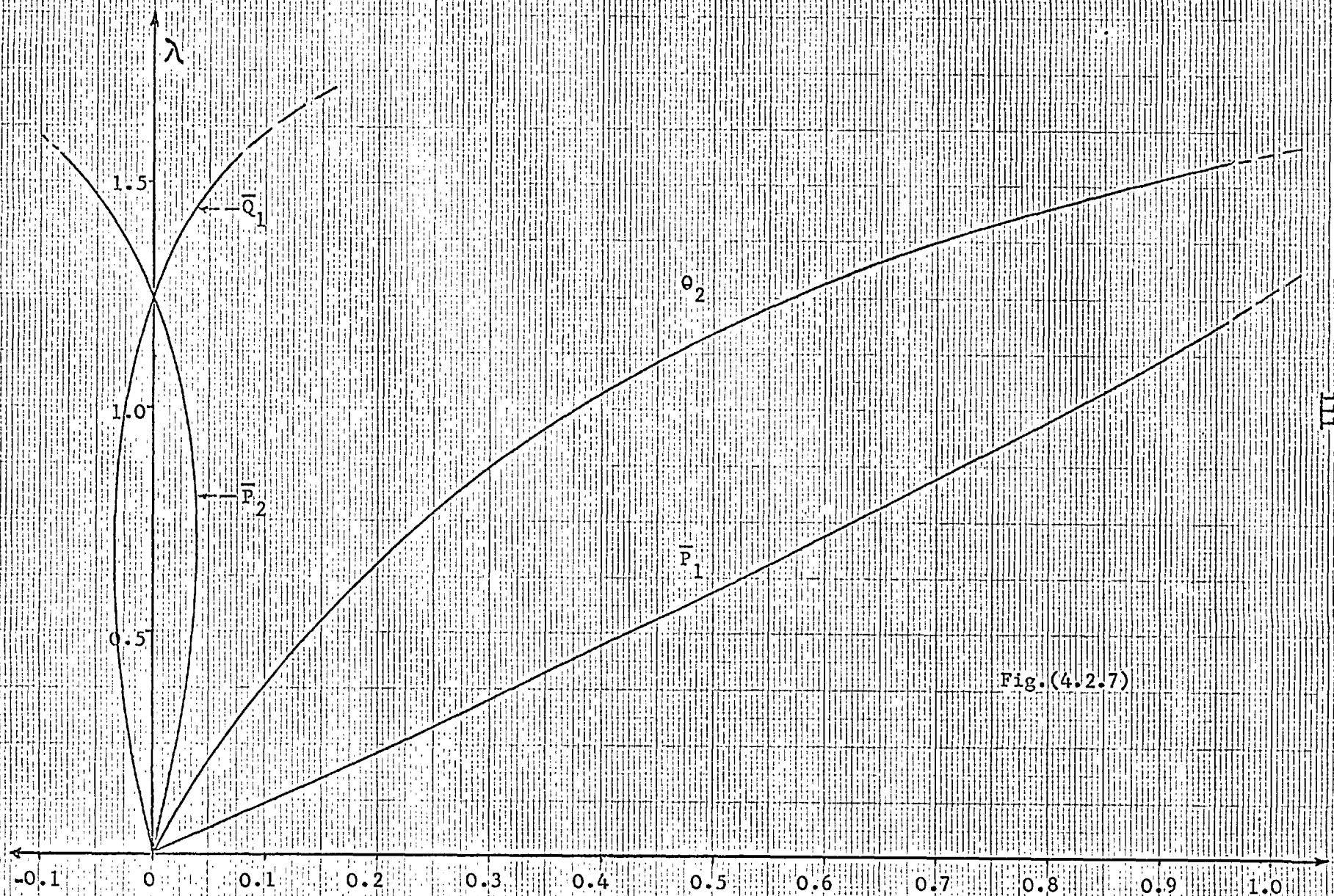


Fig.(4.2.7)

### IV.3 EQUILIBRIUM PATHS FOR FRAMES WITH SWAY

#### 4.3.1 The procedure of solution

The procedure follows closely the procedure outlined in Section (4.2.1) for frames without sway:

- (1) If the frame has a degree of indeterminacy  $N$  choose  $N$  statically independent bending moments as the "indeterminacies". For uniformity of analysis these bending moments are to be chosen at the ends of members (the numbering system for members and end-moments is as shown in Fig.(4.1.5)).
- (2) Assign the side-sway rotation of a column as the reference sway parameter  $\rho_R$  (the external loads have already been referred to this same column in Section (4.1.2) above).
- (3) Choose a small but non-zero value of  $\rho_R$ .
- (4) Initiate the values of the load factor  $\lambda$  and the indeterminate end-moments.
- (5) Evaluate the axial force at each member as given by Equ.(4.2.2), with the addition of a new term representing the influence of the axial force due to differential movement of the ends of members in the frame.
- (6) Evaluate the stability functions of all members and the primary bending terms of all loaded beams, as in Section (4.2.1).
- (7) End-moments are expressed in terms of joint rotations, initial bending moments and differential movements of the ends of the



members. Again, expressions are derived according to small-deflection assumptions. Rotations at internal joints ( $J$  of them) may be evaluated by applying the condition of moment equilibrium at all internal joints. These joint rotations are then used to evaluate end-moments (including indeterminate end-moments).

- (8) To facilitate convergence of iteration the indeterminate end-moments may be substituted back to step (5) to modify the axial forces. If this is to be adopted step (5) up to step (7) will be repeated until the values of all indeterminate moments converge.
- (9) Apply the condition of horizontal force equilibrium at the cross beam to evaluate the remaining unknown, the load factor  $\lambda$ .
- (10) Since this value of  $\lambda$  is in general not the correct one it is to be substituted back in step (5) to re-compute the axial forces. Step (5) to step (9) are repeated until the value of  $\lambda$  converges; a point on the  $\lambda - \rho_R$  curve is then located.
- (11) The subsequent points on the  $\lambda - \rho_R$  curve can be similarly found, by incrementing the reference sway parameter  $\rho_R$  in step (3). It is to be noted that step (4) may be henceforth omitted since the initial values of the load factor and the indeterminate moments are conveniently furnished by corresponding values computed for a previous point.

### 4.3.2 Formulation

Theoretical derivations will be given in this section for non-axially loaded frames subjected to sway. Computational steps following each subtitle of this section correspond to those listed in Section (4.3.1).

#### Evaluating the degree of indeterminacy (step (1))

Again, if  $M$  denotes the number of members in a frame,  $J$  the number of internal joints and  $H$  the number of hinges then the number of indeterminate end-moments  $N$  is given by Equ.(4.2.1), namely,

$$N = 3(M - J) - H. \quad (4.3.1)$$

#### Evaluation of axial forces (step (5))

As a frame sways there is differential movement of the ends of each member in the direction normal to its original centre line. Let  $\delta_j$  represents such a differential movement at the  $j$ th member ( $j = 1 \dots M$ ); then the induced bending moment at member  $j$  caused by  $\delta_j$  is equal to the product of the axial force  $P_j$  and  $\delta_j$ ; this bending moment will in turn induce axial forces in other members. Thus the axial force in the  $i$ th member of the frame is given, exactly, by Equ.(4.2.2) with the addition of a new term:

$$P_i = \lambda P_i^0 + \sum_{n=1}^N r_{in} Q_n + \sum_{j=1}^M \chi_{ij} P_j \delta_j \quad (i=1 \dots M). \quad (4.3.2)$$

The coefficients  $\chi$  can be evaluated by statics.

If the frame is to be composed of inextensible members then the differential deflections  $\delta$  of all columns are the same and those of all the beams are zero. Thus, following the notation system shown in Fig.(4.1.5),

$$\begin{cases} \delta_1 = \delta_3 = \delta_5 = \dots = \delta \\ \delta_2 = \delta_4 = \delta_6 = \dots = 0 \end{cases} \quad (4.3.3)$$

and Equ.(4.3.2) can be simplified as

$$P_i = \lambda P_i^0 + \sum_{n=1}^N r_{in} Q_n + \delta \sum_{j=1,3}^M \chi_{ij} P_j. \quad (4.3.4)$$

Let  $P_{ER}$  denotes the Euler load of the reference column having length  $L_R$ , modulus of elasticity  $E_R$  and second moment of area  $I_R$ , and let

$$\bar{P}_i = P_i / P_{ER},$$

$$\bar{P}_i^0 = P_i^0 / P_{ER},$$

$$\bar{r}_{in} = r_{in} L_R,$$

$$\bar{Q}_n = Q_n / (P_{ER} L_R),$$

$$\bar{\chi}_{ij} = \chi_{ij} L_R,$$

and

$$\rho_R = \delta / L_R,$$

then Equ.(4.3.4) may be non-dimensionalized as

$$\bar{P}_i = \lambda \bar{P}_i^0 + \sum_{n=1}^N \bar{r}_{in} \bar{Q}_n + \rho_R \sum_{j=1,3}^M \bar{\kappa}_{ij} \bar{P}_j \quad (4.3.5)$$

(i = 1...M).

Evaluation of stability functions (step (6))

The  $\phi$  value of the  $i$ th member is given by Equ.(4.2.4), namely,

$$\phi_i = \eta \sqrt{\left(\frac{|\bar{P}|}{E \bar{I}}\right)_i} L_i \quad (i = 1...M) \quad (4.3.6)$$

in which  $\bar{E}_i = E_i/E_R$ ,  $\bar{I}_i = I_i/I_R$ , and  $\bar{L}_i = L_i/L_R$ .

Stability functions  $c$  and  $s$  may then be computed according to Equ.(2.1) and Equ.(2.2), respectively.

Evaluation of primary bending terms, end-moments and joint rotations (step (6) and step (7))

If the linear elastic member shown previously in Fig.(4.2.1) is to have a rigid-body rotation  $\rho$  as shown in Fig.(4.3.1), the angular displacement at joints A and B will be given by Equ.(4.2.5) with the addition of a new term:

$$\begin{cases} \theta_A = \frac{1}{K} (c M_{AB} - s M_{BA}) + \theta_{AB}^0 + \rho \\ \theta_B = \frac{1}{K} (c M_{BA} - s M_{AB}) + \theta_{BA}^0 + \rho \end{cases} \quad (4.3.7)$$

in which  $\theta_{AB}^0$  and  $\theta_{BA}^0$  are, as defined in Section (4.2.2), primary angles due to lateral load and member imperfections, with joints A and B pinned.

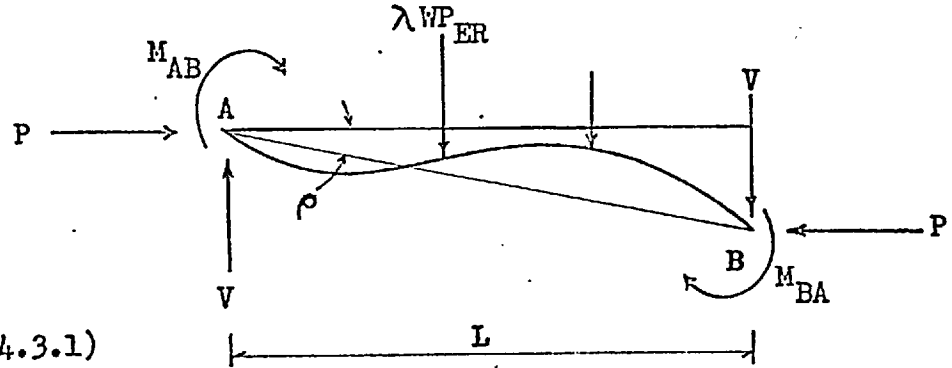


Fig.(4.3.1)

Equ.(4.3.7) may be transformed to give

$$\begin{cases} M_{AB} = K \left[ c \theta_A + s \theta_B - (c \theta_{AB}^0 + s \theta_{BA}^0) - (c + s) \rho \right] \\ M_{BA} = K \left[ c \theta_B + s \theta_A - (c \theta_{BA}^0 + s \theta_{AB}^0) - (c + s) \rho \right] \end{cases} \quad (4.3.8)$$

in which  $C = c/(c^2 - s^2)$  and  $S = s/(c^2 - s^2)$ . Again, if we denote

$$\bar{M} = M/(P_{ER} L_R),$$

$$\bar{K} = K/(P_{ER} L_R),$$

and

$$\begin{cases} T_{AB} = (c \theta_{AB}^0 + s \theta_{BA}^0) \\ T_{BA} = (c \theta_{BA}^0 + s \theta_{AB}^0) \end{cases} \quad (4.3.9)$$

then Equ.(4.3.8) becomes

$$\begin{cases} \bar{M}_{AB} = \bar{K} \left[ c \theta_A + s \theta_B - T_{AB} - (c + s) \rho \right] \\ \bar{M}_{BA} = \bar{K} \left[ c \theta_B + s \theta_A - T_{BA} - (c + s) \rho \right] . \end{cases} \quad (4.3.10)$$

The values of  $\theta_{AB}^{\circ}$  and  $\theta_{BA}^{\circ}$  for the case of  $P > 0$  are given by Equ. (4.2.9):

$$\begin{cases} \theta_{AB}^{\circ} = \frac{\lambda}{P} \sum_k \left[ W_k \left( \frac{\sin(v_k \phi)}{\sin \phi} - v_k \right) \right] + \tilde{\theta}_{AB}^{\circ} \\ \theta_{BA}^{\circ} = \frac{\lambda}{P} \sum_k \left[ W_k \left( \frac{\sin(u_k \phi)}{\sin \phi} - u_k \right) \right] + \tilde{\theta}_{BA}^{\circ} \end{cases} \quad (4.3.11)$$

in which summations are extended over all lateral loads acting on the member and  $\tilde{\theta}_{AB}^{\circ}$  and  $\tilde{\theta}_{BA}^{\circ}$  were defined as the initial imperfection angles of the member at joint A and B, respectively. In the case of  $P < 0$  hyperbolic functions should replace the circular functions in Equ. (4.3.11).

For a member with an encastré end B the moment expressions are given by Equ. (4.3.10) with  $\theta_B = 0$ . For a member pinned at end B we have  $\bar{M}_{BA} = 0$ , and the expression for  $\bar{M}_{AB}$  may be found by substituting  $\theta_B$  from the second of Equ. (4.3.10) into the first; after rearranging we have

$$\bar{M}_{AB} = \bar{K} \frac{1}{c} (\theta_A - \rho - \theta_{AB}^{\circ}). \quad (4.3.12)$$

If all horizontal loads on the frame are to be applied at the beam level we have, at each end of every column,

$$\theta^{\circ} = \tilde{\theta}^{\circ}.$$

After expressions for the end-moments have been written down

for all beams and columns the conditions for moment equilibrium at every internal joint will give  $J$  equations for the  $J$  unknown joint rotations. The end-moments, including the indeterminate moments  $Q$ , may be evaluated once these equations have been solved.

### Evaluation of $\lambda$ (step (9))

If the horizontal load  $\lambda W_h P_{ER}$  is to be applied at the beam level the equilibrium of horizontal forces acting on the beam gives

$$\frac{(\bar{M}_{12} + \bar{M}_{21})}{\bar{L}_1} + \bar{P}_1 \rho_1 + \frac{(\bar{M}_{34} + \bar{M}_{43})}{\bar{L}_3} + \bar{P}_3 \rho_3 + \dots + \lambda W_h = 0$$

or

$$\frac{(\bar{M}_{12} - \bar{M}_{24})}{\bar{L}_1} + \frac{(\bar{M}_{34} - \bar{M}_{42} - \bar{M}_{46})}{\bar{L}_3} + \dots + \sum_{j=1,3}^M \bar{P}_j \rho_j + \lambda W_h = 0 \quad (4.3.13)$$

which will be regrouped to ensure convergence of iteration as

$$\frac{\bar{M}_{24}}{\bar{L}_1} + \frac{\bar{M}_{46}}{\bar{L}_3} + \dots - \lambda W_h = \sum_{j=1,3}^M \bar{P}_j \rho_j + \left( \frac{\bar{M}_{12}}{\bar{L}_1} + \frac{\bar{M}_{34} - \bar{M}_{42}}{\bar{L}_3} + \dots \right). \quad (4.3.14)$$

If we denote

$$\begin{cases} \bar{m}_{24} = \bar{M}_{24} + \bar{K}_2 T_{24} \\ \bar{m}_{46} = \bar{M}_{46} + \bar{K}_4 T_{46} \end{cases}$$

and

$$\begin{cases} D_{24} = T_{24} / \lambda \\ D_{46} = T_{46} / \lambda \end{cases}$$

the left-hand-side of Equ.(4.3.14) may be rearranged as

$$\left(\frac{\bar{m}_{24}}{\bar{L}_1} + \frac{\bar{m}_{46}}{\bar{L}_3} + \dots\right) - \lambda \left(\frac{\bar{K}_2}{\bar{L}_1} D_{24} + \frac{\bar{K}_4}{\bar{L}_3} D_{46} + \dots\right) - \lambda W_h .$$

Thus Equ.(4.3.14) may be solved for  $\lambda$  in the form

$$\lambda = \frac{\sum_{m=1}^{N_b} \left[ \frac{\bar{m}_{2m, 2(m+1)}}{\bar{L}_{2m-1}} - \frac{\bar{M}_{2m+1, 2(m+1)} - \bar{M}_{2(m+1), 2m}}{\bar{L}_{2m+1}} - \bar{P}_{2m+1} \rho_{2m+1} \right] - \left( \frac{\bar{M}_{12}}{\bar{L}_1} + \bar{P}_1 \rho_1 \right)}{\sum_{m=1}^{N_b} \frac{\bar{K}_{2m} D_{2m, 2(m+1)}}{\bar{L}_{2m-1}} + W_h} \quad (4.3.15)$$

in which  $N_b$  denotes the number of bays in the frame.

### The iterative process

The process of locating a point on the  $\lambda - \rho_R$  curve is summarized in the simplified flow-chart shown in Fig.(4.3.2).



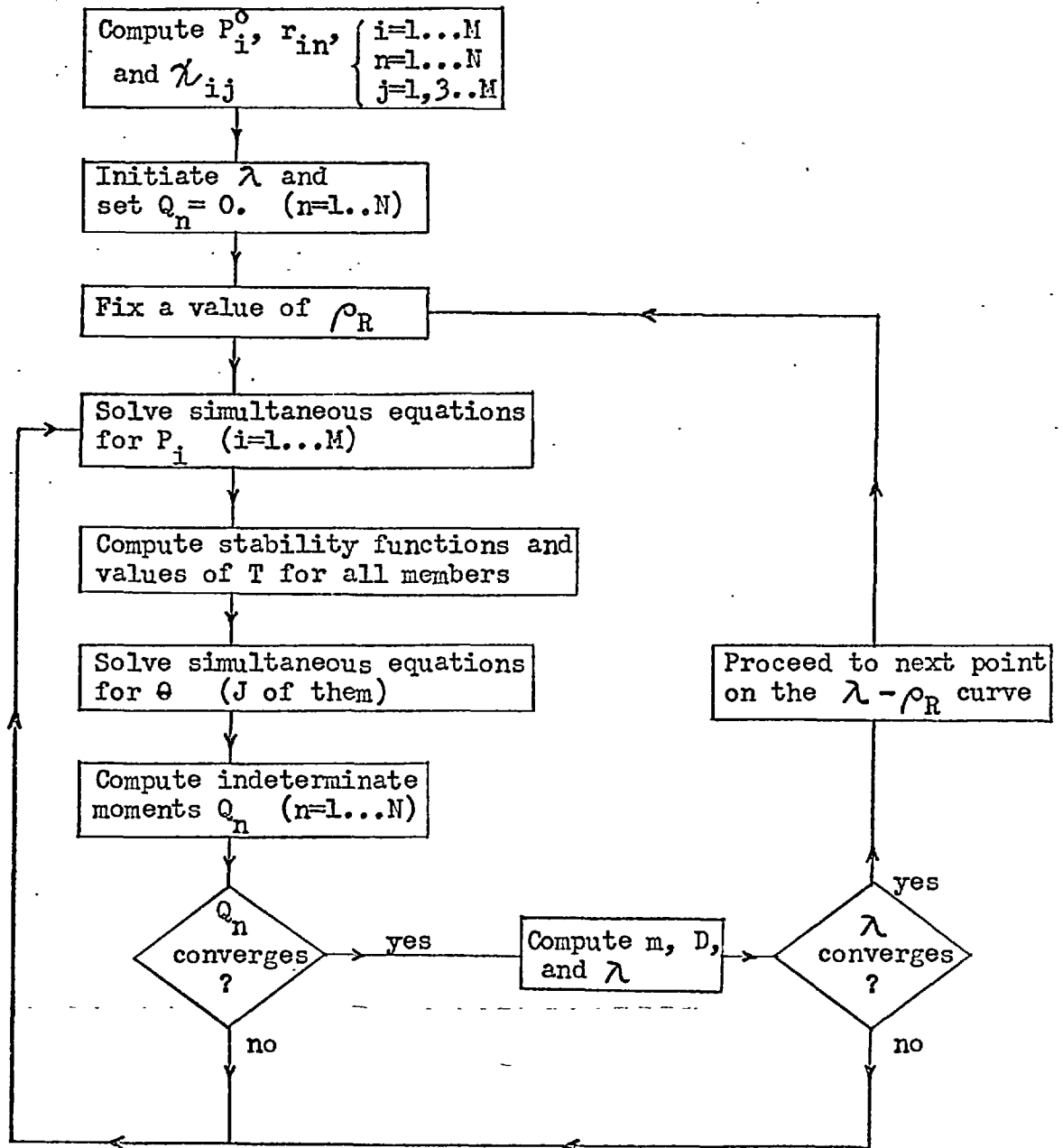


Fig.(4.3.2) Iteration flow-chart for sway problems

Example

We shall consider the two-bay frame shown in Fig.(4.3.3). For each frame member the modulus of elasticity, second moment of area and length are given as  $E_i$ ,  $I_i$ , and  $L_i$ , respectively, with  $i = 1, 2, \dots, 5$ ; there are no member imperfections.

The degree of indeterminacy for such a frame, from Equ.(4.3.1) with  $M = 5$ ,  $J = 3$ , and  $H = 3$ , is

$$N = 3(5-3) - 3 = 3.$$

If the indeterminacies are selected as shown in Fig.(4.3.4) then we have

$$\left\{ \begin{array}{l} \bar{Q}_1 = \bar{M}_{24} \\ \bar{Q}_2 = \bar{M}_{46} \\ \bar{Q}_3 = \bar{M}_{64} \end{array} \right. \quad \text{and} \quad \left\{ \begin{array}{l} \bar{P}_1^0 = W(1 - u) \\ \bar{P}_3^0 = Wu \\ \bar{P}_2^0 = \bar{P}_4^0 = \bar{P}_5^0 = 0. \end{array} \right.$$

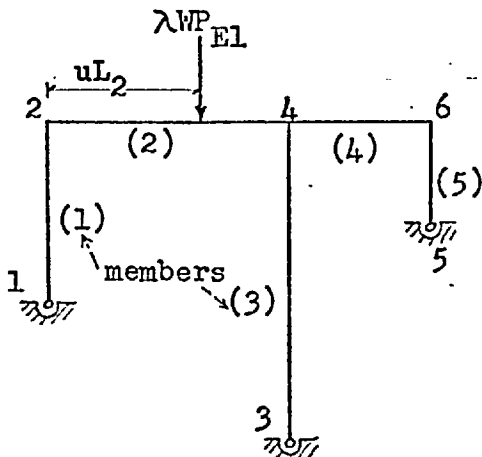


Fig.(4.3.3)

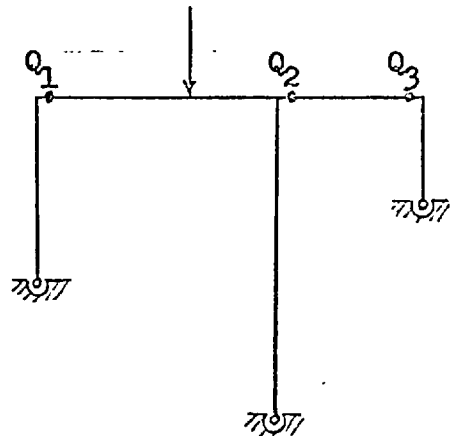


Fig.(4.3.4)

Since the load is given in terms of  $P_{E1}$  the first column is the reference column. If we denote  $\bar{L}_i = L_i/L_1$  ( $i=1\dots 5$ ) then the values of  $\bar{r}_{in}$  are as shown in Table (4.3.1);  $r_{i2}$  were prepared according to Fig.(4.3.5).

Table (4.3.1) The values of  $\bar{r}_{in}$

n \ i	1	2	3	4	5
1	$(\bar{L}_3-1)/\bar{L}_2$	-1	$(1-\bar{L}_3)/\bar{L}_2$	0	0
2	$1/\bar{L}_2$	0	$-1/\bar{L}_2 - 1/\bar{L}_4$	0	$1/\bar{L}_4$
3	$\bar{L}_3/(\bar{L}_2\bar{L}_5)$	0	$-1/\bar{L}_4 - \bar{L}_3/(\bar{L}_2\bar{L}_5)$	$1/\bar{L}_5$	$1/\bar{L}_4$

The values of  $\bar{\kappa}_{ij}$  are as shown in Table (4.3.2). For example, if  $\bar{\kappa}_{i5}$  ( $i=1\dots 5$ ) is to be computed, we would set  $P_5\delta_5$  (see Equ. (4.3.2)) equal to unity and the  $P\delta$  values of all other members equal to zero; this is equivalent to applying to member 5, alone, a positive (clock-wise) unit moment, as shown in Fig.(4.3.6). The forces induced at other members due to this unit moment can then be evaluated by statics.

Table (4.3.2) The values of  $\bar{\kappa}_{ij}$

j \ i	1	2	3	4	5
1	$-\bar{L}_3/\bar{L}_2$	1	$\bar{L}_3/\bar{L}_2$	0	0
3	$-1/\bar{L}_2$	0	$1/\bar{L}_2$	0	0
5	$-\bar{L}_3/(\bar{L}_2\bar{L}_5)$	0	$\bar{L}_3/(\bar{L}_2\bar{L}_5)$	$-1/\bar{L}_5$	0

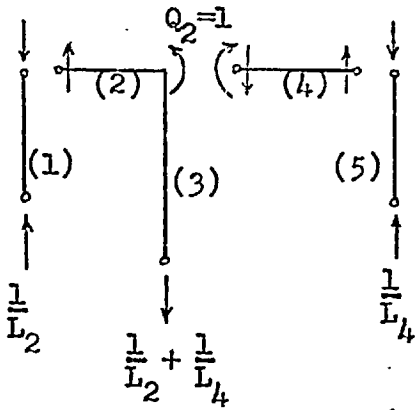


Fig. (4.3.5)

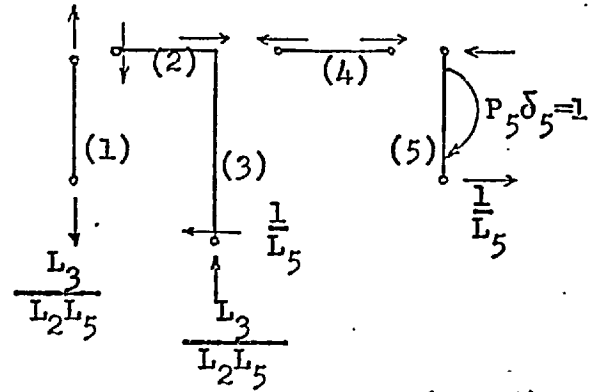


Fig. (4.3.6)

The axial forces are thus, from Equ. (4.3.5),

$$\bar{P}_i = \lambda \bar{P}_i^0 + \sum_{n=1}^3 \bar{r}_{in} \bar{Q}_n + \rho_1 \sum_{n=1,3}^5 \bar{\chi}_{ij} \bar{P}_j \quad (i=1\dots 5).$$

Stability functions  $c_i$  and  $s_i$  ( $i=1\dots 5$ ) and thus  $C_i$  and  $S_i$  may now be computed, with

$$\phi_i = \pi \sqrt{\left( \frac{|\bar{P}_i|}{\bar{E}_i \bar{I}_i} \right)_i L_i}$$

in which  $\bar{E}_i = E_i/E_1$  and  $\bar{I}_i = I_i/I_1$  ( $i=1\dots 5$ ).

Bending moments for the columns are given by Equ. (4.3.12) and those for the beams by Equ. (4.3.10); for example,

$$\bar{M}_{21} = \bar{K}_1 \frac{1}{c_1} (\theta_2 - \rho_1),$$

$$\bar{M}_{24} = \bar{K}_2 (C_2 \theta_2 + S_2 \theta_4 - T_{24}),$$

in which  $T_{24}$  is given by Equ. (4.3.9), in view of Equ. (4.3.11):

$$T_{24} = \frac{\lambda W}{\bar{P}_2} \left\{ C_2 \left[ \frac{\sin(1-u)\phi_2}{\sin\phi_2} - (1-u) \right] + S_2 \left[ \frac{\sin u \phi_2}{\sin\phi_2} - u \right] \right\}$$

for  $\bar{P}_2 > 0$ . Hyperbolic instead of circular functions should be used

for the case of  $\bar{P}_2 < 0$ .

Angles of rotation at any joint are computed by the equilibrium of moments acting at the joint. For example, at joint 2 we have  $M_{21} + M_{24} = 0$ ; this gives

$$\theta_2 = \frac{\bar{K}_1 \rho_1 / c_1 + \bar{K}_2 (T_{24} - S_2 \theta_4)}{\bar{K}_1 / c_1 + \bar{K}_2 c_2}.$$

Similar expressions for  $\theta_4$  and  $\theta_6$  can be written, and they are to be solved simultaneously with the expression for  $\theta_2$ .

With joint rotations thus determined the end-moments may be computed, and the load factor is given by Equ.(4.3.15) with  $N_b = 2$ ,  $W_h = 0$ ,  $\bar{M}_{12} = \bar{M}_{34} = \bar{M}_{56} = 0$ , and  $T_{46} = D_{46} = 0$ :

$$\lambda = \frac{\frac{\bar{m}_{24}}{\bar{I}_1} + \frac{\bar{M}_{42} + \bar{m}_{46}}{\bar{I}_3} + \frac{\bar{M}_{64}}{\bar{I}_5} - \sum_{j=1,3}^5 \bar{P}_j \rho_j}{\frac{\bar{K}_2 D_{24}}{\bar{I}_1}}$$

in which

$$\begin{cases} \bar{m}_{24} = \bar{M}_{24} + \bar{K}_2 T_{24} \\ \bar{m}_{46} = \bar{M}_{46} \end{cases} \quad \text{and} \quad \begin{cases} D_{24} = T_{24} / \lambda \\ D_{46} = T_{46} / \lambda \end{cases}.$$

For the case of equal E, I, L values for all members, and with  $W = 2$  and  $u = 0.5$ , the numerical solutions are given in Fig.(4.3.7). The computation stops at  $\rho_1 = 0.170$  (the corresponding  $\lambda = 0.233$ ). The accuracy of the method for sway problems will be investigated by model tests, to be discussed in Chapter V.

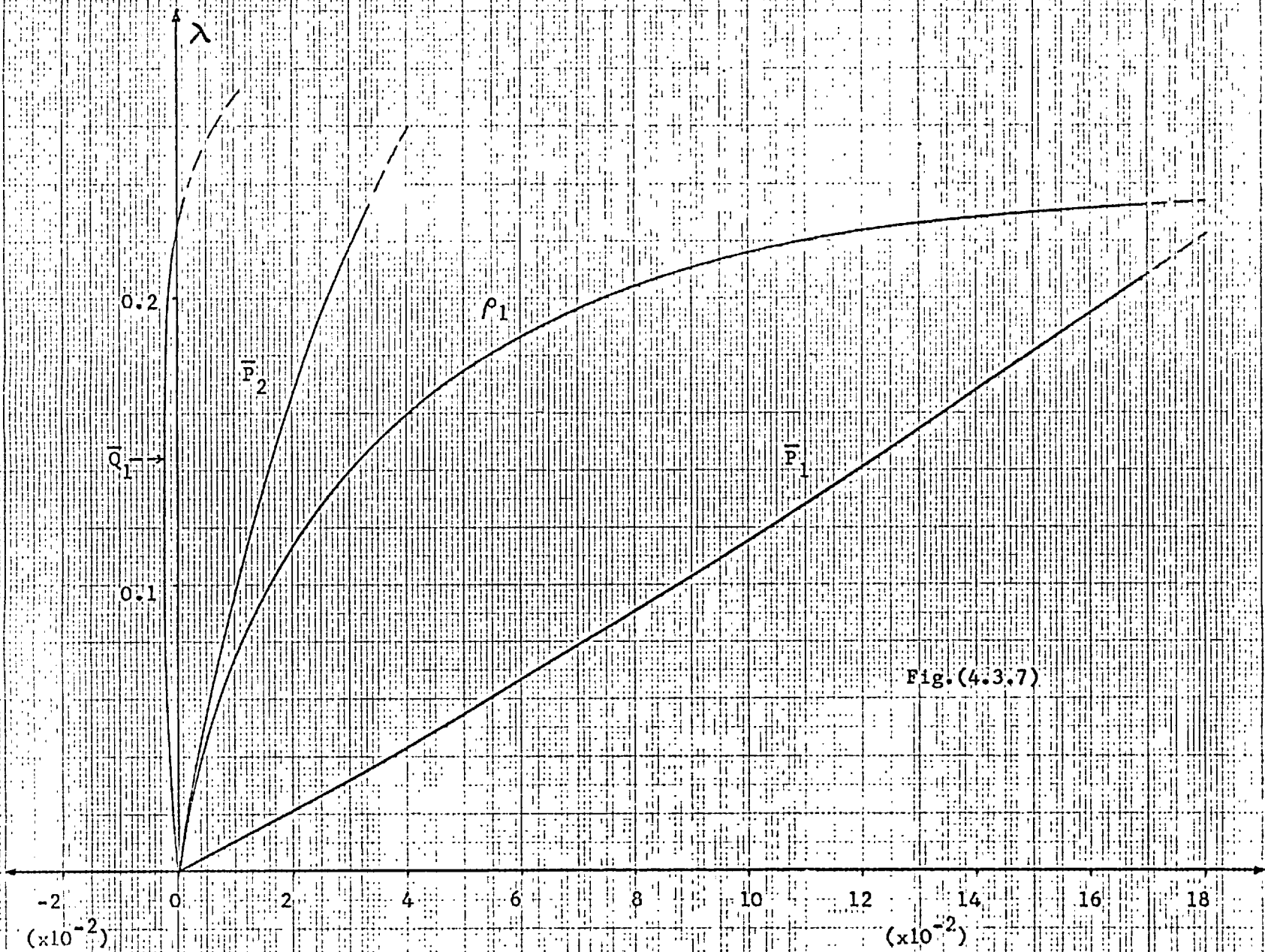


Fig.(4.3.7)

#### IV.4 BIFURCATIONAL BUCKLING

Previous investigators (see Chapter I) have given methods for finding bifurcation points for non-axially loaded frames of an appropriately symmetrical nature. Unfortunately these methods involve a great deal of labour if used to analyse frames of any complexity, and the approach to be suggested here is believed to be a considerable improvement in this respect.

The distinction between previous methods of solution and the proposed one is as follows:

(1) Previous solutions: As the load factor  $\lambda$  reaches its critical value both symmetrical and antisymmetrical configurations become equally possible; consequently the characteristic equations of these configurations should be satisfied simultaneously. Attention is thus focussed on the point of bifurcation itself (point B in Fig.(4.4.1a), in which the load factor  $\lambda$  is plotted against a reference sway parameter  $\rho_R$ ); in order to find that point both non-sway and sway behaviour have to be considered simultaneously.

(2) The proposed solution: The concept is schematized in Fig.(4.4.1b), in which  $\rho_R$  again represents a reference sway parameter. It appears that if  $\lambda$  values can be found for specified values of  $\rho_R$  our attention can be focussed solely on the sway mode, for the bifurcation load  $\lambda_c$  is located by the limiting condition

$$\lambda_c = \lambda_{\rho_R} \Big|_{\rho_R \rightarrow 0}$$

provided the symmetry of the problem assures us that  $\rho_R = 0$  before bifurcation (for the general treatment, see Section (4.1.1) above).

It follows at once that the method described in Chapter (IV.3) for evaluating the load factor corresponding to an assumed value of  $\rho_R$  can be applied without modification to the present bifurcational problem.

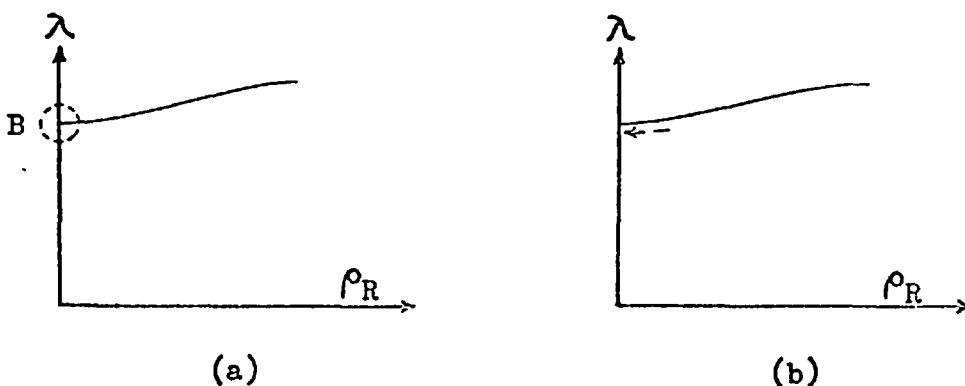


Fig. (4.4.1)

Numerical solutions will be given for three examples. Since the procedure of solution follows exactly that of the preceding section the results of computation will be given directly; the computations were performed using 8 significant figures by an IBM 7094 computer. In each example the bifurcation load may be evaluated directly by assigning an extremely small value to  $\rho_R$  (say,  $10^{-10}$ ); for the purpose of determining the post-buckling curve, however, we shall start with a  $\rho_R$  value of  $10^{-1}$  and then gradually reduce it to  $10^{-10}$ .



Example 1 The symmetrical portal proposed and solved by Chwalla (2); The frame and loading is shown in Fig.(4.4.2).

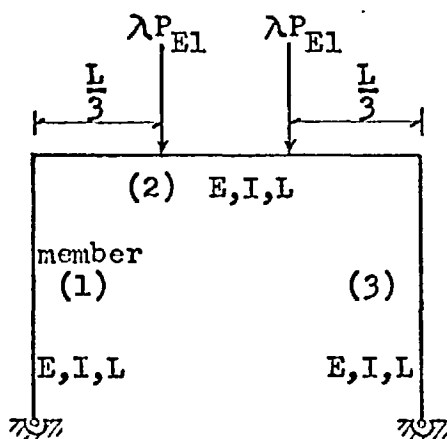


Fig.(4.4.2)

Table (4.4.1)

$\rho_1$	$\lambda$
$10^{-1}$	0.1799
$10^{-2}$	0.1798
$10^{-3}$	0.1790
$10^{-5}$	0.1790
$10^{-10}$	0.1790

The solution is shown in Table (4.4.1), in which the load factor  $\lambda$  is listed against the side-sway rotation of member 1. It thus appears that, in the context of small-deflection assumptions, the post-buckling curve is initially horizontal and consequently the equilibrium condition at bifurcation is either neutral or very nearly so.

The value of  $\lambda P_{EI}$  at bifurcation is thus  $1.767 EI/L^2$  which compares to  $1.775 EI/L^2$  given by Chwalla and by Masur et al (11), and to  $1.780 EI/L^2$  given by Horne (15); the large-deflection solution given by Lee et al (28) was  $1.751 EI/L^2$ .

Example 2 Fig.(4.4.3a) shows the frame solved by Lu (16), who extended Masur's approach to solving portal frames with uniformly distributed loads applied on the cross beam.

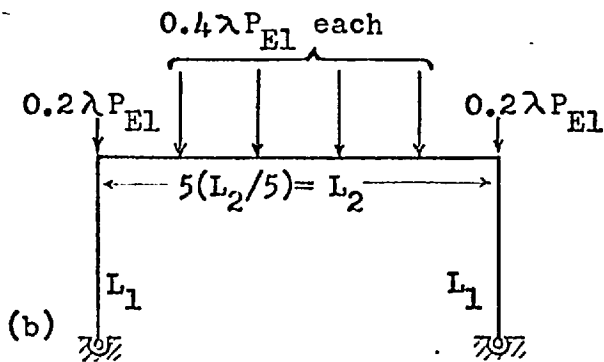
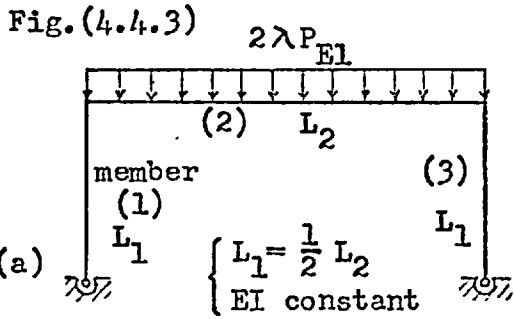


Table (4.4.2)

$\rho_1$	$\lambda$
$10^{-1}$	0.1407
$10^{-2}$	0.1402
$10^{-3}$	0.1398
$10^{-5}$	0.1398
$10^{-10}$	0.1398

In applying the present method we shall replace the distributed loads with isolated point loads as shown in Fig.(4.4.3b). The corresponding  $\lambda - \rho_1$  relation is shown in Table (4.4.2). The value of  $\lambda P_{EI}$  at bifurcation is thus  $1.38 EI/L_1^2$  which compares with  $1.39 EI/L^2$  given by Lu. For the cases of  $L_1 = L_2$  and  $L_1 = L_2/3$  the corresponding values are  $1.77 EI/L_1^2$  and  $1.07 EI/L_1^2$ , respectively, which compare to Lu's solution of  $1.79 EI/L_1^2$  and  $1.08 EI/L_1^2$ .

Example 3 The three-bay frame shown in Fig.(4.4.4); properties of the frame members are as shown in Table (4.4.3).

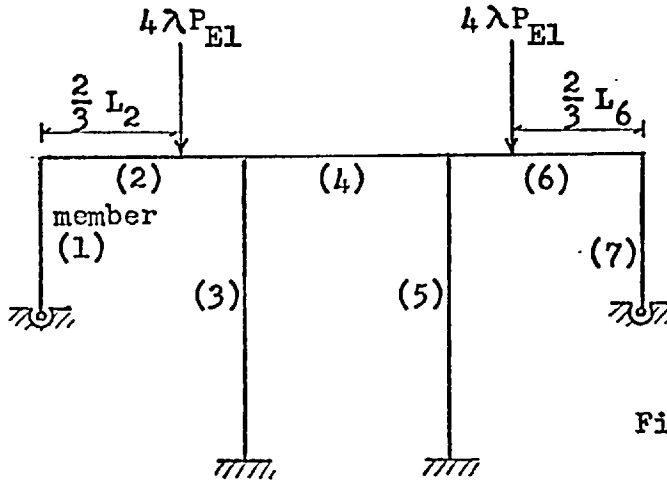


Fig.(4.4.4)

Table (4.4.3)

	Member i						
	1	2	3	4	5	6	7
$E_i/E_1$	1	1	1	1	1	1	1
$I_i/I_1$	1	1	1	1/2	1	1	1
$L_i/L_1$	1	1	2	1	2	1	1

Table (4.4.4)

$\rho_1$	$\lambda$
$10^{-1}$	0.1045
$10^{-2}$	0.1044
$10^{-3}$	0.1036
$10^{-5}$	0.1029
$10^{-10}$	0.1029

Since there are no special handling difficulties for this frame the solutions are given directly in Table (4.4.4). The value of  $\lambda$  at bifurcation is thus 0.1029.

CHAPTER V      APPLICABILITY OF SMALL DEFLECTION ANALYSESV.1      EXPERIMENTAL INVESTIGATIONS

The purpose of the present experimental investigation is to determine the non-linear response of frames under load, in order to estimate the range of applicability of the small-deflection theory.

Consequently, three different model frames were made and tested; each test represented one type of frame problems (i.e., sway, non-sway, and bifurcation problem).

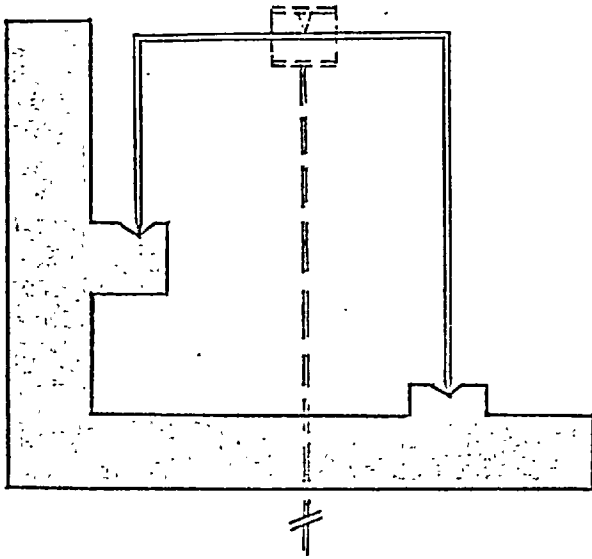
The models had high-strength aluminium alloy members, 3/4 inch wide, 1/4 to 1/2 inch thick, and from 8 to 18 inches long. The reason for selecting aluminium alloy strips was that they possess a yield-point of 60.5 ksi, which is comparable to that of mild steel, yet the modulus of elasticity  $E$  is only  $9.2 \times 10^3$  ksi. This permitted the use of relatively thick members so as to decrease the degree of initial crookedness, and at the same time kept the Euler loads of the members within reasonable limits for small-scale testing. The use of high-strength aluminium alloy strip also made it possible that large deformations would be achieved without inducing plastic strains.

The test set-ups are depicted in Fig.(5.1) while individual model frames are described in Table (5.1), in which dimensions of members are given in the order of thickness-width-length (lengths are measured between centres of joints). Table (5.2) shows the

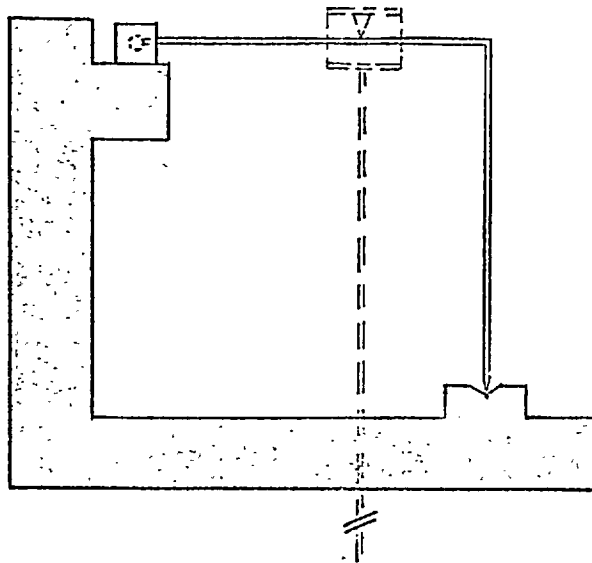
corresponding Euler load  $P_E (= \pi^2 EI/L^2)$  of each member.

Frame members in frames 1 and 2 were connected to each other by small (nominal length: one inch) rigid clamps (Fig.(5.2a)), while the stanchions in frame 3 were bolted directly to the rigid steel beam. Pinned ends were realized by knife edges, with the exception that a roller-type hinge (Fig.(5.2b)) capable of taking tension or compression was used for the horizontal member in frame 2. Loads, which were applied at the mid-width of the horizontal members through a pin connected to a loading rod (Fig.(5.2c)), were supplied by weights placed on a pan at the other end of the rod. This type of loading device was adequate for the present tests, in which post-buckling behaviour was not to be studied.

Dial gauges with an accuracy of 0.0001 inch/division were used to measure displacements at loading points and midpoints of members of frame 2. However for frames 1 and 3, which were without lateral support and thus had side-sway deflections sensitive to lateral loads, a cathetometer (sliding telescope) was used to measure lateral displacements; by this means any undesirable lateral forces that might be exerted by dial gauges were eliminated.

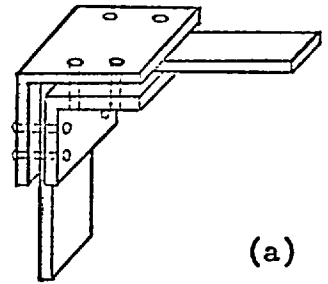


(a) Test I and Test III

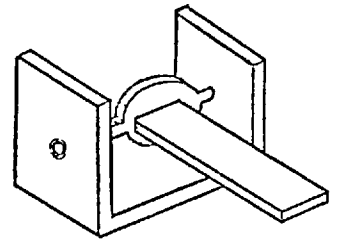


(b) Test II

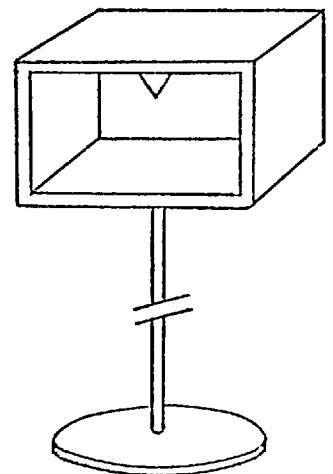
Fig.(5.1) Test set-up



(a)



(b)



(c)

Fig.(5.2)

Table (5.1) Dimension (inches)

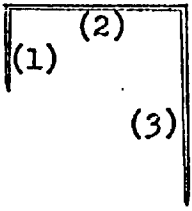
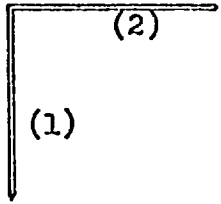
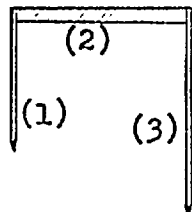
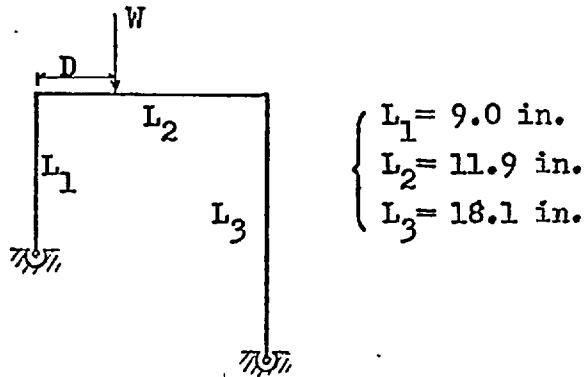
Frame	Member	Thickness	width	length
	1	0.129	0.746	9.00
	2	0.253	0.752	11.86
	3	0.129	0.746	18.06
	1	0.129	0.746	18.06
	2	0.129	0.746	18.06
	3	—	—	—
	1	0.129	0.746	8.00
	2 (steel)	1.00	0.746	8.00
	3	0.129	0.746	12.00

Table (5.2)  
 Values of  $P_E (= \pi^2 EI/L^2)$  (lbs)

Member	Frame 1	Frame 2	Frame 3
1	151.2	37.5	191.4
2	662.3	37.5	$2.89 \times 10^5$
3	37.5	—	85.1

Test I

The frame was to be tested without lateral support (Fig.(5.1a)). The load was applied at a distance  $D$  of 4.0 inches along the cross beam from the joint connecting the shorter column:



Snap buckling of the frame was observed at a load of 57 lbs (which will be referred to as  $W_1^c$ ), at which point the side-sway deflection of the frame increased rapidly and was checked only by a limiting pin. The experimental results are given in Fig.(5.3) and Fig.(5.4); corresponding solutions given by the small-deflection analysis, as described in Chapter IV.3, are presented by curve A in the same figures. The frame members regained their original straightness upon unloading, so the test was within the elastic range of the frame.

It is observed from Fig.(5.3) that the small-deflection analysis gives good approximations to the vertical deflection  $\delta_v$ . For example, at  $W = 0.85 W_1^c$ , the error in estimating  $\delta_v$  is about 10%. However, an error of 10% in estimating the side-sway deflection  $\delta_h$  occurs at  $W = 0.47 W_1^c$ , as indicated by Fig.(5.4).



A similar test was conducted with the load applied at a distance  $D$  of 6.0 inches instead of 4.0 inches. Snap buckling of the frame was observed at a load of 59 lbs (which will be referred to as  $W_2^c$ ); again, the frame members resumed their original straightness upon unloading.

Experimental results are shown in Fig.(5.5) and Fig.(5.6); corresponding solutions given by the small-deflection analysis are shown by curve A in the same figures.

It is observed from Fig.(5.5) that the small-deflection analysis again gives good approximations to the vertical deflection  $\delta_v$ . For example, at  $W = 0.87 W_2^c$ , the error in estimating  $\delta_v$  is about 10%. However, Fig.(5.6) indicates that an error of 10% in estimating the side-sway deflection  $\delta_h$  occurs at  $W = 0.42 W_2^c$ .

It is to be noted that if the effects of gusseted connections on the model frame could have been removed the experimental maximum load would have been slightly reduced. For example, if the increase of buckling strength in the model frame due to gussets was about 10% (see Bowles and Merchant (6)), the corresponding maximum load for the two tests would be  $W_1^c = 52$  lbs and  $W_2^c = 54$  lbs, respectively. The adjusted analytical solutions at a region near to the maximum loads are as shown by curve B in Fig.(5.3) to Fig.(5.6).

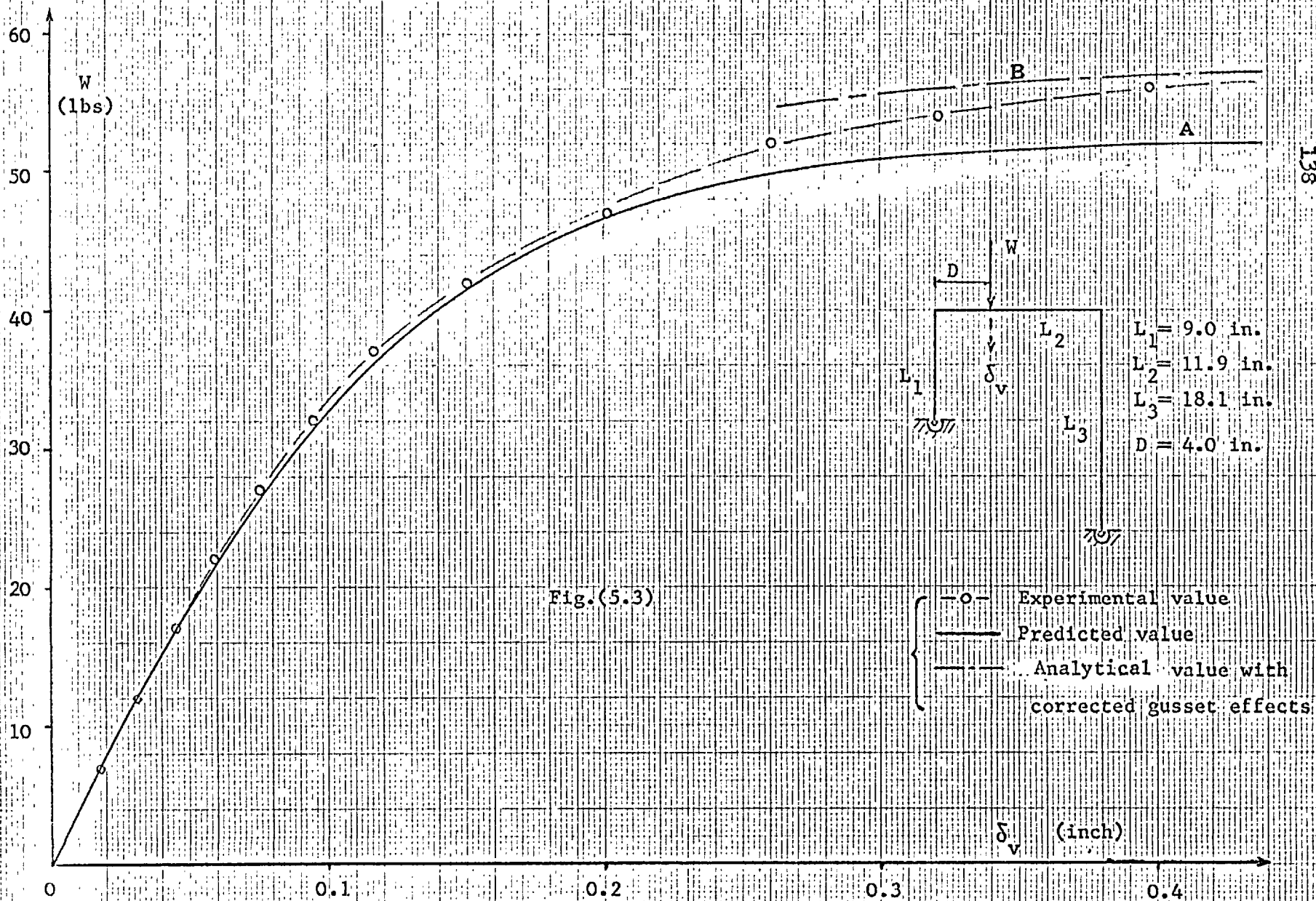
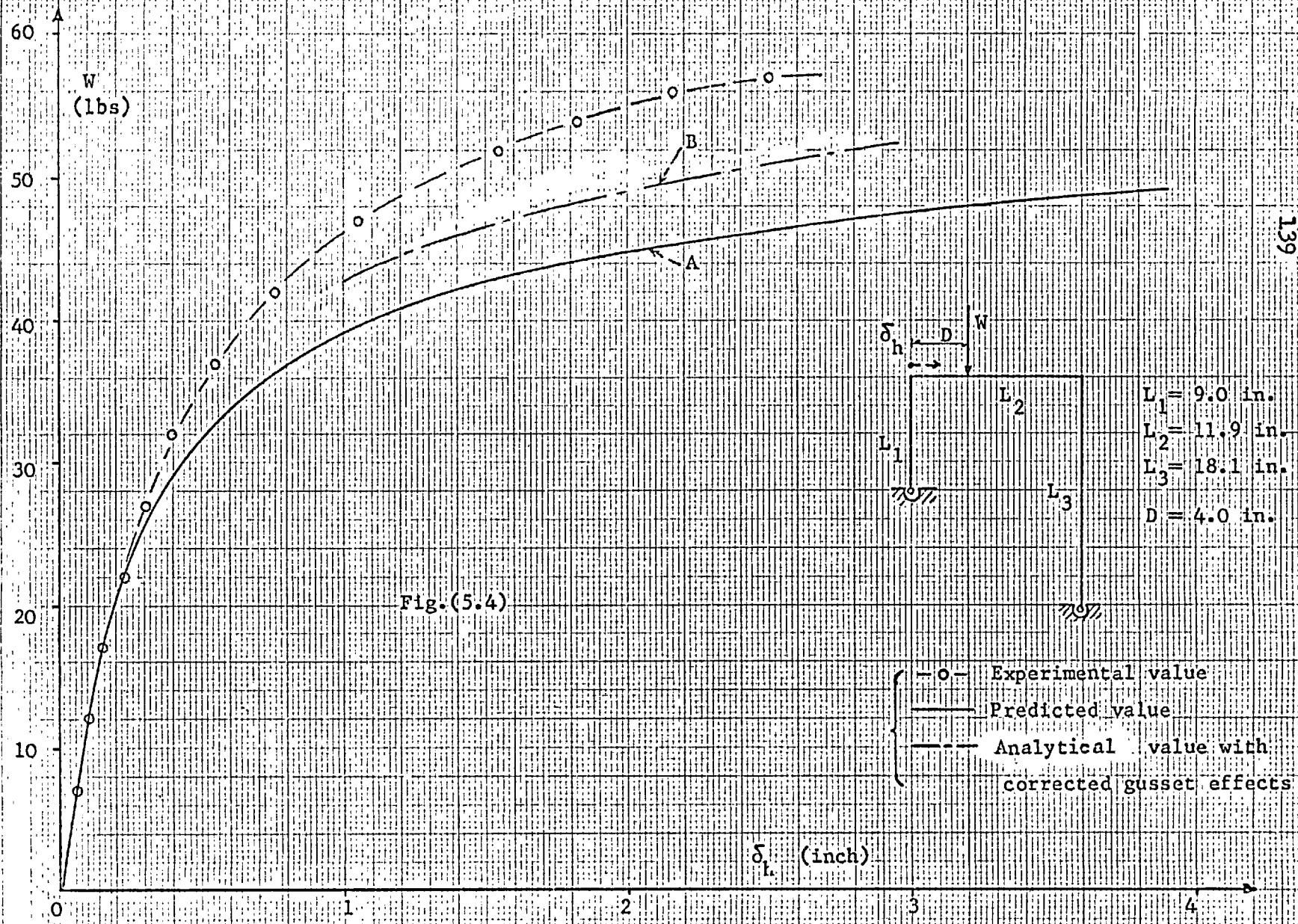
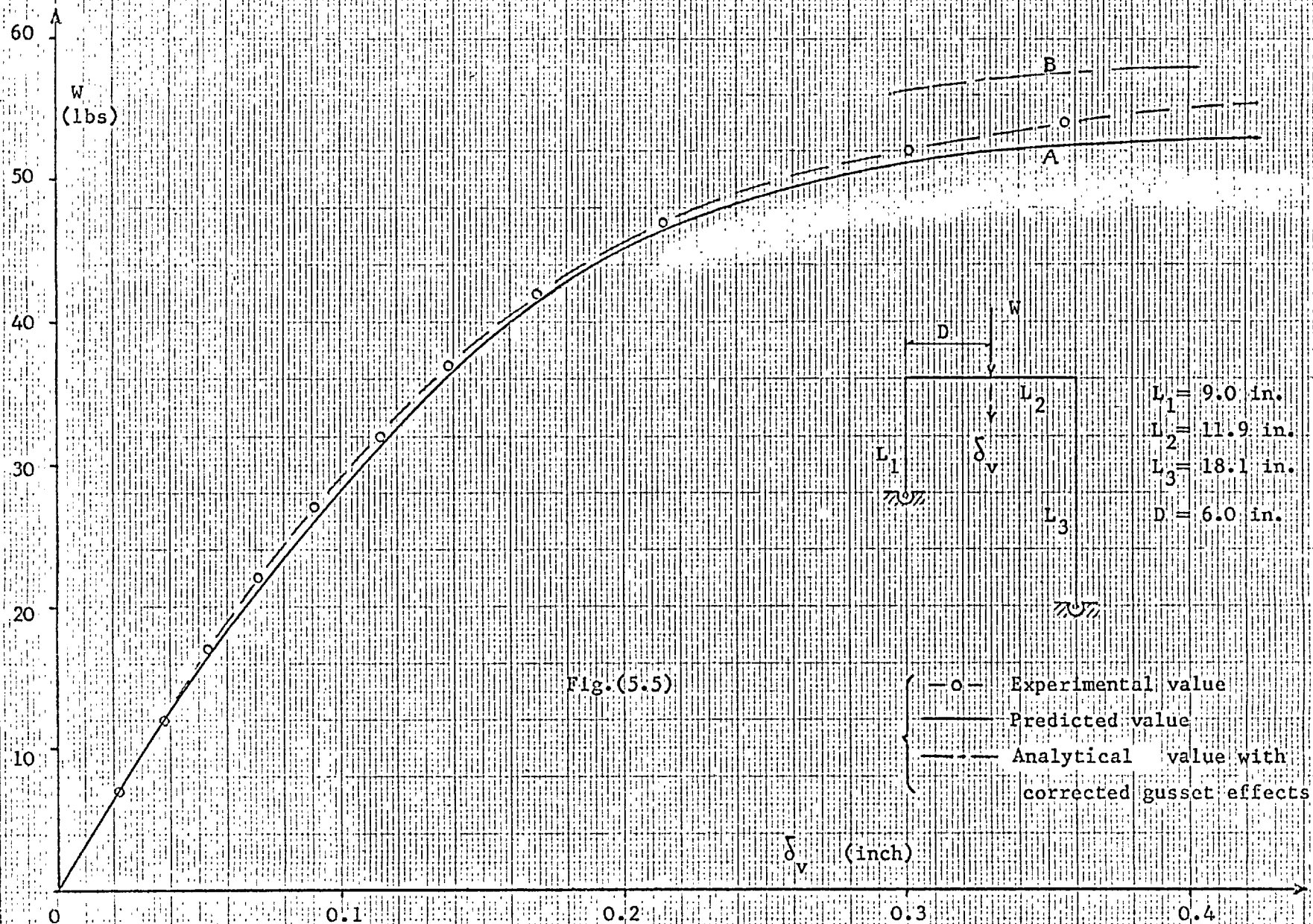
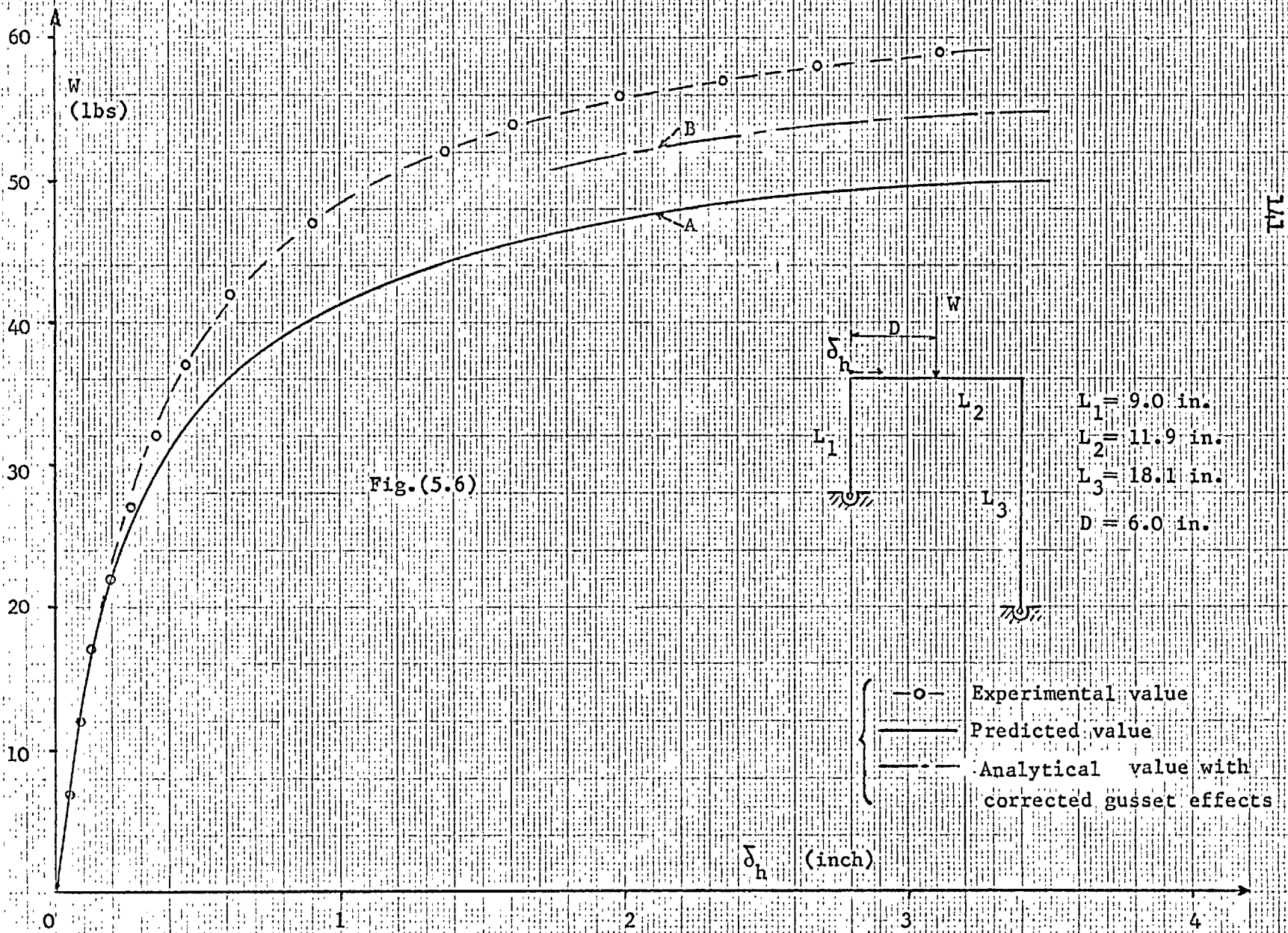


Fig. (5.3)

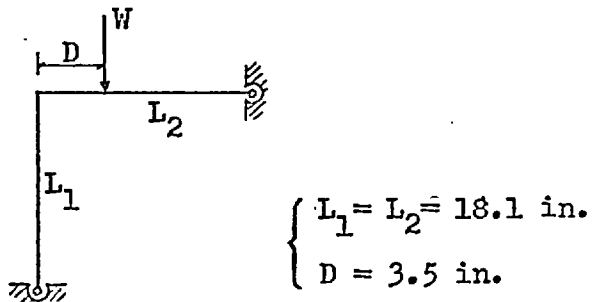






Test II

The column of the frame in this test had an Euler load  $P_E$  of 37.5 lbs. The frame was to be tested with a lateral support provided by the hinge at one end of the beam as shown in Fig.(5.1b); the hinge was securely mounted to the rigid test frame in such a way that it allowed only rotational freedom in the plane of the frame. The load was applied at a distance of 3.5 inches along the beam from the joint connecting the column:



At a test load of about 36 lbs the frame started to yield and plastic deformation occurred under the loading point until about 44 lbs, at which load the test was ended.

The occurrence of yielding, however, did not impede the purpose of the test, since at a load of 36 lbs the vertical deflections at the loading point and at mid-span of the beam were already more than 1.4 inches and 2.2 inches, respectively, and these deflections were probably already too large to be predicted satisfactorily by a small-deflection analysis.

The experimental result is shown in Fig.(5.7) where the load is plotted against the vertical deflection at loading point,  $\delta_v$ ; curve A

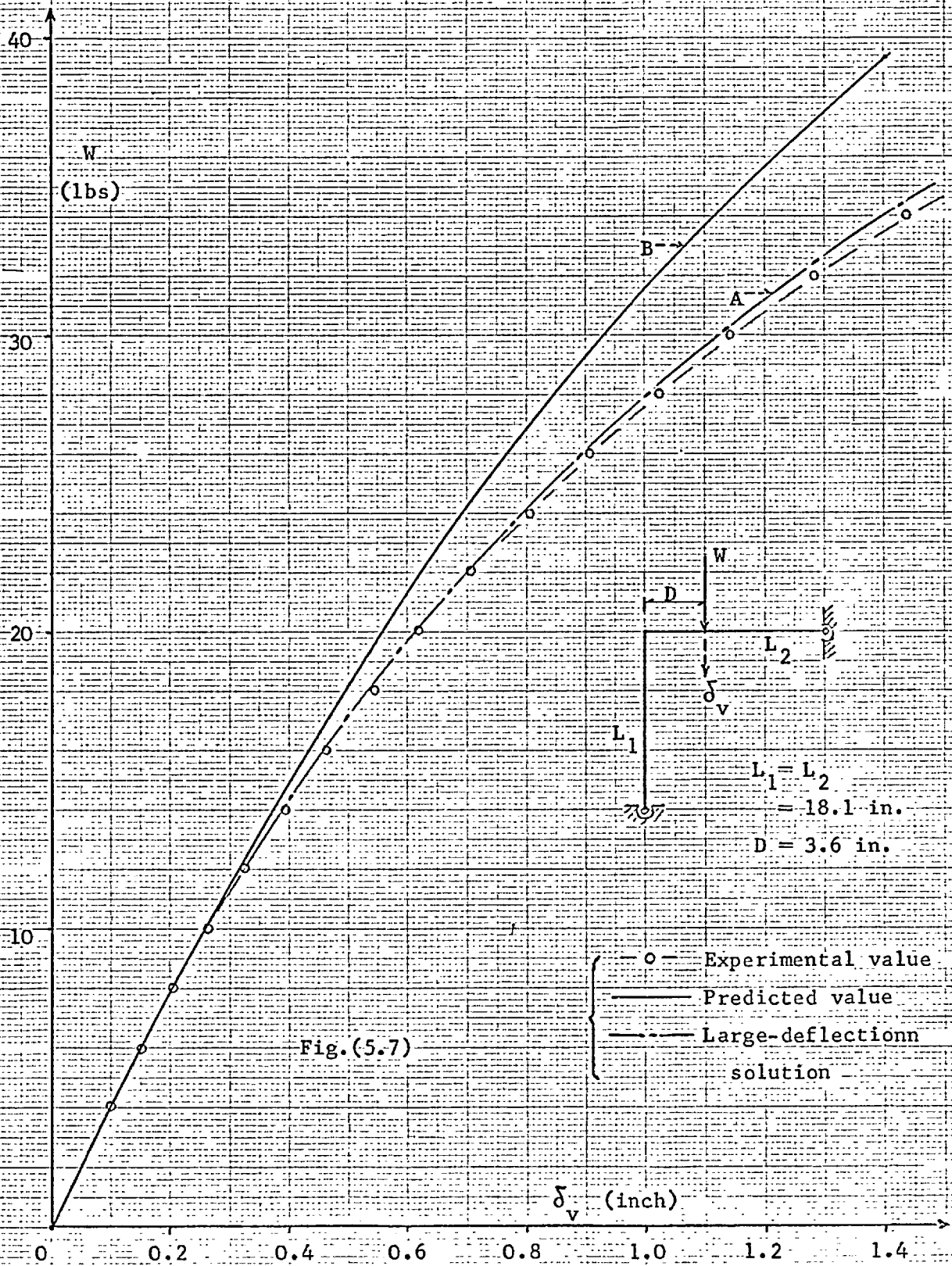


in the same figure represents the large-deflection solution, estimated from the original diagram given in small scale by Lee et al (28).

The corresponding small-deflection solution, as described in Chapter IV.2, is given by curve B (Fig.(5.7)) which registers an error of about 10% in estimating  $\delta_v$  at  $W = 0.5 P_E$ . At the load of 36 lbs, which is the maximum recorded load before yielding occurs, the corresponding error is about 30%.

The mid-span deflections of the frame members are also plotted against load in Fig.(5.8).

Adjustment of the theoretical values for gusset effects may be neglected in the present test. Fig.(4.2.7) shows that at a low load level the absolute value of the end-moment  $Q_1$  is small, and that its value increases very rapidly as the load approaches its maximum equilibrium value; consequently the effect of the gussets, which is to reduce the curvature locally and so influence the load-deflection relation of the frame, is negligible in the present test when the load level is relatively low. Furthermore the ratio of gusset length to column length, which is one of the factors that determine the gusset effect ((25), pp.67-72), is relatively small in the present model.





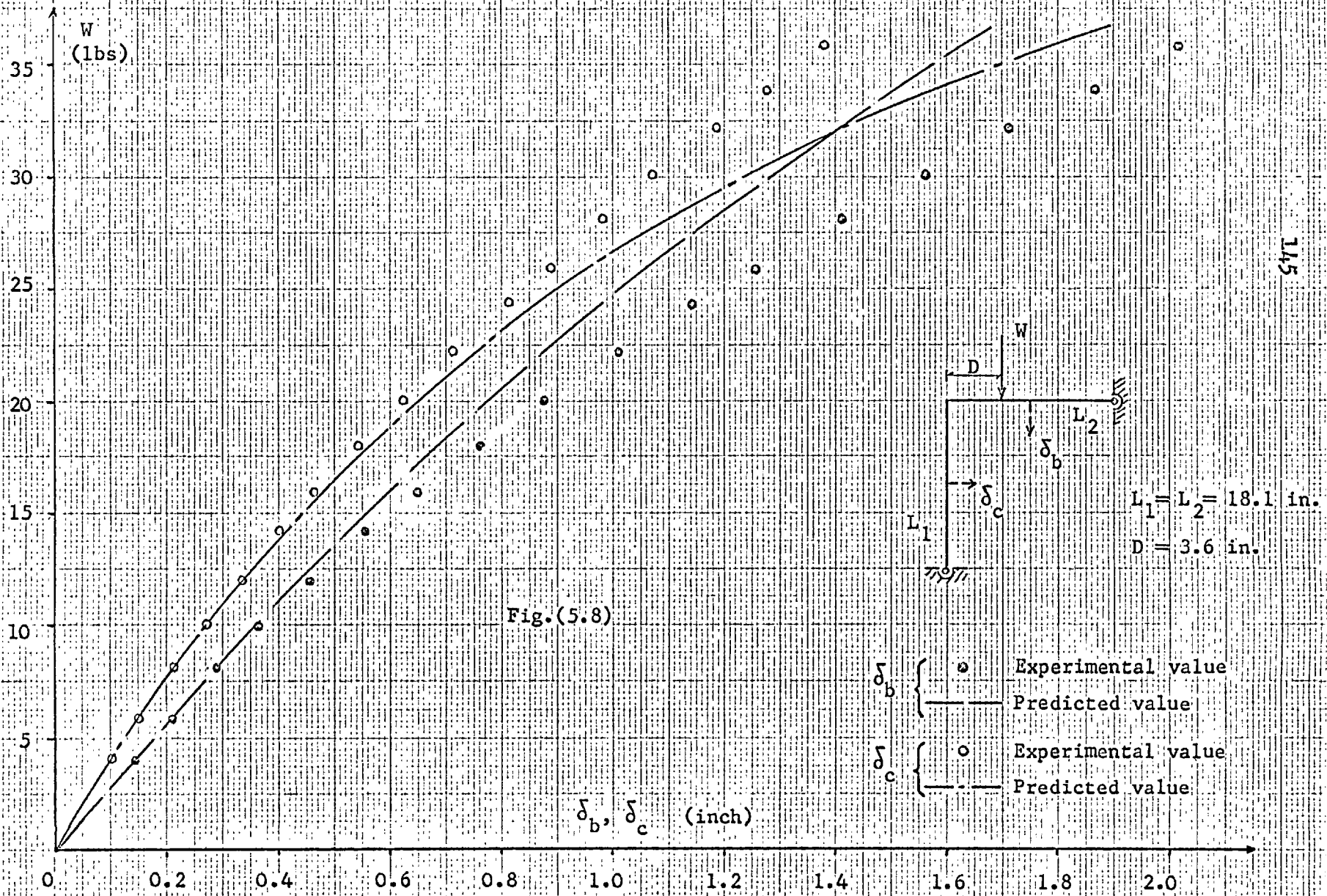


Fig.(5.8)

Test III

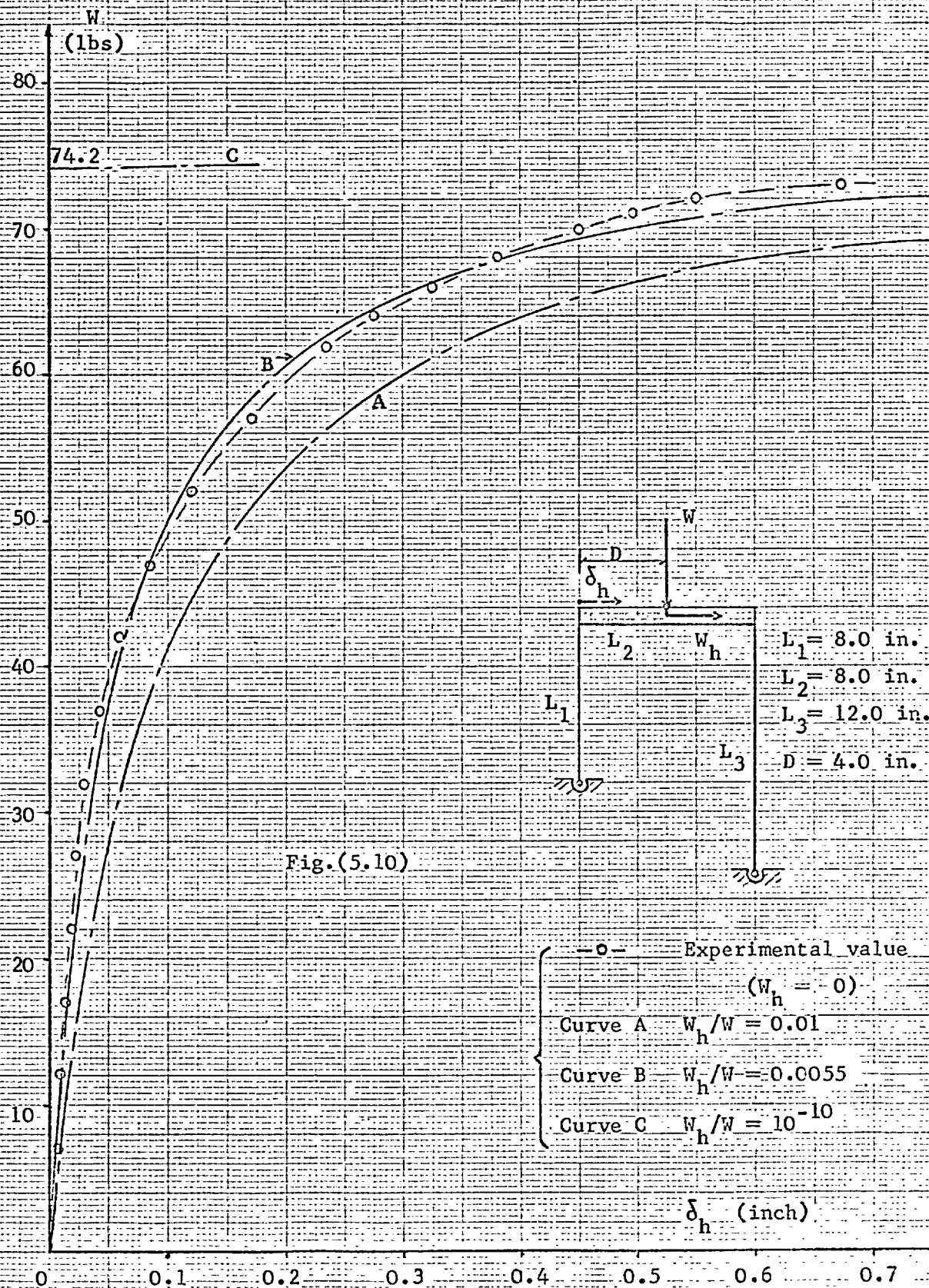
The frame (Fig.(5.9a)) in this test had a cross beam which was virtually rigid in comparison with its connecting members (see Table (5.1)); there was no lateral load applied to the frame. Then it can readily be shown that before bifurcation the condition of equilibrium of horizontal shears precluded sway, and as a result the columns were subjected only to axial loads at an arbitrary load level. The test therefore represented a bifurcational problem. In actual test, however, minor imperfections were expected in the straightness of members and the perpendicularity of the columns and the rigid beam. These initial imperfections caused bowing of the columns, bending moments, and side-sway of the frame, affects which were magnified as the load was increased.

The experimental load-deflection curve is given in Fig.(5.10). The maximum load was 76 lbs; the frame members resumed their original straightness after unloading, showing again that the load-deflection relation was within its elastic range.

As an estimate of the order of magnitude that the effect of imperfection might have had, the frame was analysed with an imperfection of the direction of loading, giving a horizontal disturbing force  $W_h$  as shown in Fig.(5.9b).

Curve A and curve B in Fig.(5.10) represent the load-deflection curve of the frame (Fig.(5.9b)) with  $W_h/W$  equal to 0.1 and 0.0055,





## V.2 DISCUSSION

### (1) Axial loading problems

The frame shown in Fig.(5.11) is subjected to axial loading and its inextensible members are free from initial geometrical imperfections. For such a perfect frame deformation will not occur until the load factor  $\lambda$  reaches its critical value. Consequently solutions given by small-deflection analysis for this type of frame problem, as discussed in Chapter II, are exact as long as the assumption of inextensibility remains valid for all the members composing the frame.

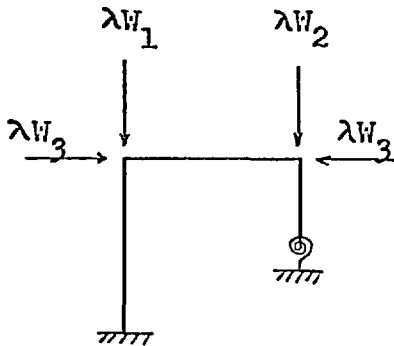
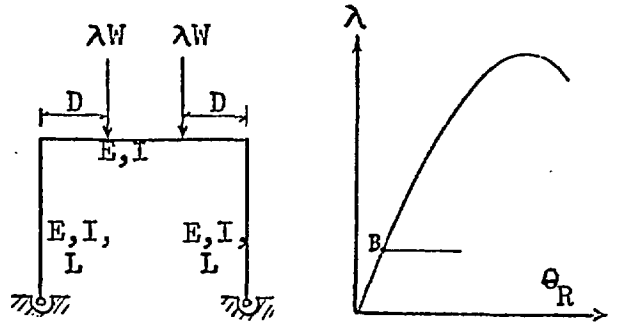


Fig.(5.11)



(a)

(b)

Fig.(5.12)

### (2) Bifurcational non-axial loading problems

This type of frame problem is exemplified by the frame proposed by Chwalla; the frame is shown in Fig.(5.12a). If the load factor  $\lambda$  is plotted against a reference joint rotation  $\theta_R$  the resulting load-deflection relation will be as shown in Fig.(5.12b), in which point B represents the point of bifurcation from the non-sway mode

to a sway mode. In this case deformation, without side-sway, will occur at any non-zero load level, and consequently only the large-deflection theory is capable of providing an exact answer. However, due to the fact that bifurcation generally occurs at a relatively low load level and thus the corresponding deformations remain small, a solution given by the small-deflection theory in predicting the bifurcation load should usually be satisfactory.

The bifurcation load of Chwalla's frame given by Lee et al (28), using large-deflection theory, is about 2% less than that given by small-deflection analysis. The discrepancy is mainly due to the fact that a large-deflection analysis takes into account the flexural shortening of the cross beam due to bowing, which causes additional eccentricity of the column load.

### (3) General non-axial loading problem

The frame and loading shown in Fig.(5.13a) typically represent such a problem. The general shape of the load-deflection curve is shown in Fig.(5.13b), in which  $\delta_R$  represents a general deflection parameter.

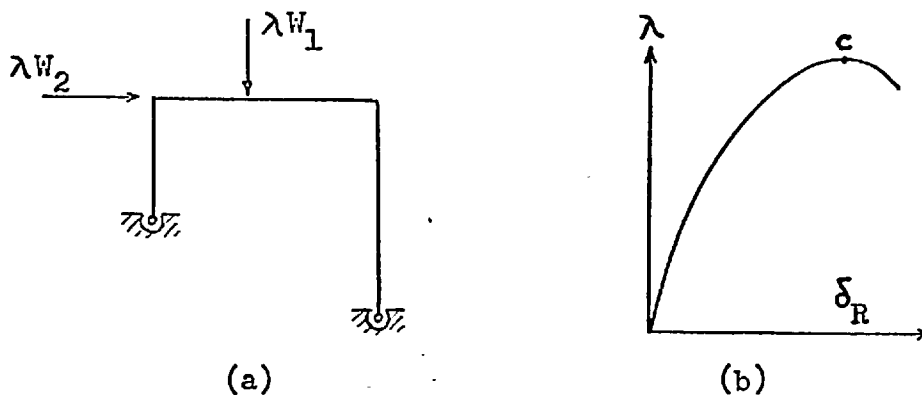


Fig.(5.13)

Depending on the properties and proportion of frame members and the pattern of loading, the frame may undergo very large deflections as the load factor approaches its local maximum (point C in Fig. (5.13b)) and consequently the small-deflection assumption can no longer hold.

In reality, however, there is always opportunity for the application of a small-deflection analysis, for structural failure may in general be viewed as either the collapse of a structure (failure in strength) or the occurrence of excessive deformation in it so that the structure loses its serviceability (failure in stiffness); consequently, for civil engineering structures, there is normally a limit of deformation imposed on a practical structure. The allowable deformation varies according to circumstances and codes of practice, but its order of magnitude is invariably small. Fig. (5.3) to Fig. (5.8) show that small-deflection theory gives a good approximation in each case provided that the measured deflection is less than about  $1/50$  of the corresponding member length, and this is well above the limiting deflection which would be considered acceptable in any building frame.

## CHAPTER VI CONCLUSIONS

### Axial loading problems

Two methods of evaluating the critical loads of axially-loaded rectangular frames have been proposed in this thesis. They are manual methods (as opposed to methods for electronic computation) and, as such, are much quicker than existing methods. The proposed methods are:

(1) The  $\gamma$  method (Chapter II):

The  $\gamma$  method is an exact method of analysis for portal-type structures which consist of open loops. The method is thus applicable to structures such as continuous beams, multi-bay bents, and multistorey single-bay frames of an appropriately symmetrical nature (since such frames can be divided, across the line of symmetry, into two continuous "open-loop" bents with known support conditions). The characteristic of the  $\gamma$  method is that it proceeds by successive trial estimates of the critical load value, at which the stiffnesses  $\gamma$  are computed for every member of the frame.

(2) The stability function transformation method (Chapter III):

This is an approximate method in which stability problems are solved in algebraic terms. Any portal-type structure, either open-looped or closed-looped, can be solved by this method. When applied to open-looped structures it can give specific



information on the behaviour of individual members under load. However, when applied to closed-looped structures the method invokes the concept of an equivalent column, so it can only give information on the behaviour of the frame as a whole, although the contribution of each individual member to the buckling strength of the frame is still recognisable during the process of forming the equivalent column.

The method offers two possible approaches of solution:

(a) The direct approach (Section (3.3) to Section (3.6)):

For an open-looped structure consisting of  $N_s$  loaded members the critical load may be evaluated directly by solving a polynomial of degree  $N_s$ . The behaviour of a multistorey structure may be approximated by an equivalent column, so a frame having  $N_s$  storeys and  $N_c$  continuous columns may be transformed into an equivalent column (which is an open-looped structure) consisting of  $N_s$  loaded members. In this case therefore the direct approach is applicable. In general the direct approach is recommended when  $N_s < 3$ ; for frame problems in which  $N_s \geq 3$  a trial-and-error type of solution (Approach (b)) will be preferred.

(b) The trial-and-error approach (Section (3.7) and Section (3.9)): This approach may be applied with advantage when  $N_s \geq 3$ . The method is to assume a distribution of

$S$  (the rotational stiffness of beams) at the ends of each column so that the load-carrying capacity of each loaded member may be evaluated; a successful trial is represented by the condition that the load-carrying capacities thus computed are equal (or nearly so) to their mean value. The method is easy to apply and powerful in obtaining a satisfactory solution. The speed of convergence is further enhanced by initiating the trial-and-error process at a probable "critical column", whereby the critical load may be more quickly approximated. Furthermore, since this critical load value has to be maintained throughout the structure the values of  $\gamma$  at all columns may be computed accordingly, and the effort of guessing the  $\gamma$  values is greatly reduced.

The main feature of the stability function transformation method is that the load-carrying capacity of a column (or an equivalent one) under either a no shear or a non-sway condition may be evaluated by separate consideration of its end conditions. This is believed to be of value in the process of preliminary design of a structure and of its subsequent modification. For example, Equ.(3.12) and Equ.(3.21) (or Table (3.7)) show that it is more profitable to fix the base of a column subjected to sway than to fix a similar column prevented from sway (since the buckling strength in the former case will increase fourfold while that of

the latter case will increase only twofold), and that in both cases the increase in strength is independent of the boundary condition at the other end of the column. Table (3.7) also shows that for a column subjected to sway a slight degree of fixity at one end will considerably improve the load-carrying capacity, and the rate of improvement decreases rapidly as the degree of fixity increases; therefore we realize that the provision of full fixity at the base of a column subjected to sway may not always be worth the effort.

Both the method of stability function transformation and the  $\gamma$  method are able to depict the physical phenomenon of buckling throughout the process of computation: the  $\gamma$  method shows the effect on the stiffness of individual members of the buckling load, while the transformation method shows the effect on the buckling load of the stiffness of the individual members. Consequently these methods have a definite advantage over computer methods and most other manual methods.

When computer methods are used they can of course provide exact solutions to complex stability problems, but the validity of the solution is difficult to verify because of the non-linear nature of the problem. In this situation the proposed methods are especially useful, as they give a rapid procedure for the desk calculation of an approximation to the critical load.

Non-axial loading problems

An iterative method was proposed (Chapter IV) to determine the equilibrium paths of rigidly-jointed rectangular frames under non-axial loading, according to small-deflection theory. The characteristic of this approach is that a reference deformation parameter, rather than the load factor, is treated as the independent variable.

The main advantage of this approach is that bifurcation buckling can be solved directly, without resorting to laborious formulations based on the existing bifurcation criteria. The saving in labour of formulation and of obtaining a solution may be gauged by the fact that the proposed method need only consider the bifurcated (asymmetrical) mode of deformation, while the existing methods have to consider simultaneously the symmetrical and asymmetrical modes. Furthermore, for frame problems where distributed loads are present the proposed method requires no additional formulation effort.

The method was also applied to non-bifurcational problems so as to estimate the approximate range of applicability of the small-deflection theory, by comparing solutions thus found with the experimental results obtained from model tests (Chapter V). In each test the small-deflection analysis gives a good approximation provided the measured deflection is less than about  $1/50$  of the corresponding member length, and this is well above the limiting deflection which would be considered acceptable in any building frame.

NOTATION

$$A_b = \alpha_{tc} + \alpha_{bu}$$

$$A_t = \alpha_{bc} + \alpha_{tv}$$

$C = c/(c^2 - s^2)$  for non-axial loading problems;  
coefficient of axial forces for axial loading problems.

$C_f$  coefficient for frame problems where  $\rho = 0$

$C_s$  coefficient for frame problems where  $V = 0$

$$D = T/\lambda$$

$E$  modulus of elasticity

$E_R$  the value of  $E$  of a reference member

$$\bar{E} = E/E_R$$

$F$  kinematic degree of freedom

$H$  the number of hinges in a frame

$I$  second moment of area

$I_R$  the value of  $I$  of a reference member

$$\bar{I} = I/I_R$$

$J$  the number of internal joints in a frame

$$K = EI/L$$

$$\bar{K} = K/(P_{ER} L_R)$$

$L$  length of member

$L_R$  the value of  $L$  of a reference member

$$\bar{L} = L/L_R$$

- M non-subscripted: the number of members in a frame  
subscripted: bending moment
- $\bar{M}$  =  $M/(P_{ER} L_R)$
- N the number of indeterminate end-moments in a frame
- $N_b$  the number of bays in a frame
- $N_c$  the number of column lines in a frame ( $= N_b + 1$ )
- $N_s$  the number of storeys in a frame
- $N_w$  the number of transverse loads acting on a beam
- P axial force
- $P_E$  the Euler load of a member ( $= \pi^2 EI/L^2$ )
- $P_{ER}$  the value of  $P_E$  of a reference member
- $\bar{P}$  =  $P/P_R$
- $P^0$  axial force in a determinate frame
- $\bar{P}^0$  =  $P^0/P_R$
- Q indeterminate end-moment
- $\bar{Q}$  =  $Q/(P_{ER} L_R)$
- R the number of support reactions in a frame
- S =  $s/(c^2 - s^2)$  for non-axial loading problems;  
rotational stiffness for axial-loading problems.
- T primary bending term
- V shearing force
- W external load

$W_h$	horizontal external load
$W_v$	vertical external load
a	$= -1/(\phi \tan\phi)$ , for $P > 0$
b	$= 1/\phi^2$ , for $P > 0$
c	$= (1 - \phi \cot\phi)/\phi^2$ , for $P > 0$ ; suffix for the critical column.
d	$= s^2 - c^2$
e	the base of natural logarithms
f	general mathematical function
i	index
j	index
k	index
m	index
n	index
r	influence coefficient of axial force in a frame due to an indeterminate end-moment
$\bar{r}$	$= r L_R$
s	$= (\phi \csc\phi - 1)/\phi^2$ , for $P > 0$
u	suffix for the column located above a critical column
v	suffix for the column located below a critical column
w	eigenfunction deflection

$\alpha$	stability coefficient, $= \alpha_t \alpha_b$
$\alpha_b$	the value of $\alpha$ at the bottom of a column
$\alpha_t$	the value of $\alpha$ at the top of a column
$\gamma$	$= M/(K \theta)$
$\delta$	differential displacement of the ends of a member
$\delta_h$	horizontal displacement
$\delta_v$	vertical displacement
$\epsilon$	remainder
$\theta$	angle of rotation at a joint
$\theta^o$	primary angle of rotation due to lateral load
$\tilde{\theta}^o$	initial imperfection slope at an end of a member
$\lambda$	load factor
$\nu$	$= \gamma/C_f$ for frame problems where $\rho = 0$ ; $= \gamma/C_s$ for frame problems where $V = 0$ .
$\pi$	$= 3.14159265$
$\rho$	rigid-body rotation of a member
$\phi$	$= \sqrt{H/EI} L$
$\chi$	coefficient of axial force due to differential movement of frame members
$\bar{\chi}$	$= \chi L_R$



REFERENCES

- (1) S.P. Timoshenko, "Theory of elastic stability", McGraw-Hill Book Co., Inc., 1936
- (2) E. Chwalla, "Die Stabilitat lotrecht belasteter Rechteckramen", Der Bauingenieur, Vol.19, 1938
- (3) W.T. Koiter, "Over de stabiliteit van het elastisch evenwicht", Thesis Delft, 1945. A concise summary of the work was given in "Non-linear Problems; elastic stability and post-buckling behavior", edited by R.E. Langer, the Univ. of Wisconsin Press, 1963
- (4) F. Bleich, "Buckling strength of metal structures", McGraw-Hill Book Co., Inc., 1952
- (5) W. Merchant, "Critical loads of tall building frames", Structural Engineer, Vol.33, 1955
- (6) R.E. Bowles and W. Merchant, "Critical loads of tall building frames, Part III", Structural Engineer, Vol.34, 1956
- (7) A.H. Chilver, "Buckling of a simple portal frame", J.Mech. Phys. Solids, Vol.5, 1956
- (8) R.K. Livesley and D.B. Chandler, "Stability functions for structural frameworks", Manchester Univ. Press, 1956
- (9) E. Lightfoot, "The analysis for wind loading of rigid jointed multistorey building frames", Civil Engineering, July and August, 1956
- (10) D.E. Johnson, "Lateral stability of frames by energy method", J. ASCE, EM.4, August, 1960
- (11) E.F. Masur, I.C. Chang, and L.H. Donnell, "Stability of frames in the presence of primary bending moments", J. ASCE, EM.4, August, 1961

- (12) J.E. Goldberg, "Buckling of one-storey frames and buildings", Trans. ASCE, Vol.126, Part 2, 1961
- (13) S.J. McMinn, "The determination of the critical loads of plane frames", Structural Engineering, July, 1961
- (14) S.J. McMinn, "Matrices for structural analysis", E. & F.N. Spon Ltd., 1962
- (15) M.R. Horne, "The effect of finite deformations in elastic stability of plane frames", Proc. Royal Society, London, Vol.226, 1962
- (16) L.W. Lu, "Stability of frames under primary bending moments", J. ASCE, ST.3, June, 1963
- (17) S.A. Saafan, "Non-linear behavior of structural plane frames", J. ASCE, ST.4, August, 1963
- (18) S.J. Britvec and A.H. Chilver, "Elastic buckling of rigidly-jointed frames", J. ASCE, EM.6, December, 1963
- (19) J.M. Gere, "Moment distribution", D. Van Nostrand Co., Inc., 1963
- (20) J.M.T. Thompson, "Basic principles in the general theory of elastic stability", J. Mech. Phys. Solids, Vol.2, 1963
- (21) F.W. Williams, "An approach to the non-linear behaviour of the members of a rigid jointed plane framework with finite deflections", Qtly. J. Mech. Appl. Math., Vol.17, November, 1964
- (22) C.N. Kerr, "Large deflections of a square frame", Qtly. J. Mech. Appl. Math., Vol.17, November, 1964
- (23) J.M.T. Thompson, "Discrete branching points in the general theory of elastic stability", J. Mech. Phys. Solids, Vol.13, 1965

- (24) M.J. Sewell, "The static perturbation technique in buckling problems", J. Mech. Phys. Solids, Vol.13, 1965
- (25) M.R. Horne and W. Merchant, "The stability of frames", Pergamon Press Ltd., 1965
- (26) M.H.R. Godley and A.H. Chilver, "The elastic post-buckling behaviour of unbraced plane frames", Int. J. Mech. Sci., Vol.9, 1967
- (27) M. Gregory, "Elastic instability", E. & F.N. Spon, Ltd., 1967
- (28) S.L. Lee, F.S. Manuel, and E.C. Rossow, "Large deflections and stability of elastic frames", J. ASCE, EM.2, April, 1968
- (29) E.H. Brown, "Virtual work theorems for frame stability problems", 12th Int. Cong. Appl. Mech., Stanford, August, 1968
- (30) E.H. Brown, "The failure of frames", to be published.